The Case of Extended Supersymmetry and A Study in Superspace

A Dissertation Presented

by

Dharmesh Jain

to

The Graduate School

in Partial Fulfillment of the

Requirements

for the Degree of

Doctor of Philosophy

in

Physics and Astronomy

Stony Brook University

May 2014

Stony Brook University

The Graduate School

Dharmesh Jain

We, the dissertation committee for the above candidate for the

Doctor of Philosophy degree, hereby recommend

acceptance of this dissertation.

Warren Siegel – Dissertation Advisor
Professor, C. N. Yang Institute for Theoretical Physics,
Department of Physics and Astronomy

Peter van Nieuwenhuizen – Chairperson of Defense
Distinguished Professor, C. N. Yang Institute for Theoretical Physics,
Department of Physics and Astronomy

Christopher Herzog – Committee Member
Associate Professor, C. N. Yang Institute for Theoretical Physics,
Department of Physics and Astronomy

Dmitri Tsybychev – Committee Member
Assistant Professor, Department of Physics and Astronomy

Marcus Khuri – Outside Member
Associate Professor, Department of Mathematics

This dissertation is accepted by the Graduate School.

Charles Taber
Dean of the Graduate School

Abstract of the Dissertation

The Case of Extended Supersymmetry and A Study in Superspace

by

Dharmesh Jain

Doctor of Philosophy

in

Physics and Astronomy

Stony Brook University

2014

In this dissertation we study quantum field theories with extended supersymmetry in four and three dimensions. In $d = 4$ we study $\mathcal{N} = 2$ supersymmetric theories using projective superspace formalism extensively. We discover the full non-Abelian action for super Yang-Mills (SYM) theory in projective superspace by studying its relation to harmonic superspace under a suitable Wick rotation of the latter's internal two-dimensional sphere. We also show that a Chern-Simons action for SYM in 'full' $\mathcal{N} = 2$ superspace can be written down that reproduces both the harmonic and projective SYM actions. The projective formalism allows simplifications in computing Feynman supergraphs because the $\mathcal{N} = 2$ rules imply simpler D-algebra than the $\mathcal{N} = 1$ case. Also, integrals over its one-dimensional internal space are simpler to handle than the two-dimensional counterparts in the harmonic case. Furthermore, these calculations are simplified drastically in background field formalism and to construct it in projective formalism, we have to choose different representations for quantum and background fields. This also means that the standard power counting arguments are applicable and finiteness beyond 1-loop for $\mathcal{N} = 2$ SYM becomes manifest. We then study the hyperkähler moduli space of $\mathcal{N} = 2$

SYM compactified on a circle. Recently, it was shown that the Darboux coordinates on the moduli space are an efficient description of the hyperkähler metric and we give a simple construction of the integral equation describing these coordinates using projective superspace. We apply this result to study the moduli space of $d = 5$ $\mathcal{N} = 1$ SYM compactified on a torus and we obtain results in agreement with the literature. Lastly, in $d = 3$ we study the free energy of $\mathcal{N} = 3$ Chern-Simons theories associated with affine ADE quivers and conjecture a general expression for free energy of D_n quivers. Through the AdS/CFT correspondence, this leads to a prediction for the volume of certain class of tri-Sasaki Einstein manifolds. As a consistency check of our expression, we add massive fundamental flavour fields and verify that the free energy decreases in accordance with F-theorem once they are integrated out.

To Sir, with gratitude...
&
To my Superpartner!

Table of Contents

List of Figures

List of Tables

Acknowledgements

I am extremely grateful to

- My advisor Warren Siegel for his advanced QFT courses, for being always available to listen to ideas and issues in my ongoing research leading to long and intense discussions (both Physics & non-Physics!), for allowing me freedom to choose my research projects, for being a significant contributor to the YITP forum, and most importantly for his sense of humour.

- Peter van Nieuwenhuizen for teaching all those advanced and in-depth courses every semester, for sharing equally detailed notes, for (founding &) participating in Friday seminars, for giving me an opportunity to teach a class in his Susy & Sugra course (a small part of those notes feature here) and for constant support over the years.

- Martin Roček for insightful discussions on projective superspace formalism, for suggesting to look at GMN's paper and sharing with us unpublished notes on which chapter 4 is based, for helpful advice and encouragement throughout my stay here, including the Friday seminars.

- Christopher Herzog for suggesting the work discussed in chapter 5, for illuminating explanations, helpful suggestions and being available for discussions just a room away.

- Shantanu Agarwal and Siddhartha Santra for being just a phone call away when I needed to vent out some interesting breakthrough in my research or just had to indulge in some *Sher-o-Shayari*.

- Marcos Crichigno for being a constant presence ever since we started collaborating in chapter 4, which has led me to being 'worldly-wise' regarding not just Physics but also the 'world'.

- Chia-Yi Ju and Jun Nian for coming up with interesting ideas in our collaborations, for listening patiently to me explaining why they won't work and figuring out something that works despite that.

- Yu-tin Huang for helpful discussions while some of the work presented in chapter 2 was done and for encouraging discussions from time to time during his visits to YITP.

- Prerit Jaiswal for useful discussions on Feynman diagrams, Physics beyond Standard Model, Phenomenology, Computaional Physics, and almost everything else under the sun.

Further thanks are in order to

- George Sterman for his 1-year QFT course, for his encouraging presence in Friday seminars (at least during my talks) and for making it possible for me to stay and research at YITP for all these years.

- Ozan, Wolfger, Madalena, Mao, Yi-wen, Pedro, Wenbin, Melvin, Cheesheng, $\cdots$ for being in the same office room, making it 'fun' to research in and remembering to close the door when everyone left.

- Sujan, Abhijit, Elli, $\cdots$ for being in the other office room and dropping by sometimes to make our room more 'fun'.

- YITP and DPA for allowing my long stay here at SBU to be pleasant and academically productive. I would specially thank Betty and Sara for answering my frequent queries in the last year with ease and efficiency.

- Visitors: Babak Haghighat and Stefan Vandoren for helpful discussions on the 5D theory content of chapter 4. Greg Moore and Rikard von Unge for encouraging discussions and Sergey Cherkis for useful suggestions about the paper manuscript on which chapter 4 is based. Daniel Gulotta for various discussions and clarifications regarding the work presented in chapter 5. Daniel Butter for insightful discussions on projective and harmonic superspaces.

- IIT KGP (Profs. SK, SPK, SB, $\cdots$) and TIFR (Profs. ST, Sμ & SM) where I got first exposure to QFT and Supersymmetry without which the research I have done here would have been close to impossible.

- My friends (whose names do not appear above) and family (JKMSMKJ & $\cdots$), very few of them for understanding what I was doing and the rest for not understanding it!

- Last but not the least, my research was supported in part by National Science Foundation Grant No. PHY-0653342, PHY-0969739 and PHY-1316617.

Chapter 1

Introduction

Supersymmetry is currently the most studied yet unobserved aspect of the real world. The most relevant supersymmetry for the physical $d = 4$ spacetime is labelled $\mathcal{N} = 1$, which has four fermionic supercharges (worth 'one' Majorana or Weyl spinor) in addition to expected generators of the Poincaré group. However, the $\mathcal{N} \geq 2$ theories, with the virtue of having more symmetries, have simpler UV properties and allow greater control over possible exact computations, which have applications even to the 'real world' QCD.

For the major part of this thesis we will concentrate on $\mathcal{N} = 2$ supersymmetric field theories in $d = 4$. To study these theories, we will use the language of projective (and harmonic) superspace. In general, superspace is the most efficient tool to study supersymmetric quantum field theories. It keeps supersymmetry manifest at all stages of computations and simplifies a lot of calculations (so-called miraculous cancellations). Superspace also has deep connections with the mathematics of complex geometry. As is well-known, $\mathcal{N} = 1$ superspace is intimately related to Kähler geometry and here we will continue that discussion to $\mathcal{N} = 2$ superspace and explore its relation to hyperkähler manifolds in some detail. We will also take a small tour of $\mathcal{N} = 3$ theories in $d = 3$ and compute their 'exact' partition functions using matrix model techniques. We will not use superspace here but a common thread that ties it with the rest of the chapters is that supersymmetry simplifies calculations and in this case, even allows extraction of exact results.

To kick-start our treatment of $d = 4$, $\mathcal{N} = 2$ supersymmetric theories, we first discuss here the reason for using projective (and/or harmonic) superspace. That is, why does a naïve extension of the well-known $\mathcal{N} = 1$ superspace (called ordinary in the case of $\mathcal{N} = 2$) turns out to be insufficient for describing the $\mathcal{N} = 2$ theories.

1.1 Why Not Ordinary Superspace?

Let us first consider the massless $\mathcal{N}=2$ scalar multiplet (scalar hypermultiplet [1]) in ordinary superspace. It consists of two complex scalars ϕ^i (where $i=1,2$ is an $SU(2)$ index) and two Weyl spinors $\psi_\alpha, \bar{\kappa}_{\dot{\alpha}}$ forming a Dirac spinor. Upgrading to a superfield requires addition of fermionic coordinates so the full set of coordinates is

$$X^M = \{x^\mu, \theta^\alpha_i, \bar{\theta}^{\dot{\alpha}i}\}. \tag{1.1.1}$$

Also, the super-covariant derivatives satisfy[1]

$$\{D^i_\alpha, \bar{D}_{\dot{\alpha}j}\} = -2i\delta^i_j \partial_{\alpha\dot{\alpha}}\,; \quad \{D^i_\alpha, D^j_\beta\} = 0\,. \tag{1.1.2}$$

Here we have used that for massless theories the central charge Z is zero. A natural choice for a superfield describing the physical fields mentioned above would be a superfield Φ^i such that its lowest components read

$$\phi^i = \Phi^i_|\,; \quad \psi_\alpha = D_{\alpha i}\Phi^i_|\,; \quad \bar{\kappa}_{\dot{\alpha}} = \bar{D}_{\dot{\alpha}i}\Phi^i_|\,, \tag{1.1.3}$$

where $_|$ denotes setting all θ's to zero. But a general superfield has too many components so we have to put some constraints on Φ^i (like a chiral superfield in $\mathcal{N}=1$). The following constraints [2] produce only the physical fields in (1.1.3)

$$D^{(i}_\alpha \Phi^{j)} = \bar{D}^{(i}_{\dot{\alpha}} \Phi^{j)} = 0\,. \tag{1.1.4}$$

However, we now show that these constraints are too strong and put these physical fields on-shell:

$$\begin{aligned}
\bar{D}^k_{\dot{\alpha}} \left[D^{(i}_\alpha \Phi^{j)}\right] &= 0 \\
\Rightarrow D^\alpha_i \left[-2i\epsilon^{k(i}\partial_{\alpha\dot{\alpha}}\Phi^{j)} - D^{(i|}_\alpha \bar{D}^k_{\dot{\alpha}}\Phi^{|j)}\right] &= 0 \\
\Rightarrow \epsilon_{kj}\left[-2i\left(D^{\alpha k}\partial_{\alpha\dot{\alpha}}\Phi^j + \epsilon^{kj}\partial_{\alpha\dot{\alpha}}D^\alpha_i\Phi^i\right) - D^\alpha_i D^j_\alpha\left(-\tfrac{1}{2}\epsilon^{ki}\right)\bar{D}^m_{\dot{\alpha}}\Phi_m\right] &= 0 \\
\Rightarrow -2i\left(\partial_{\alpha\dot{\alpha}}D^\alpha_j\Phi^j + 2\partial_{\alpha\dot{\alpha}}D^\alpha_i\Phi^i\right) &= 0 \\
\Rightarrow \partial_{\alpha\dot{\alpha}}\psi^\alpha &= 0
\end{aligned} \tag{1.1.5}$$

[1] The $SU(2)$ indices i,j are raised and lowered with ϵ^{ij} and ϵ_{ij} according to the 'north-west rule': $v^i = \epsilon^{ij}v_j$ and $v_i = v^j\epsilon_{ji}$ with $\epsilon^{ij} = \epsilon_{ij}$ and $\epsilon_{12} = \epsilon^{12} = 1$. Then $\{D^i_\alpha, \bar{D}^j_{\dot{\alpha}}\} = 2i\epsilon^{ij}\partial_{\alpha\dot{\alpha}}$, $\{D_{\alpha i}, \bar{D}^j_{\dot{\alpha}}\} = 2i\delta^j_i\partial_{\alpha\dot{\alpha}}$ and $\{D_{\alpha i}, \bar{D}_{\dot{\alpha}j}\} = 2i\epsilon_{ij}\partial_{\alpha\dot{\alpha}}$. We further define $(\theta^i_\alpha)^\dagger = \bar{\theta}_{\dot{\alpha}i}$ and $(\theta_{\alpha i})^\dagger = \bar{\theta}^i_{\dot{\alpha}}$ but $(\theta^{\alpha i})^\dagger = -\bar{\theta}^{\dot{\alpha}}_i$ and $(\theta^\alpha_i)^\dagger = -\bar{\theta}^{\dot{\alpha}i}$. Spinor indices are raised and lowered with $\epsilon_{\alpha\beta} = \epsilon^{\alpha\beta} = -\epsilon_{\dot{\alpha}\dot{\beta}} = -\epsilon^{\dot{\alpha}\dot{\beta}}$ also according to the north-west rule, for example $\theta_{\alpha i} = \theta^\beta_i\epsilon_{\beta\alpha}$ and $\bar{\theta}^{\dot{\alpha}i} = \epsilon^{\dot{\alpha}\dot{\beta}}\bar{\theta}^i_{\dot{\beta}}$. Then $(\epsilon^{\alpha\beta}\theta_{\beta i})^\dagger = -\epsilon^{\dot{\alpha}\dot{\beta}}(\theta_{\beta i})^\dagger = -\bar{\theta}^{\dot{\alpha}i}$.

where we used that $D_i^\alpha D_\alpha^i = 0$. A similar result holds for $\bar{\kappa}^{\dot{\alpha}}$ if we start from the other constraint. To see that ϕ^i is also put on-shell, we need to start from $\partial_{\alpha\dot{\alpha}} D^{\alpha i}\Phi^j = 0$. This equation is true since the symmetric part (ij) vanishes because of (1.1.4) and the vanishing of the antisymmetric part $[ij]$ was proven above. Now we act with $\bar{D}^{\dot{\alpha}k}$ on it as follows

$$\begin{aligned} \bar{D}^{\dot{\alpha}(k|}\partial_{\alpha\dot{\alpha}} D^{\alpha i}\Phi^{|j)} &= 0 \\ \Rightarrow 2i\partial_{\alpha\dot{\alpha}}\partial^{\alpha\dot{\alpha}}\epsilon^{i(k}\Phi^{j)} - \partial_{\alpha\dot{\alpha}} D^{\alpha i}\bar{D}^{\dot{\alpha}(k}\Phi^{j)} &= 0 \\ \Rightarrow \Box\phi^j &= 0\,. \end{aligned} \tag{1.1.6}$$

Thus, we see that all the physical fields satisfy the on-shell condition, i.e.,

$$\partial_{\alpha\dot{\alpha}}\psi^\alpha = 0\,, \qquad \partial_{\alpha\dot{\alpha}}\bar{\kappa}^{\dot{\alpha}} = 0 \qquad \& \qquad \Box\phi^i = 0\,. \tag{1.1.7}$$

To have these fields remain off-shell, we could try relaxing the constraints but that approach does not go too far. It gives the tensor multiplet, the relaxed multiplet, etc. (with finite sets of auxiliary fields) [3, 4] but they have some disadvantages. Their coupling to super Yang-Mills theory is not straightforward (in fact, impossible in the case of the tensor multiplet). Also these multiplets have scalars in real representations of $SU(2)$ R-symmetry as opposed to the field content we considered above.

Now we argue that a complex representation can not be accommodated in the ordinary superspace with a finite number of auxiliary fields [5, 6]. Off-shell, the auxiliary fields along with the physical fields form representations of massive multiplet(s). This implies we would need some auxiliary fermions. These auxiliary fermions should appear in the action as pairs of Dirac spinors, like $\bar{\chi}\eta$, and because the physical spinor ψ is in a real representation of $SU(2)_R$ (the singlet representation), the auxiliary spinors should belong to complex non-singlet representations. Let us count the total number of real fermionic field components.

Needed: pairs of **Dirac spinors** in $SU(2)$ representations $\boldsymbol{I_j}$ and the **physical ones** $\Rightarrow \sum_j[2\times 8\times(2I_j+1)] + 8 = 16q + 8$.

Expected: half the number of states in a **complex** irreducible $\boldsymbol{\mathcal{N} = 2}$ **supermultiplets** in $SU(2)$ representations $\boldsymbol{J_i} \Rightarrow \sum_i \frac{1}{2}\times 2\times 2^{2\times 2}\times(2J_i + 1) = 16p$.

Here, p and q are integers and it is clear that these two counting results do not match. This means we can not construct an off-shell superfield describing the massless $\mathcal{N} = 2$ scalar multiplet with a finite number of auxiliary fields. The way to circumvent this 'no-go' theorem is to have an infinite number of auxiliary fields.

As we will see the $\mathcal{N} = 2$ projective (and harmonic) superspaces achieve that by introducing extra bosonic coordinates on which the superfields are now allowed to depend. Since these coordinates are bosonic, the superfield's expansion in terms of the relevant functions (spherical harmonics for harmonic and Taylor/Laurent series for projective) does not terminate and we get an infinite number of auxiliary fields. As such, our arguments above apply only to the complex scalar hypermultiplet and it is possible to describe a vector (Yang-Mills) hypermultiplet in a 'chiral' $\mathcal{N} = 2$ superspace with finite number of auxiliary fields since it is real. However, unlike $\mathcal{N} = 1$, a prepotential formulation does not exist (at least one that can be satisfactorily quantized) so projective and harmonic superspaces are indispensable in describing the vector hypermultiplet. A prepotential can be constructed in these two approaches that allows a vector action (which can be quantized) to be written down. These aspects will become clear as we proceed further. We end this chapter by summarizing the upcoming chapters:

Origins of Projective Superspace is based on [7,8] (with W. Siegel) where we discuss the derivation of various hypermultiplets in projective superspace from those in harmonic, including the 'first' appearance of full nonabelian action for Yang-Mills theory in projective superspace.

Exploring Projective Superspace consolidates [9–11] (with W. Siegel) and hence includes derivation of Feynman rules for scalar (both massless and massive) and vector hypermultiplets, a significant amount of loop calculations using those rules and the 'first-ever' construction of a background field formalism in projective superspace.

Applying Projective Superspace discusses the work in [12] (with P. M. Crichigno) where we derive a general expression for Darboux coordinates on hyperkähler manifolds described by $\mathcal{O}(2p)$ hypermultiplets using projective superspace, which is then used to reproduce two existing results in the literature: Coulomb branch moduli space metric for $d = 4$, $\mathcal{N} = 2$ SYM compactified on S^1 and $d = 5$, $\mathcal{N} = 1$ SYM on T^2.

Quiver Chern-Simons Theories presents the work done in [13] (with P. M. Crichigno and C. P. Herzog) where we conjecture an expression for free energy of $d = 3$, $\mathcal{N} = 3$ $\widehat{D}_n$ quiver Chern-Simons theories using matrix model techniques and provide various checks, including an interesting connection with 'signed' graph theory.

Chapter 2

Origins of Projective Superspace

As mentioned in the introduction, there are two competing (but closely related) formalisms for effectively dealing with $\mathcal{N} = 2$ supermultiplets ('hypermultiplets' [1]) in $\mathcal{N} = 2$ superspace ('hyperspace'), in four dimensions (or simple supersymmetry in six): projective (ĬΠ) [14–16] and harmonic (♫) [17–20]. Projective hyperspace has the advantage of 1 less R-symmetry coordinate, which results in all the coordinates fitting neatly into a square matrix, whose hyperconformal transformations take the form of fractional linear transformations [21–25], hence the term 'projective'.

Although the relations between various multiplets in the two formalisms has been frequently discussed, in this chapter we will provide a direct derivation of multiplets, gauge transformations, and actions for the projective formalism from those of the harmonic. The derivation is mostly straightforward: The basic step is to start with the usual complex coordinates y and $\bar{y}$ of the 2-sphere, which is the space of the SU(2)(/U(1)) R-symmetry, and treat them as independent, which can be accomplished by Wick rotation. Due to the change in topology from compact to non-compact, the standard equations of motion and gauge conditions of the harmonic formalism, which involve only the (SU(2)- and gauge-)covariant $\bar{y}$ derivatives, no longer put the theory on shell. We solve the equations of motion or gauge conditions for explicit $\bar{y}$ dependence of the hyperfields in terms of 'coefficients' that depend on y, and perform the $\bar{y}$ integral in the action. (Instead of gauge fixing we can also define the projective gauge field in terms of the line integral of the harmonic one across the range of $\bar{y}$.) Effectively, the theory has been reduced to its 'boundary' in $\bar{y}$, for both the hyperfields and their residual gauge invariance. This is not the true boundary of the Wick-rotated theory, but symmetry under finite SU(2) R-transformations is maintained on this one-dimensional space y. (The exception is projective actions for nonrenormalizable theories that require integration over a specific contour in their definition, such as for the tensor

multiplet, past which SU(2) can move singularities. Such theories are SU(2) invariant under infinitesimal, but not finite transformations. They also do not have SU(2) covariant forms in the harmonic formalism.) This Wick rotation also accounts for the modified definition of charge conjugation used in such spaces [26]. The remaining coordinate can consistently be treated as real, even though the SU(2) transformations are complex, by treating them as being on the fields, rather than on the coordinates, since the fields that appear in the Laurent expansion in y are complex (but may be subject to reality conditions based on charge conjugation consistent with SU(2)).

Previously [27], the equivalent was accomplished by replacing regular functions on the sphere with singular functions there in the harmonic formalism (or by taking a singular limit of regular functions), which allowed projective multiplets to be obtained after minor modifications, but altered the harmonic interpretation. Here we do not modify the definition of the harmonic fields or action; the singularities of the projective fields in y follow directly from the regular harmonic expansion of the harmonic fields.

We also give further analysis of hypergraphs in the 2 formulations, and evaluate the 1-scalar-hypermultiplet-loop divergence with an arbitrary number of external (nonabelian) vector-multiplet lines. In particular, we give for the first time the complete projective action for nonabelian $\mathcal{N} = 2$ super Yang-Mills (SYM), which could be guessed from the similar harmonic action, particularly by noting its coupling with the scalar hypermultiplet. However, we go a step further and derive even the harmonic action for SYM from a Chern-Simons (CS) action which can be written in 'full' hyperspace ($d^4x\, d^8\theta$) supplemented by the internal SU(2) space (d^3y). Since the CS action doesn't know about the geometry of the space, we can choose a 'different' internal space as long as integration over this space can be consistently defined. Thus, choosing a space with a boundary (amounts to a suitable Wick-rotation of SU(2)) is desirable as the (local) CS action can then be 'reduced' to the (non-local) SYM action of the harmonic hyperspace on this boundary. This also means that the sphere is not the only possibility for the harmonic internal space and other spaces can be chosen as we will see later, which facilitate further reduction to projective hyperspace.

2.1 R-symmetry Coordinates

We begin with some conventions, and our definition for evaluation of the simple $\bar{y}$ integrals that convert harmonic hyperfields to projective ones. We will ignore questions of representation with respect to the usual superspace coordinates until later, and focus mostly on just R-space. We begin with a conventional

parametrization of an element of SU(2) as

$$g = \begin{pmatrix} e^{i\varphi/2} & 0 \\ 0 & e^{-i\varphi/2} \end{pmatrix} \frac{1}{\sqrt{1+y\bar{y}}} \begin{pmatrix} 1 & -\bar{y} \\ y & 1 \end{pmatrix} \equiv \begin{pmatrix} \bar{u} \\ u \end{pmatrix}, \tag{2.1.1}$$

where the angle φ parametrizes the element of U(1) factored out to leave the projective complex conjugate coordinates y and $\bar{y}$ of the sphere. The currents $g^{-1}dg$ and $(dg)g^{-1}$ then define the dual SU(2) generators G and covariant derivatives d, respectively, as usual:

$$G_0 = y\partial_y - \bar{y}\partial_{\bar{y}} - i\partial_\varphi \tag{2.1.2}$$
$$G_y = \partial_y + \bar{y}^2\partial_{\bar{y}} + i\bar{y}\partial_\varphi \tag{2.1.3}$$
$$G_{\bar{y}} = y^2\partial_y + \partial_{\bar{y}} - iy\partial_\varphi \tag{2.1.4}$$
$$d_0 = -i\partial_\varphi \tag{2.1.5}$$
$$d_y = e^{i\varphi}\left[(1+y\bar{y})\partial_y - i\bar{y}\partial_\varphi\right] \tag{2.1.6}$$
$$d_{\bar{y}} = e^{-i\varphi}\left[(1+y\bar{y})\partial_{\bar{y}} + iy\partial_\varphi\right]. \tag{2.1.7}$$

We then make the change of variables

$$\bar{y} \;\to\; t = \frac{1}{1+y\bar{y}}\,.$$

The convenience can be seen from the change of (Haar) measure for the coset (sphere):

$$\frac{1}{2\pi i}\int \frac{dyd\bar{y}}{(1+y\bar{y})^2} \;\to\; \frac{1}{2\pi i}\int \frac{dy}{y}\int_0^1 dt\,,$$

normalized so that the integral of 1 is 1. (We will suppress the factor $\frac{1}{2\pi i}$ in integrals from now on.)

At this point we are already effectively treating y and $\bar{y}$ (now t) as Wick rotated coordinates, so they can be integrated independently. (This corresponds to independent deformations of contours of integration of the 2 real coordinates of the sphere.) The triviality of the measure for t implies that covariant differential equations in that coordinate will also be. The range of t follows from the positivity of $y\bar{y}$ on the sphere; we'll keep this restriction after Wick rotation to reproduce the usual projective hyperspace formalism. (Although extending the range to the boundary of the Wick-rotated space at $t = \infty$ should lead to the usual holography, we have not been able to derive a corresponding hyperspace formalism.) The y integral will then be interpreted as a (closed) contour integral. (Reality conditions will be discussed below.)

Another useful change of variables is

$$e^{-i\varphi} \to e^{-i\phi} = e^{-i\phi}t \Rightarrow \partial_\varphi = \partial_\phi, \tag{2.1.8}$$

so d_0 is still integer or half-integer. (A similar variable was used, with y and $\bar{y}$, in [27].) After switching from harmonic to projective hyperspace, this complex redefinition allows the complex gauge condition $\phi = 0$. Another interpretation is to replace the R-sphere with a true $\mathbb{CP}^1$: 2 complex coordinates with a complex scale invariance, allowing metrics that differ from the sphere by a Weyl scale (including flat R-space). Then $\phi = 0$ is a choice of that complex scale. So our final parametrization of the group element is

$$g = \begin{pmatrix} e^{\frac{i}{2}\phi} & 0 \\ 0 & e^{-\frac{i}{2}\phi} \end{pmatrix} \begin{pmatrix} t & -\frac{1-t}{y} \\ y & 1 \end{pmatrix}. \tag{2.1.9}$$

The symmetry generators and covariant derivatives are now

$$G_0 = y\partial_y - i\partial_\phi \tag{2.1.10}$$
$$G_y = \partial_y - \tfrac{1}{y}(1-t)\partial_t \tag{2.1.11}$$
$$G_{\bar{y}} = y^2\partial_y - y(t\partial_t + 2i\partial_\phi) \tag{2.1.12}$$
$$d_0 = -i\partial_\phi \tag{2.1.13}$$
$$d_y = e^{i\phi}\left[\partial_y - \tfrac{1}{y}(1-t)(t\partial_t + 2i\partial_\phi)\right] \tag{2.1.14}$$
$$d_{\bar{y}} = -e^{-i\phi}y\partial_t. \tag{2.1.15}$$

Determination of $\bar{y}$ dependence of hyperfields is simple, since the free field equations or gauge conditions we solve take the form $d_{\bar{y}} = 0$ or ${d_{\bar{y}}}^2 = 0$, so the harmonic hyperfield consists of 1 or 2 projective ones by simple Taylor expansion in t. Together with the determination of ϕ dependence by the isotropy constraint, which determines the eigenvalue of d_0 for the harmonic hyperfield Ψ, we find

$$d_0\Psi = n\Psi, \qquad (d_{\bar{y}})^m\Psi = 0 \qquad \Rightarrow \qquad \Psi = e^{in\phi}\sum_{j=0}^{m-1}\psi_j(y)t^j. \tag{2.1.16}$$

The analyticity properties of the projective superfields ψ_j in y then follow from the regularity of the original (off-shell) Ψ on the sphere; we'll discuss each case individually below. Since the field equations are no higher than second order in derivatives, the projective hyperfields can be associated with 'boundary values' (at $t = 0$ or 1) of the harmonic ones.

The usual charge conjugation of the projective and harmonic formalisms (with respect to just SU(2); again we ignore the generalization to the full projective hyperspace [26]) is defined by the pseudoreality of the defining representation of SU(2), as given here by the group element (with respect to just the symmetry group): Left-multiplication of g^* (where '$*$' is ordinary complex conjugation) by an antisymmetric matrix gives back the same representation. So

$$\mathcal{C}u = \bar{u} \quad \Rightarrow \quad (\mathcal{C}y)^* = -\tfrac{1}{y}, \quad (\mathcal{C}t)^* = 1 - t, \quad (\mathcal{C}e^{-\frac{i}{2}\phi})^* = ye^{-\frac{i}{2}\phi}. \tag{2.1.17}$$

Thus in projective hyperspace, which doesn't have t, C switches a projective hyperfield associated with $t = 0$ with one associated with $t = 1$. So from the above solution in terms of projective hyperfields ψ of the field equations on a harmonic hyperfield Ψ we have,

$$(\mathcal{C}\Psi)(z) = [\Psi(\mathcal{C}z)]^* \quad \Rightarrow \quad (\mathcal{C}\psi)(z) = y^{-2n}[\psi(\mathcal{C}z)]^* \tag{2.1.18}$$

(We include all coordinates in z, so C acts also on x and θ, which we haven't discussed.) Hyperfields that have integer eigenvalue of d_0 are called 'real' if they are equal to their charge conjugates (whereas half-integer ones are pseudoreal representations of SU(2)).

2.2 Fermion Representations

Representations with respect to spinor derivatives differ slightly in the two formalisms because of the (non)appearance of $\bar{y}$. Just as the covariant R-derivatives of the harmonic formalism are invariant under the global SU(2) (commute with the generators), the usual covariant spinor derivatives need to be multiplied by the group element g to replace their SU(2) transformations with those of the isotropy U(1):

$$\begin{pmatrix} d_\theta \\ d_\vartheta \end{pmatrix} = g \begin{pmatrix} d_{(1)} \\ d_{(2)} \end{pmatrix} \tag{2.2.1}$$

$$\Rightarrow \qquad d_\vartheta = e^{-\frac{i}{2}\varphi}\sqrt{t}(d_{(2)} + yd_{(1)}), \qquad d_\theta = e^{\frac{i}{2}\varphi}\sqrt{t}(d_{(1)} - \bar{y}d_{(2)}) \tag{2.2.2}$$

where d_ϑ vanishes on projective hyperfields. Here we use six-dimensional SU*(4) matrix notation for spinors (and vectors): In the 'real' representation, $d_{(1)}$ and $d_{(2)}$ are hermitian conjugates of each other up to an antisymmetric 4×4 matrix; they form the usual pseudoreal isospinor representation of the

global SU(2). Their anticommutation relations are

$$\{d_{(1)}, d_{(2)}\} = -\{d_{(2)}, d_{(1)}\} = -i\partial_x, \qquad \{d_{(1)}, d_{(1)}\} = \{d_{(2)}, d_{(2)}\} = 0, \quad (2.2.3)$$

where the sign is due to the antisymmetry of the 4×4 matrix ∂_x (6 coordinates for $d = 6$, but easily reduced to $d = 4$).

In terms of our redefined SU(2) coordinates,

$$d_\vartheta = e^{-\frac{i}{2}\phi}(d_{(2)} + y d_{(1)}), \qquad d_\theta = e^{\frac{i}{2}\phi}\left[t d_{(1)} - (1-t)\frac{1}{y} d_{(2)}\right] \quad (2.2.4)$$

Clearly d_θ needs to be redefined for the projective formalism: Fixing any value of t will preserve the spinor-derivative anticommutation relations; $t = 1$ is the choice that relates directly to the usual projective formalism, as well as giving the simplest y dependence. Similar remarks apply to d_y.

The real representation is the least useful one for the projective formalism. The representations that are more useful are obtained by supercoordinate transformations $x \to x \pm \frac{1}{2} i\vartheta\theta$:

$$d_{(1)} = \partial_\theta + i\vartheta\partial_x, \quad d_{(2)} = \partial_\vartheta \quad \text{or} \quad d_{(1)} = \partial_\theta, \quad d_{(2)} = \partial_\vartheta - i\theta\partial_x \quad (2.2.5)$$

The former leads to the 'analytic' representation in the harmonic formalism after a further redefinition involving the R-coordinates $\theta \to \theta \pm \vartheta y$. After manipulations like the above, similar (but not identical) representations can be obtained for projective hyperspace.

However, the desired representations can be both obtained and explained more directly in projective hyperspace: We first note that the (4D) hyperconformal group can be represented directly on the projective coordinates via fractional linear transformations (as for other projective spaces, such as SU(2) on $\mathbb{CP}^1$). Under this representation of the hyperconformal group, simple translations of the coordinates yield the usual x translations, half the hypersymmetries, and some of the R-symmetry. We call this the 'projective representation'. But there is another representation where it is the corresponding covariant derivatives that are just partial derivatives, instead of the generators of this subgroup of the hyperconformal group. The existence of this other representation is clear if we consider the hyperspace coordinates in terms of hyperconformal group elements. At first we ignore the isotropy group, which is generated by a subset of the covariant derivatives. Then there is a symmetry between hyperconformal generators and covariant derivatives as they are generated by left and right action on the group element. These representations can easily be switched by the coordinate transformation that replaces

the group element by its inverse:

$$g' = g_L g g_R \quad \Rightarrow \quad (g^{-1})' = g_R^{-1} g^{-1} g_L^{-1} \tag{2.2.6}$$

$$g \to g^{-1} \quad \Rightarrow \quad g_L \to g_R^{-1}, \quad g_R \to g_L^{-1} \tag{2.2.7}$$

In practice, it's more convenient to replace this transformation with one that can be obtained continuously from the identity, by in addition performing a sign change for all the coordinates. These 2 transformations would cancel for exponential parametrization of the group element. But for the more standard parametrization as a 'product' of exponentials, this combination just reverses the ordering of the exponential factors. In this case, it is equivalent to a hyperconformal transformation on the projective coordinates (and not ϑ) with ϑ acting as the parameter, of the form described above.

The resulting 'reflective' representation is essentially one of the twisted-chiral representations described above (with $t \to 1$). The projective representation is like the other one, but requires in addition a y-dependent hypercoordinate transformation. The net result for the covariant derivatives d and corresponding symmetry generators G of the 2 representations is

d's & G's	Projective (Й)	Reflective (Я)
d_x	∂_x	∂_x
d_θ	$\partial_\theta + i\vartheta\partial_x$	∂_θ
d_y	$\partial_y - \vartheta\partial_\theta - i\frac{1}{2}\vartheta\vartheta\partial_x$	∂_y
d_ϑ	∂_ϑ	$\partial_\vartheta + y\partial_\theta - i\theta\partial_x$
G_x	∂_x	∂_x
G_θ	∂_θ	$\partial_\theta - i\vartheta\partial_x$
G_y	∂_y	$\partial_y + \vartheta\partial_\theta - i\frac{1}{2}\vartheta\vartheta\partial_x$
G_ϑ	$\partial_\vartheta - y\partial_\theta + i\theta\partial_x$	∂_ϑ

Table 2.1: Covariant derivatives and symmetry generators in two different representations.

The advantages of the projective representation are that projective hyperfields depend on just the projective coordinates, hyperconformal transformations are simpler, and scattering amplitudes are simpler because their hyperspace form (as derived, e.g., from hypertwistors) contains explicit hypersymmetry conservation δ-functions $\delta\left(\sum G_\theta\right)$ for $G_\theta = \partial_\theta$. The advantage of the reflective representation is that the y-nonlocal action for $\mathcal{N} = 2$ SYM (see below) can be written simply. (The same is true for gauge-covariant derivatives, written in a similar form.) The corresponding expressions in the projective representation are more complicated, because the y-dependent transformation

from a real (or reflective) representation to the projective one (which isn't needed from real to reflective) is different at each y. This is related to the fact that such actions have explicit ϑ-dependence. However, it is possible to perform the ϑ integration; the result contains derivatives in a form that is not manifestly covariant. (By analogy, consider an $\mathcal{N} = 1$ action of the form $\int d^4\theta \mathcal{L}(\Phi, d_\alpha \Phi)$ depending only on the chiral Φ and not antichiral $\bar{\Phi}$.)

2.3 Scalar Hypermultiplet

Our general procedure for deriving projective actions from harmonic ones is to solve the field equation (for scalar multiplets) or the gauge condition (for the vector multiplet), both of which involve t-derivatives, and plug the solution back into the action. (For application of this idea to nonlinear sigma models, refer to D. Butter [28].)

For scalar multiplets the procedure is similar to the JWKB approximation in the path-integral formalism: The 'classical' contribution is given by substituting the solutions of the equations of motion in terms of the boundary values (at 'initial' and 'final' times). In our case, these boundary values of the harmonic hyperfields at $t = 0$ and 1 are the projective hyperfields.

There are two versions of the scalar hypermultiplet in harmonic hyperspace, but both reduce to the same one in projective hyperspace. The one that's easier to treat is also the one that appears for the usual Faddeev-Popov ghosts: Its free Lagrangian is

$$\mathcal{L}_1 = \tfrac{1}{2}(d_{\bar{y}}\omega)^2, \qquad d_0\omega = 0, \qquad \mathcal{C}\omega = \omega. \tag{2.3.1}$$

As described in the previous section, the solution to its field equation is

$$\omega = \omega_0(y) + t\omega_1(y) \quad \Rightarrow \quad d_{\bar{y}}\omega = -e^{-i\phi} y \omega_1(y). \tag{2.3.2}$$

In terms of the boundary values,

$$\omega_i(y) = \omega|_{t=0} = \omega_0, \quad \omega_f(y) = \omega|_{t=1} = \omega_0 + \omega_1 \tag{2.3.3}$$

$$\Rightarrow \omega = (1-t)\omega_i + t\omega_f, \tag{2.3.4}$$

we find the reality condition $\omega_f(y) = (\omega_i)^\dagger \left(-\frac{1}{y}\right)$.

Regular functions on the sphere can be expanded in terms of spherical harmonics, or equivalently in terms of U(1)-invariant products of the SU(2) group element. In the present case (integer isospin), these can be obtained

from symmetrized products of those for isospin 1, namely

$$\frac{(y,\bar{y},1-y\bar{y})}{1+y\bar{y}} = \left(ty, \frac{1-t}{y}, 2t-1\right) = \begin{cases} (0,\frac{1}{y},-1) & \text{for } t=0 \\ (y,0,1) & \text{for } t=1 \end{cases} \tag{2.3.5}$$

So such harmonic fields will have only nonpositive powers of y at $t=0$ (ω_i), and only nonnegative powers at $t=1$ (ω_f). This is just the usual definition of the scalar multiplet Υ in projective hyperspace, regular at $y=0$, so we identify $\Upsilon = \omega_f, \quad \bar{\Upsilon} \equiv (\Upsilon)^\dagger(-\frac{1}{y}) = \omega_i$.

The projective Lagrangian is then the usual

$$\int_0^1 dt\, \mathcal{L}_1 = -e^{-2i\phi}y^2 \left(\int_0^1 dt\right) \bar{\Upsilon}\Upsilon = -e^{-2i\phi}y^2 \bar{\Upsilon}\Upsilon. \tag{2.3.6}$$

The fermionic coordinates cancel the ϕ dependence. The $\frac{1}{y}$ in the harmonic measure reduces the y^2 factor to y, a weight factor for charge conjugation [26], as the Lagrangian is a hyperconformal density in projective hyperspace. We have dropped the Υ^2 and $\bar{\Upsilon}^2$ terms, which vanish after y (and θ) integration from lack of $\frac{1}{y}$ poles.

The other version of the free scalar hypermultiplet is described by the Lagrangian

$$\mathcal{L}_2 = \bar{q} d_{\bar{y}} q, \quad d_0 q = -\tfrac{1}{2} q, \tag{2.3.7}$$

(where $\bar{q} = \mathcal{C}q$). The solution to its field equation is [27]

$$q = e^{-\frac{i}{2}\phi} q_0(y), \quad \bar{q} = e^{-\frac{i}{2}\phi} y (q_0)^\dagger \left(-\frac{1}{y}\right) \equiv e^{-\frac{i}{2}\phi} y \bar{q}_0(y). \tag{2.3.8}$$

The Lagrangian would then seem to vanish, but we know from path integrals for fermions in quantum mechanics that a more careful, discretized-'time' analysis can lead to nonvanishing results, depending on the boundary conditions. In particular, for a first-quantized Lagrangian of the form $\bar{\Psi}\dot{\Psi}$, time independence of Ψ and $\bar{\Psi}$ by the equations of motion implies that the propagator gives just the inner product, *i.e.*, the same result as $t_f = t_i$. So, if the boundary conditions are chosen so that the initial wave function depends on $\bar{\Psi}$ while the final depends on the canonical conjugate Ψ, the 'classical' action found from the JWKB expansion is just $\bar{\Psi}_i \Psi_f$, whose exponentiation gives the 'plane wave' inner product. Effectively, the result is the same as dropping the derivative, as for a 'boundary term' that might result on integration by parts.

In this case, this leads to the result

$$\int_0^1 dt\, \mathcal{L}_2 = \bar{q}[-e^{-i\phi}y]q = -e^{-2i\phi}y^2\bar{q}_0 q_0, \tag{2.3.9}$$

which is again the projective scalar hypermultiplet action, identifying $\Upsilon = q_0$. The regularity of Υ at $y = 0$ follows from associating q_0 with the original q at $t = 1$, and $\bar{q}_0$ with $t = 0$. (4D massive scalar hypermultiplets are found from 6D massless by dimensional reduction as will be detailed in next chapter.)

2.4 Vector (Yang-Mills) Hypermultiplet

Unlike the scalar hypermultiplets, the reduction of the vector hypermultiplet follows from applying the gauge condition, rather than the field equation. Solving the gauge condition is equivalent to (but more convenient than) working directly in terms of gauge-invariant variables. The residual gauge invariance (in either method) is that of the projective formalism: The gauge condition trivializes $\bar{y}$ dependence in both the gauge field and the gauge parameters.

Again from the above analysis, solving the usual gauge condition gives [27]

$$d_{\bar{y}}A_{\bar{y}} = 0, \quad d_0 A_{\bar{y}} = -A_{\bar{y}} \quad \Rightarrow \quad A_{\bar{y}} = -ie^{-i\phi}yV(y) \tag{2.4.1}$$

where we have defined $A_{\bar{y},0} = yV$ by analogy with $d_{\bar{y}}$. (V is Hermitian with respect to C.) In the Abelian case, using the covariant current

$$J^{\bar{y}} = d\bar{y}\, e^{i\phi}t^2 = dt\, e^{i\phi}\tfrac{1}{y}$$

(from $(dg)g^{-1}$), where $J^{\bar{y}}d_{\bar{y}} = d\bar{y}\partial_{\bar{y}} = dt\partial_t$, to define the covariant line integral

$$\text{Abelian}: \quad V \equiv i\int_0^1 J^{\bar{y}}A_{\bar{y}} = \int_0^1 dt\, V = V \tag{2.4.2}$$

we see the gauge-independent definition of V is consistent with the above gauge condition. For the nonabelian case, we instead define the (complexified) group element

$$e^V \equiv \mathcal{P}\left[e^{i\int_0^1 J^{\bar{y}}A_{\bar{y}}}\right], \tag{2.4.3}$$

again consistent with the above gauge. (C gives an extra sign change from switching $t \leftrightarrow 1-t$, so hermitian conjugation with C gives 2 canceling path reversals.)

The regularity of $A_{\bar{y}}$ (in arbitrary gauges) tells us it has the above type of singularities in y at $t = 0$ or 1. Thus, V must have singularities at both

$y = 0$ and ∞, as in the usual projective formalism. Furthermore, examining the abelian gauge transformation applied to the gauge-independent definition of V as a line integral

$$\text{Abelian:} \quad \delta A_{\bar{y}} = -d_{\bar{y}} K, \quad d_0 K = 0 \quad \Rightarrow \quad -i\delta V = K|_{t=0}^{1}, \tag{2.4.4}$$

and using the correspondence between the scalar multiplet ω and gauge parameter K in harmonic hyperspace on the one hand, and the scalar multiplet Υ and gauge parameter Λ in projective hyperspace on the other hand (except for different conformal weights), we recognize the usual Abelian projective gauge transformation

$$\text{Abelian:} \quad \delta V = i\left(\Lambda - \bar{\Lambda}\right); \qquad \Lambda = K|_{t=1}, \quad \bar{\Lambda} = K|_{t=0}. \tag{2.4.5}$$

Because of the path ordering in the gauge-independent definition, this can be seen to generalize directly to the nonabelian case as

$$e^{V'} = e^{-i\bar{\Lambda}} e^{V} e^{i\Lambda}. \tag{2.4.6}$$

2.4.1 Coupling to Scalar

Before looking at the action, we examine the coupling to matter. In the above gauge, even in the nonabelian case, the $\bar{y}$ covariant derivative can be written as

$$\mathcal{D}_{\bar{y}} = d_{\bar{y}} + iA_{\bar{y}} = e^{tV} d_{\bar{y}} e^{-tV}$$

This modifies the solution to the matter field equations: e.g.,

$$\omega = e^{tV}(\omega_0 + t\omega_1) \quad \Rightarrow \quad \omega_i = \omega_0, \quad \omega_f = e^{V}(\omega_0 + \omega_1) \tag{2.4.7}$$

$$\Rightarrow \quad \omega = e^{tV}(1-t)\omega_i + e^{-(1-t)V} t\omega_f \tag{2.4.8}$$

$$\Rightarrow \quad d_{\bar{y}}\omega = -e^{-i\phi} e^{tV} y\omega_1 = e^{-i\phi} y(e^{tV}\omega_i - e^{-(1-t)V}\omega_f) \tag{2.4.9}$$

Since ω must be a real representation of the Yang-Mills group, the group generators are antisymmetric, so

$$\mathcal{L}_1 = \tfrac{1}{2}(d_{\bar{y}}\omega)^T d_{\bar{y}}\omega = -e^{-2i\phi} y^2 \omega_f e^{V} \omega_i \tag{2.4.10}$$

again after dropping non-cross terms, whose V dependence cancels, and so vanish after integration as before. The result is the usual modification by e^V, which restores gauge invariance. If we write e^V as a gauge-covariant path-ordered exponential of the integral of $A_{\bar{y}}$, we recognize this modification as

gauge-covariant point splitting in t. Similarly, for the other multiplet we have

$$q = e^{-\frac{i}{2}\phi} e^{tV} q_0, \qquad \bar{q} = e^{-\frac{i}{2}\phi} y \bar{q}_0 e^{(1-t)V} \tag{2.4.11}$$

yielding the same result [27].

The nonabelian gauge transformation of V can be derived from the above expression for that of e^V. An alternate method is to solve for the residual gauge invariance in the above gauge. This is equivalent to solving the equations of motion for the Faddeev-Popov ghosts. The equation to solve is

$$0 = \delta(d_{\bar{y}} A_{\bar{y}}) = -d_{\bar{y}}[\mathcal{D}_{\bar{y}}, K]$$

Plugging in the above expression for $A_{\bar{y}}$ in this gauge yields

$$\partial_t e^{tV} \partial_t e^{-tV} K = 0$$

where we now write K as a column vector (so V is in the adjoint representation) for convenience. The solution, in notation analogous to that for ω above, is

$$K = e^{tV} K_0 + \frac{1}{V}(e^{tV} - 1) K_1 = \frac{1}{e^V - 1} \left[(e^V - e^{tV}) K_i + (e^{tV} - 1) K_f \right] \tag{2.4.12}$$

(Upon Taylor expansion, there are no inverse powers of V.) The transformation law is then

$$\delta V = -\tfrac{i}{2} V \left[\left(\bar{\Lambda} + \Lambda \right) + \coth\left(\tfrac{1}{2} V \right) \left(\bar{\Lambda} - \Lambda \right) \right] \tag{2.4.13}$$

in analogy to the $\mathcal{N} = 1$ result.

In an arbitrary gauge, we have

$$\mathcal{D}_{\bar{y}} = \mathcal{P} \left[e^{i \int_0^t J^{\bar{y}} A_{\bar{y}}} \right] d_{\bar{y}} \mathcal{P} \left[e^{i \int_t^0 J^{\bar{y}} A_{\bar{y}}} \right] \tag{2.4.14}$$

if we assume the boundary condition $A_{\bar{y}}|_{t=0} = 0$. (This might also be an asymptotic gauge condition, but it seems reasonable as a boundary condition since $d_{\bar{y}}$ has a factor of $\frac{1}{t}$ multiplying $\partial_{\bar{y}}$.) This uses the explicit gauge transformation for going to the gauge $A_{\bar{y}} = 0$. Repeating the above manipulations then produces the same results but in terms of the gauge-covariant definition of V given above. This construction is reminiscent of the construction for $\mathcal{N} = 1$, where $e^V = e^{\Omega} e^{\bar{\Omega}}$, with $\bar{\Omega}$ corresponding to the $\int_0^t$ piece and Ω to the $\int_t^1$. This allows transformations to different gauge representations where the covariant derivatives transform with only one of $K \equiv K(t)$, $\Lambda \equiv K(1)$, or $\bar{\Lambda} \equiv K(0)$.

2.5 Hypergraphs

A few $\mathcal{N}=2$ supergraphs have been evaluated in both approaches. The rules and tricks were similar, due to the fact that the harmonic formalism [29,30] differs from the projective one [31–34] only by the appearance of additional auxiliary multiplets, coming from extra $\bar{y}$ (or t) dependence. We summarize these rules here in our notation. Those that are (almost) the same are (in real/reflective representations, or those that differ by only y-independent coordinate transformations):

$$\text{scalar multiplet propagator: } \frac{d^4_{1\vartheta} d^4_{2\vartheta}}{y_{12}^3} \frac{\delta^8(\theta_{12})}{p^2}$$

$$\text{vector multiplet propagator: } d^4_\vartheta \delta(y_{12}) \frac{\delta^8(\theta_{12})}{p^2} \quad \text{(Fermi-Feynman gauge)}$$

$$\text{scalar multiplet vertex: } \int d^4\theta dy, \quad \text{but use } \int d^4\theta d^4_\vartheta = \int d^8\theta$$

$$\text{vector multiplet (only) vertex: } \int d^8\theta dy_1 ... dy_n \frac{1}{y_{12} y_{23} ... y_{n1}}$$

where $\theta_{12} \equiv \theta_1 - \theta_2$, etc. (The rules above are for the q scalar multiplet in the harmonic formalism, which is simpler, and more similar to the projective case.) There are also the identities common to both:

$$d_{2\vartheta} d^4_{1\vartheta} = y_{21} d_{1\theta} d^4_{1\vartheta} \quad \Rightarrow \quad \delta^8(\theta_{12}) d^4_{2\vartheta} d^4_{1\vartheta} \delta^8(\theta_{12}) = y^4_{12} \delta^8(\theta_{12}) \,. \tag{2.5.1}$$

The former is used when integrating a spinor derivative by parts from one propagator across a vertex to an adjacent propagator; alternatively, the latter can be used when only 4 such derivatives are moved in the last step of θ integration.

The differences in the above expressions in the two formalisms are the number of R-coordinates and the $i\epsilon$ prescription:

Def.	Harmonic	Projective
'$\int dy$'	$\int \frac{dy\, d\bar{y}}{2\pi i (1+y\bar{y})^2}$	$\oint \frac{dy}{2\pi i}$
'$\delta(y_{12})$'	$2\pi i \,(1+y\bar{y})^2 \delta(y_{12}) \delta(\bar{y}_{12})$	$2\pi i \, \delta(y_{12})$
'$\frac{1}{y_{12}}$'	$\frac{1}{y_{12} + \frac{\epsilon}{\bar{y}_{12}}}$	$\frac{1}{y_{12} + \epsilon(y_1+y_2)}$

Table 2.2: Differences between harmonic and projective hyperspaces.

In manipulations involving integrating '$\frac{1}{y}$' to make results more R-local, in the harmonic formalism one needs various identities that generate $\bar{y}$ derivatives

to apply

$$\partial_{\bar{y}} \frac{1}{y + \frac{\epsilon}{\bar{y}}} = \pi \delta^2(y), \tag{2.5.2}$$

which is easy to integrate. On the other hand, in the projective formalism one just immediately evaluates standard contour integrals. There is also an ordering for the projective formalism: $\frac{1}{y_{12}+\epsilon(y_1+y_2)}$, for y_1 and y_2 on the same contour, is for $\langle \Upsilon(1)\bar{\Upsilon}(2)\rangle$. This means that effectively one integrates with the y_2 contour enclosing y_1 (and 0), or the y_1 contour inside y_2 (and ∞). For example, for contours counterclockwise around the origin, we have

$$\frac{1}{y_{12} + \epsilon(y_1 + y_2)} + \frac{1}{y_{21} + \epsilon(y_1 + y_2)} = 2\pi i\, \delta(y_{12}). \tag{2.5.3}$$

Another source of differences is the relation of the spinor derivatives in the 2 approaches: We have seen that the projective ones follow from the harmonic ones effectively by setting $t = 1$. (We also gauge $\phi = 0$ in both cases.) So for the harmonic relations

$$\{d_{1\vartheta}, d_{2\vartheta}\} = -iu_1 \cdot u_2 \partial_x, \tag{2.5.4}$$
$$\{d_{1\theta}, d_{2\vartheta}\} = -i\bar{u}_1 \cdot u_2 \partial_x, \tag{2.5.5}$$
$$\{d_{1\theta}, d_{2\theta}\} = -i\bar{u}_1 \cdot \bar{u}_2 \partial_x \tag{2.5.6}$$

we have in general

$$u_1 \cdot u_2 = y_{12}, \quad \bar{u}_1 \cdot u_2 = t_1 + (1 - t_1)\tfrac{y_2}{y_1}, \quad \bar{u}_1 \cdot \bar{u}_2 = t_2(1 - t_1)\tfrac{1}{y_1} - t_1(1 - t_2)\tfrac{1}{y_2} \tag{2.5.7}$$

but only for the projective case do the latter 2 simplify:

$$u_1 \cdot u_2 = y_{12}, \qquad \bar{u}_1 \cdot u_2 = 1, \qquad \bar{u}_1 \cdot \bar{u}_2 = 0 \qquad \text{(projective)} \tag{2.5.8}$$
$$\Rightarrow \{d_{1\vartheta}, d_{2\vartheta}\} = -iy_{12}\partial_x, \quad \{d_{1\theta}, d_{2\vartheta}\} = -i\partial_x, \quad \{d_{1\theta}, d_{2\theta}\} = 0. \tag{2.5.9}$$

Moving spinor derivatives from propagators around loops requires evaluating expressions of the form

$$d_{i\vartheta} ... d_{j\vartheta} d^4_{1\vartheta}$$

which results in repeated use of the above anticommutators, so the harmonic formalism also has these t-dependent factors to deal with. (The example above that gave the same result in the 2 approaches needed only $u_1 \cdot u_2$.) However, one should be able in general to use $d_{(1)}$ in place of d_θ in the harmonic approach to mimic the projective and get the same simplifications, since only d_ϑ appears in the Feynman rules.

There is also some Legendre transformation involved in the 'duality', which accounts for the minor differences in the action, such as coupling to $iA_{\bar{y}}$ vs. $e^V - 1$ (subtracting out the '1' for the kinetic term). Also, the rules for the ω multiplet (and the ghosts) are a little more complicated than the q multiplet for the harmonic formalism. (For the most part, the extra $d_{\bar{y}}$ in the vertex converts the ω propagator into a q propagator.)

The bottom line is that although the final results in the two approaches are almost the same (to the same extent as the Feynman rules), the harmonic formalism requires some extra algebra (for R-space).

2.6 Yang-Mills Action in Harmonic Hyperspace

The action for nonabelian Yang-Mills multiplet in the harmonic case was written as an infinite series expansion in terms of the prepotential. This action turned out to be non-local in the internal R-coordinates. Even though the origin of the Abelian action could be understood via the action written in chiral hyperspace, the nonabelian action did not have such a direct origin. Its origin was explained by Zupnik in [19] where the 'series' action was summed to a logarithm of a pseudo-differential operator.

We now review the construction of SYM action in harmonic hyperspace. The following constraints define the SYM in harmonic hyperspace:

$$\{\mathcal{D}_\vartheta, \mathcal{D}_\vartheta\} = \{\mathcal{D}_\vartheta, \bar{\mathcal{D}}_\vartheta\} = \{\bar{\mathcal{D}}_\vartheta, \bar{\mathcal{D}}_\vartheta\} = 0 \tag{2.6.1}$$

$$[\mathcal{D}_+, \mathcal{D}_\vartheta\left(\bar{\mathcal{D}}_\vartheta\right)] = \mathcal{D}_\theta\left(\bar{\mathcal{D}}_\theta\right) \tag{2.6.2}$$

$$[\mathcal{D}_+, \mathcal{D}_\theta\left(\bar{\mathcal{D}}_\theta\right)] = 0 \tag{2.6.3}$$

$$[\mathcal{D}_-, \mathcal{D}_\vartheta\left(\bar{\mathcal{D}}_\vartheta\right)] = 0 \tag{2.6.4}$$

$$[\mathcal{D}_-, \mathcal{D}_\theta\left(\bar{\mathcal{D}}_\theta\right)] = \mathcal{D}_\vartheta\left(\bar{\mathcal{D}}_\vartheta\right) \tag{2.6.5}$$

$$[\mathcal{D}_0, \mathcal{D}_\vartheta\left(\bar{\mathcal{D}}_\vartheta\right)] = -\mathcal{D}_\vartheta\left(\bar{\mathcal{D}}_\vartheta\right) \tag{2.6.6}$$

$$[\mathcal{D}_0, \mathcal{D}_\theta\left(\bar{\mathcal{D}}_\theta\right)] = \mathcal{D}_\theta\left(\bar{\mathcal{D}}_\theta\right) \tag{2.6.7}$$

$$[\mathcal{D}_-, \mathcal{D}_+] = 2\mathcal{D}_0 \tag{2.6.8}$$

$$[\mathcal{D}_0, \mathcal{D}_\pm] = \pm\mathcal{D}_\pm \tag{2.6.9}$$

where $\mathcal{D}$'s are gauge covariant derivatives: $\mathcal{D} = d + iA$. We use here $(+, -, 0)$ as an alternate notation for $(y, \bar{y}, \phi)$. The coordinate denoted by '0' corresponds to U(1) in the coset SU(2)/U(1) due to which the corresponding derivative is not covariantized, *i.e.*, $A_0 = 0$. The above constraints are then solved in the following way to get the SYM action:

1. Choose the gauge (λ-frame): $A_\vartheta = \bar{A}_\vartheta = 0$.

2. A_- becomes a harmonic hyperfield due to equation (2.6.4). It is also the 'prepotential'.

3. Then (2.6.2) just gives $A_\theta = -d_\vartheta A_+$.

4. A_+ is solved as a series in terms of A_- from equation (2.6.8):

$$A_+ = \sum_{n=1}^{\infty} \left(\prod_{i=1}^{n} \int d^2 y_i \right) \frac{A_{1-} \dots A_{n-}}{(y - y_1) y_{12} \dots (y_n - y)}. \tag{2.6.10}$$

   where d^2y is the volume element of S^2, $A_{i-} \equiv A_-(x, \theta, \vartheta, y_i)$ and $y_{12} = (y_1 - y_2)$ with a relevant $\epsilon-$prescription defined later.

5. The Abelian action is written as $A_- A_+$ (derived from the chiral version) which is generalized in the nonabelian case to a series with an extra factor of $\frac{1}{n}$:

$$\mathcal{S}_{\text{♫}} = -\frac{\text{tr}}{2g^2} \int dx\, d^8\theta \sum_{n=2}^{\infty} \frac{(-i)^n}{n} \left(\prod_{i=1}^{n} \int d^2 y_i \right) \frac{A_{1-} A_{2-} \dots A_{n-}}{y_{12}\, y_{23} \dots y_{n1}}. \tag{2.6.11}$$

2.7 Chern-Simons Action

We now work with 'curved' SU(2) derivatives, $\partial_m (m = 1, 2, 3)$ instead of the 'flat' ones, $d_a (a = +, -, 0)$ used above:

$$\begin{aligned} d_a &= e_a{}^m \partial_m \\ [d_a, d_b] &= f_{ab}{}^c d_c \to [\partial_m, \partial_n] = 0 \end{aligned} \tag{2.7.1}$$

where $f_{ab}{}^c$'s are the SU(2) structure constants (can be read from equations (2.6.8) & (2.6.9)) and we require that $e_a{}^m$ is a dreibein satisfying

$$e_-{}^1 = e_-{}^3 = 0. \tag{2.7.2}$$

Introducing gauge covariant derivatives $\partial_m \to \nabla_m = \partial_m + iA_m$ in equation (2.7.1), we get:

$$[\nabla_m, \nabla_n] = F_{mn} = 0 \tag{2.7.3}$$

Let us now check how the spinorial covariant derivatives act on the 'curved' SU(2) connections (conjugate derivatives give similar results):

$$[\mathcal{D}_a, \mathcal{D}_\vartheta] = f_{a\vartheta}{}^\eta \mathcal{D}_\eta \to [\nabla_m, \mathcal{D}_\vartheta] = e_m{}^a f_{a\vartheta}{}^\eta \mathcal{D}_\eta \tag{2.7.4}$$

$$\Rightarrow d_\vartheta A_2 = 0 \tag{2.7.5}$$

where the non-zero constants are: $f_{0\theta}{}^{\theta} = -f_{0\vartheta}{}^{\vartheta} = f_{+\vartheta}{}^{\theta} = f_{-\theta}{}^{\vartheta} = 1$ (read from eqs. (2.6.4)−(2.6.7)), which imply A_2 is a harmonic hyperfield. This result is valid in general due to the condition in equation (2.7.2).

Finally, the constraints in equation (2.7.3) can be derived as equations of motion from a CS action:

$$\mathcal{S}_3 = \frac{\mathrm{tr}}{2g^2}\int dx\, d^8\theta\, d^3y\, \epsilon^{mnp}\left[\frac{1}{2}A_m\partial_n A_p + \frac{1}{3}A_m A_n A_p\right]. \tag{2.7.6}$$

This action is reminiscent of the $\mathcal{N}=3$ SYM action in harmonic superspace [35]. An important difference is that while in the case of $\mathcal{N}=3$ all the A's are 'harmonic', only one of them is in $\mathcal{N}=2$ SYM and the above action has 'full' hyperspace measure with 8 Fermionic coordinates whereas the $\mathcal{N}=3$ SYM action has only harmonic superspace measure also with 8 θ's instead of all the twelve. Also, the y-integration in (2.7.6) is over three real coordinates corresponding to SU(2)=S^3 (or its Wick-rotated versions) whereas for $\mathcal{N}=3$ SYM, the integration is over three complex coordinates corresponding to the coset $SU(3)/U(1)^2$.

2.8 Reduction from CS Action to Harmonic

As mentioned in the introduction, we are not restricted to use the compact SU(2) manifold as the internal 3-manifold for the CS action since the geometry does not affect it. Hence, we can choose the internal 3-manifold for the CS action to have a boundary at $y^3 = 0$, which basically amounts to a 'Wick-rotation' of SU(2) to SU(1,1). We do not put any boundary conditions on A at this boundary due to which the variation of action (2.7.6) reads:

$$\delta\mathcal{S}_3 = \frac{\mathrm{tr}}{4g^2}\int dx\, d^8\theta\, d^3y\, \epsilon^{mnp}\left[2\partial A_m F_{np} - \partial_m\left(A_n\partial A_p\right)\right]. \tag{2.8.1}$$

The first term gives the usual equations of motion and the second (boundary) term breaks gauge invariance in general[1]. Ignoring this subtlety, we can rewrite the action (2.7.6) as:

$$\mathcal{S}_3 = \frac{\mathrm{tr}}{4g^2}\int dx\, d^8\theta\, d^3y\, \epsilon^{ij}\left[2F_{ij}A_3 - A_i\partial_3 A_j - \partial_i\left(A_j A_3\right)\right], \tag{2.8.2}$$

[1]The action can be made gauge invariant by imposing suitable boundary conditions on A or by adding additional boundary degrees of freedom as shown in [36–38]. The gauge invariance can also be retained if we allow the gauge parameter to vanish at the boundary, but we do not do that.

where $i = 1, 2$. The total derivative term vanishes as there are no boundaries along y^i. Here, A_3 acts as a Lagrange multiplier and being an unconstrained hyperfield imposes the constraint $F_{12} = 0$, whose solution can be substituted back to get a simplified action[2]. In other words, we substitute the solution of the equation of motion of A_3 so that the action has only harmonic hyperfields:

$$F_{12} = \partial_1 A_2 - \partial_2 A_1 + i[A_1, A_2] = 0 \quad \& \quad A_1 = \sum_n A_1^{(n)} \tag{2.8.3}$$

$$\begin{aligned}
\Rightarrow A_1^{(1)}(y) &= \partial_1 \int d^2y' \frac{A_2'(y')}{y^1 - y^{1\prime} + \frac{\epsilon}{y^{2\prime} - y^2}} = -\int d^2y' \frac{A_2'(y')}{\left(y^1 - y^{1\prime}\right)^2}, \\
A_1^{(2)}(y) &= -i \int d^2y' d^2y'' \frac{A_2'(y') A_2''(y'')}{\left(y^1 - y^{1\prime\prime}\right)\left(y^{1\prime\prime} - y^{1\prime}\right)\left(y^{1\prime} - y^1\right)}, \quad \text{and so on...} \\
\Rightarrow A_1 &= \sum_{n=1}^{\infty} (-i)^{n+1} \int d^2y' \ldots d^2y^{(n)'} \frac{A_2' \ldots A_2^{(n)'}}{\left(y^1 - y^{1\prime}\right) \ldots \left(y^{1(n)'} - y^1\right)}
\end{aligned} \tag{2.8.4}$$

where $d^2y \equiv dy^1 dy^2$ and the $\epsilon-$term is present in all denominator factors. The following identity is used to prove that the solution in (2.8.4) indeed makes the curvature vanish (equation (2.8.3)):

$$\partial_2 \left(\frac{1}{y^{1\prime} - y^1 + \frac{\epsilon}{y^{2\prime} - y^2}} \right) \sim \delta^2(y' - y). \tag{2.8.5}$$

Plugging this solution back in action (2.8.2), we get:

$$\mathcal{S}_3 = -\frac{\mathrm{tr}}{4g^2} \int dx\, d^8\theta\, d^2y\, dy^3 \left(A_1 \partial_3 A_2 - A_2 \partial_3 A_1\right) \tag{2.8.6}$$

$$\begin{aligned}
&= -\frac{\mathrm{tr}}{2g^2} \int dx\, d^8\theta \int_0^{\infty} dy^3 \sum_{n=2}^{\infty} \frac{(-i)^n \partial_3}{n} \left(\int d^2y\, d^2y' \ldots d^2y^{(n-1)'} \times \right. \\
&\qquad \left. \times \frac{A_2\, A_2' \ldots A_2^{(n-1)'}}{\left(y^1 - y^{1\prime}\right) \ldots \left(y^{1(n-1)'} - y^1\right)} \right)
\end{aligned} \tag{2.8.7}$$

The equation (2.8.7) can be written with the factor $\frac{1}{n}$ because all A_2's depend on same y^3 (no primes). Assuming A_2 is well-behaved at $y^3 = \infty$, we can

[2]Usually, the connections A_i are chosen to be flat at this point and written as $A_i = (\partial_i U)\, U^{-1}$, which gives the well-know Wess-Zumino action.

integrate over y^3 and write a '2D' action on the boundary at $y^3 = 0$:

$$\mathcal{S}_2 = -\frac{\mathrm{tr}}{2g^2}\int dx\, d^8\theta \sum_{n=2}^{\infty}\frac{(-i)^n}{n}\int d^2y\, d^2y' \ldots d^2y^{(n-1)'}\frac{A_2\, A_2' \ldots A_2^{(n-1)'}}{(y^1-y^{1'})\ldots\left(y^{1(n-1)'}-y^1\right)} \tag{2.8.8}$$

where A_2's are evaluated at the boundary, effectively removing the y^3 dependence. Furthermore, equation (2.8.6) implies that $A_{1,2}$ do not depend on y^3 on-shell. This is the same as imposing $F_{23} = F_{31} = 0$ and $A_3 = 0$ everywhere. We can even substitute these 'remaining' equations of motion above in action (2.8.8), which completely removes the y^3-dependence of A_2's. We also note that though the CS action as we started with is not gauge invariant, the resulting harmonic action on the boundary space is gauge invariant under a familiar gauge transformation: $\delta A_2 = -\mathcal{D}_2 K$.

Finally, to connect the above construction with the usual harmonic action, we use a specific dreibein $(e_a{}^m)$ parameterizing the Wick-rotated coset SU(2)/U(1) given in Section 2.1:

$$g = \begin{pmatrix} t & y \\ \frac{t-1}{y} & 1 \end{pmatrix}\begin{pmatrix} e^{\frac{i}{2}\phi} & 0 \\ 0 & e^{-\frac{i}{2}\phi} \end{pmatrix} \tag{2.8.9}$$

$$\Rightarrow \begin{cases} d_0 = -2i\partial_\phi \\ d_+ = e^{i\phi}\left[\partial_y + \frac{1}{y}(t-1)(t\,\partial_t + 2i\partial_\phi)\right] \\ d_- = e^{-i\phi} y\,\partial_t \end{cases} \tag{2.8.10}$$

where $\bar{y} \to t = \frac{1}{1+y\bar{y}}$ and the subgroup U(1) acts on the right. We can now rewrite the above action in terms of 'flat' connections and recover the well-known harmonic SYM action:

$$\mathcal{S}_{\text{♫}} = -\frac{\mathrm{tr}}{2g^2}\int dx\, d^8\theta \sum_{n=2}^{\infty}\frac{(-i)^n}{n}\left(\prod_{k=1}^{n}\int\frac{dy_k\, dt_k}{y_k}\right)\frac{A_{1-}A_{2-}\ldots A_{n-}}{y_{12}\, y_{23}\ldots y_{n1}}. \tag{2.8.11}$$

where $y_{12} = \left(y_1 - y_2 + \frac{\epsilon}{\bar{y}_1-\bar{y}_2}\right)$ and the volume element is explicitly written in terms of 'modified' stereographic coordinates for the coset described above.

Furthermore, we could also use a different coset construction for the internal space that has a different generator as a subgroup and is a 'contraction' of

the earlier coset:

$$g = \begin{pmatrix} 1 & y \\ 0 & 1 \end{pmatrix} \begin{pmatrix} e^{\frac{\phi}{2}} & 0 \\ 0 & e^{-\frac{\phi}{2}} \end{pmatrix} \begin{pmatrix} 1 & 0 \\ \bar{y} & 1 \end{pmatrix} \tag{2.8.12}$$

$$\Rightarrow \begin{cases} d_0 = 2\partial_\phi + 2\bar{y}\partial_{\bar{y}} \\ d_+ = e^{\phi}\partial_y - \bar{y}^2\partial_{\bar{y}} - 2\bar{y}\partial_\phi \\ d_- = \partial_{\bar{y}}\,. \end{cases} \tag{2.8.13}$$

We have to exchange $y^2 \leftrightarrow y^3$ to see that the dreibein does satisfy the conditions of (2.7.2) at the boundary $y^2 = 0$ now. This gives us a 'different' harmonic hyperspace in which the SYM action reads almost the same as above (2.8.11) except that the connection A_- gets replaced with A_0 and the internal space has a different volume element. This internal 2-manifold has a degenerate metric (just $d\phi^2$) but the volume element is properly defined from the 3-manifold's volume element as $\bar{y} \to 0$ and is simply: $e^{-\phi} dy\, d\phi$.

2.9 Reduction from Harmonic to Projective

We basically have to reduce the Wick-rotated 2D harmonic y-space to 1D projective y-space. The integration over y as the usual contour integration needs to be carefully defined. We show that the choice of contour is invariant under finite SU(2) transformations and the integration can be consistently defined. For that purpose, we choose the Wick-rotated coset SU(1,1)/U(1) ($\sim$ SO(2,1)/SO(2) $\sim \mathbb{RP}^2$) as defining the 2D harmonic internal space for the rest of this section.

2.9.1 Internal Space

In stereographic coordinates, the projective plane $\mathbb{RP}^2$ has a circular boundary that is given by $y\bar{y} = 1$. It can be shown that it is invariant under the symmetry group SU(1,1) as follows: Given that $\left(\begin{smallmatrix} a & b \\ c & d \end{smallmatrix}\right) \in$ SU(1,1) and the group 'metric' is $\left(\begin{smallmatrix} 1 & 0 \\ 0 & -1 \end{smallmatrix}\right)$, the matrix entries of the group element get related: $c = \bar{b}$ & $d = \bar{a}$. Then, if $y \to \frac{ay+b}{cy+d}$, it is easy to see that $y\bar{y} = 1$ is an invariant. Thus, the usual contour integration definition over this boundary can be used for the y-coordinate, where the $\bar{y}-$coordinate takes a fixed value and is redundant:

$$\oint \frac{dy}{2\pi i} \frac{1}{y^{n+1}} = \delta_{n,0}\,. \tag{2.9.1}$$

The same procedure still works if we Wick-rotate the isotropy group SO(2)

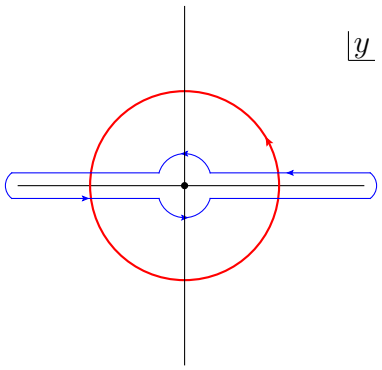

Figure 2.1: Contours in y-plane.

to SO(1,1), which is optional at the level of harmonic hyperspace but required when reducing to projective hyperspace given by the coset SO(2,1)/SO(1,1)× ISO(1). This can be achieved by 'Wick-rotating' $\bar{y} \to \frac{1}{\bar{y}}$ such that the boundary $y\bar{y} = 1$ becomes $y = \bar{y}$, which is the 'real' axis. This change basically corresponds to choosing an antisymmetric basis for the unitary 'metric', *i.e.*, $\left(\begin{smallmatrix} 0 & -i \\ i & 0 \end{smallmatrix}\right)$ (which is usually chosen for SL(2,R) group) instead of the usual diagonal one as chosen above such that the modified group element now has purely real entries and reads (modulo the U(1)≡GL(1)-factor):

$$
\begin{aligned}
g = \frac{1}{\sqrt{(1-y\bar{y})}} \begin{pmatrix} 1 & \bar{y} \\ y & 1 \end{pmatrix} \quad &\xrightarrow{WR} \quad \frac{1}{\sqrt{\left(1-\frac{y}{\bar{y}}\right)}} \begin{pmatrix} 1 & \frac{1}{\bar{y}} \\ y & 1 \end{pmatrix} \\
&\xrightarrow{CT} \frac{1}{\sqrt{-2i\bar{y}\left(1-\frac{y}{\bar{y}}\right)}} \begin{pmatrix} 1 & \frac{1}{\bar{y}} \\ y & 1 \end{pmatrix} \begin{pmatrix} 1 & i \\ \bar{y} & -i\bar{y} \end{pmatrix} \\
\Rightarrow g = \frac{1}{\sqrt{\frac{i(y-\bar{y})}{2}}} &\begin{pmatrix} 1 & 0 \\ \frac{y+\bar{y}}{2} & \frac{i(y-\bar{y})}{2} \end{pmatrix}. \qquad (2.9.2)
\end{aligned}
$$

The full transformation involves both the Wick-rotation (WR) and a coordinate transformation (CT). After this, the circular contour gets modified to a contour enclosing the 'real' axis (see Figure 2.1) and effectively, the earlier definition of the contour integral can still be used by analytic continuation[3]. This change now leads to transformation of the metric in stereographic coordinates to that in Poincaré coordinates and the corresponding volume elements

[3]If y is to be treated as a complex coordinate, then this Wick-rotation is not required.

read:

$$\frac{dy\,d\bar{y}}{(1-y\,\bar{y})^2} \xrightarrow{WR} \frac{dy\,d\bar{y}}{(y-\bar{y})^2}\,. \tag{2.9.3}$$

2.9.2 Yang-Mills Action

We now redefine $y \equiv y^1$ and $y^i = \{y^2, y^3\} \equiv \{\bar{y}\,(t), \phi\} \in [0,1]$ to set the notation for projective hyperspace. We make a 'special' Abelian gauge transformation for A_y:

$$\delta A_y = -\partial_y \left(\int_0^{y^i} dy^{i'} A_{y^i}(y, y^{i'}) \right) \equiv -\partial_y K\,, \tag{2.9.4}$$

where we assume $A_{y^i}|_{y^i=0} = 0$. This relates the harmonic connection A_y to the projective one as follows:

$$\text{♫}: \quad A_y = \partial_y \int \frac{d^2y'}{y'-y} A'_{y^i}\,; \quad \frac{1}{y'-y} = P\left(\frac{1}{y'-y}\right) + \pi i \delta(y-y')\theta(y^i - y^{i'}) \tag{2.9.5}$$

$$\check{\Pi}: \quad A_y = \mp i\,\partial_y \int \frac{dy'}{y'-y} V'\,;\; V' = \pm i \int_0^1 dy^{i'}\, A'_{y^i} \quad \text{with} \tag{2.9.6}$$

$$\frac{1}{y'-y} + \frac{1}{y-y'} = 2\pi i \delta\,(y'-y)$$

Now, we can use this transformation to write down the action for Abelian SYM in projective space characterized by a 1D y-space:

$$\mathcal{S}^{(2)}_{\check{\Pi}} = \frac{1}{2g^2} \int dx\, d^8\theta dy_1 dy_2 \frac{V_1 V_2}{y_{12}\, y_{21}} \tag{2.9.7}$$

where y_{12} is defined via equation (2.9.6) and the $\epsilon-$prescription consistent with it reads $y_{12} = y_1 - y_2 + \epsilon\,(y_1 + y_2)$. This Abelian action is invariant under the following linear gauge transformation after identifying $K|_{y^i=1} = \Lambda$ and $K|_{y^i=0} = \bar{\Lambda}$:

$$\delta V = i\left(\Lambda - \bar{\Lambda}\right). \tag{2.9.8}$$

Thus we connect back to our discussion of Section 2.4 with this explicit reduction of harmonic action using the connection A_y. The nonabelian generalization of V in (2.9.6) was already given in (2.4.3) via path-ordered exponentiation, which lifts the above abelian transformation of V to the nonabelian one given below:

$$\delta\left(e^V\right) = i\left(\Lambda\, e^V - e^V \bar{\Lambda}\right). \tag{2.9.9}$$

One main difference between harmonic and projective that we have already seen is that while in the harmonic case q couples to $iA_{\bar{y}}$, in the projective case Υ couples to $\left(e^V-1\right)$. Drawing this analogy and staring at $\mathcal{S}_{\text{♫}}$, we can write down the full nonabelian projective SYM action that generalizes (2.9.7) and is invariant under the nonabelian gauge transformation (2.9.9) as:

$$\mathcal{S}_{\check{\text{I}}\text{I}} = \frac{\text{tr}}{g^2}\int dx\, d^8\theta \sum_{n=2}^{\infty}\frac{(-1)^n}{n}\left(\prod_{k=1}^{n}\int dy_k\right)\frac{\left(e^{V_1}-1\right)\ldots\left(e^{V_n}-1\right)}{y_{12}\,y_{23}\ldots y_{n1}}. \tag{2.9.10}$$

On a concrete note, however, a way to derive this full action is from looking at the divergent part of a scalar multiplet loop in a vector background [29]. The calculation is almost the same in the two formalisms: To keep the most divergent part, keep all spinor derivatives inside the loop when integrating them by parts, and keep the ∂_x terms (vs. yd_θ^2 terms) generated by pushing d_ϑ's past d_θ's. Thus almost every d_ϑ^4 integrated by parts produces a y^2p^2. The result after performing all θ integration (except the usual final one) is that every $\frac{1}{y^3}$ is replaced by a $\frac{1}{y}$, while only two $\frac{1}{k^2}$'s remain (associated with the two d_ϑ^4's killing the next-to-last $\delta^8(\theta)$, as in the identity (2.5.1)), yielding the logarithmic divergence. This 1-loop calculation then precisely leads to the projective action (2.9.10).

There is also a 'dual' version, coming from reverse ordering of the loop, corresponding to starting with the action as $\Upsilon e^{-V}\bar{\Upsilon}$ rather than $\bar{\Upsilon}e^V\Upsilon$. The result is to everywhere change the signs on V and y. For such real representations $V^T=-V$, so transposing reproduces the above form.

The check of gauge invariance is similar to the harmonic case, but again no derivatives $d_{\bar{y}}$ are involved. We start with

$$\delta(e^V-1) = -i\left(\bar{\Lambda}-\Lambda\right) - i\left[\bar{\Lambda}(e^V-1)-(e^V-1)\Lambda\right].$$

Then, as in the harmonic case, the inhomogeneous contribution to the 'n-point' (in y) contribution to the action will cancel the linear contribution to the $(n-1)$-point. The exception is the homogeneous contribution to the 2-point, which vanishes by itself after θ integration. (However, one should not try to define each contour enclosing the previous simultaneously, implying a Penrose staircase. Keeping all contours the same is consistent with the $i\epsilon$ prescription.) The details of both the proof of action being gauge invariant and the loop calculation outlined above leading to the action itself are given in the next chapter.

2.10 Discussion

Our explicit construction of the relation between the projective and harmonic formalisms shows that in the appropriate notation the two are almost the same, sharing similar (dis)advantages. The only significant difference is the extra R-coordinate of harmonic hyperspace, which appears in so simple a way as to have little effect.

We have shown that a local CS action for $\mathcal{N}=2$ SYM is equivalent to the usual action written in harmonic hyperspace. In fact, it seems that as long as consistent integration over the internal space of the harmonic formulation can be defined, the internal space need not be restricted to S^2 but can be spaces with boundaries like SO(2,1)/SO(2) or even degenerate spaces like its contraction SO(2,1)/ISO(1). We then showed that the 2D internal space(s) of the(se) harmonic hyperspace(s) when properly reduced to 1D reproduce the same projective hyperspace as one would expect.

We have not been able to construct the projective covariant derivatives and field strengths, which would be the fundamental ingredients in the background field formalism for $\check{\Pi}$. However, we have an ansatz for the full nonabelian connection A_y in terms of V that comes very close to being the right one:

$$A_y = \sum_{n=1}^{\infty}(-1)^{n+1}\left(\prod_{k=1}^{n}\int dy_k\right)\frac{e^V\left(e^{V_1}-1\right)...\left(e^{V_n}-1\right)}{(y-y_1)\;y_{12}...\;(y_n-y)} \tag{2.10.1}$$

because it produces the correct equation(s) of motion:

$$d_\vartheta^4 A_y = 0 \Rightarrow d_\vartheta^2 W = \bar{d}_\vartheta^2 \bar{W} = 0. \tag{2.10.2}$$

However, A_y in (2.10.1) does not vary as a connection should, as can be checked with a straightforward calculation. We expect that 'regularizing' the divergent integrals by adding some projective terms should fix A_y but we have not been able to find the correct pieces yet. Despite this 'lack' of the connections in terms of V, we will be able to construct the background field formalism in the next chapter. Before that, we will also look at the ordinary Feynman rules and quantize the multiplets directly in projective hyperspace without referring to the harmonic results in the next chapter.

Chapter 3

Exploring Projective Superspace

Having derived the non-Abelian $\mathcal{N} = 2$ SYM action in projective hyperspace in the previous chapter, we put it to use for some computations in this chapter. The hypermultiplets in projective hyperspace have been long known since the work of Lindström and Roček [15, 16]. The Feynman rules were derived for scalar and vector hypermultiplets in three successive papers by Gonzalez-Rey, et al [31–33]. Some one-loop calculations involving scalar hypermultiplet's contributions to effective action were done in [34] but as the non-Abelian action was lacking, not much could be accomplished as far as calculations involving vector hypermultiplet were concerned.

Analogous (but slightly better) situation exists in the case of harmonic hyperspace developed by GIKOS [17, 18, 20]. One-loop two-point functions for SYM effective action and four-point functions (both divergent and finite) with external scalar hypermultiplets were computed by them in [29, 30]. The $n-$point calculations were accomplished by Buchbinder, et al [39] but these are contributions to the effective action for the Abelian case only. Even a direct computation of the β-function for $\mathcal{N} = 2$ SYM has not been done, which requires a $3-$point calculation with ordinary Feynman rules. However, a $3-$point calculation is unnecessary in the case of background field formalism, which does exist for harmonic hyperspace [40, 41] and which we will construct later in this chapter for the projective case. Using this formalism, even a $4-$point S-matrix calculation in $\mathcal{N} = 4$ SYM has been done in [42], which also includes effective potential calculations similar to those in [34].

In this chapter, we extend the possible set of loop calculations in projective hyperspace and show that the hypergraphs are easier to handle than their $\mathcal{N} = 1$ counterparts. We calculate both the divergent and finite parts of 1-hoop 2, 3 & $4-$point functions. It turns out that both the massless and massive scalar hypermultiplet actions (along with their coupling to vector hypermultiplet) are not renormalized at any loop order. We also find that the

divergent (and some finite) 1-loop corrections to SYM effective action have the same form as the classical action (modulo their momentum dependence) proving its renormalizability.

Both the wavefunction and coupling constant are linearly renormalized at 1-loop for $\mathcal{N} = 2$ SYM, which is not the case when $\mathcal{N} = 1$ supergraph methods are used [43–46]. An independent (non-linear) wavefunction renormalization is required in that case to keep the effective action renormalizable. Additionally, we learn from using hypergraph rules that there is effectively only one renormalization factor as is encountered when using background field formalism, which we also develop in the last section of this chapter.

These 1-hoop calculations enable us to compute the well-known β-function for $\mathcal{N} = 2$ SYM coupled to scalar hypermultiplet (matter) in any representation of the gauge group. We also perform a few 'selected' 2-hoops calculations to prove its two-loop finiteness. All these calculations and a few 'miraculous' cancellations also show that the β-function of $\mathcal{N} = 4$ SYM vanishes at 1 & 2-loop(s)[1].

In the next section, we give the coset construction of projective hyperspace. After that, we write various hypermultiplet actions (including that for massive scalar hypermultiplet) to derive the propagators and vertices, which enable us to present the revised 'complete' Feynman rules to evaluate any possible hypergraph. Then, as mentioned above, we present some examples of 1 & 2-hoop(s) hypergraph calculations and the resulting consequences for $\mathcal{N} = 2$ & 4 theories. Finally, we will construct the background field formalism for theories in projective hyperspace.

3.1 General Theory

We review the (relevant) generalities of Projective Hyperspace that are discussed in gory details in [53].

3.1.1 Hyperspace

We start with SU(2,2|2) group element $g_{\mathcal{M}}{}^{\mathcal{A}}$. The SU(2) bosonic (Latin) and SU(2,2) fermionic (Greek) indices contained in the group indices are divided into two parts and shuffled such that $\mathcal{M} = \{M, M'\} = \{(m, \mu), (m', \dot{\mu})\}$ with

[1] Using $\mathcal{N} = 1$ supergraph methods, finiteness of $\mathcal{N} = 4$ SYM has been shown till 3-loops explicitly in [47–50]. Using $\mathcal{N} = 2$ superfields and background field formalism, such cancellations leading to UV finiteness of $\mathcal{N} = 2$ & 4 theories were explained in [51, 52] for all loop orders.

their values being $\{1,(1,2),1',(\dot{1},\dot{2})\}$. Since the bosonic indices take only one value, they will be suppressed.

The projective coordinates $(4\,x's, 4\,\theta's \,\&\, 1\,y)$ are arranged in an off-diagonal square matrix ${w_M}^{A'}$ inside ${g_{\mathcal{M}}}^{\mathcal{A}}$. The rest of the fermionic coordinates $(\vartheta_\mu, \vartheta^{\dot{\alpha}})$ are contained in the diagonal parts of g and can be understood by the method of projection given below:

$$g: \quad {g_{\mathcal{M}}}^{\mathcal{A}} \to {\bar{z}_{\mathcal{M}}}^{A'} \tag{3.1.1}$$

$$g^{-1}: \quad {g_{\mathcal{A}}}^{\mathcal{M}} \to {z_A}^{\mathcal{M}} \tag{3.1.2}$$

$$\text{Constraint}: \quad {z_A}^{\mathcal{M}} {\bar{z}_{\mathcal{M}}}^{A'} = 0 \tag{3.1.3}$$

$$\text{Solution}: \quad \begin{cases} {\bar{z}_{\mathcal{M}}}^{A'} = \left({w_M}^{N'}, \delta^{N'}_{M'}\right) {\bar{u}_{N'}}^{A'}; \\ {z_A}^{\mathcal{M}} = {u_A}^N \left(\delta^M_N, -{w_N}^{M'}\right). \end{cases} \tag{3.1.4}$$

The coordinates in w, u, $\&\,\bar{u}$ are arranged as follows:

$${w_M}^{A'} = \begin{pmatrix} y & \bar{\theta}^{\dot{\alpha}} \\ \theta_\mu & {x_\mu}^{\dot{\alpha}} \end{pmatrix} \tag{3.1.5}$$

$${u_M}^A = \begin{pmatrix} I & 0 \\ \vartheta_\mu & I \end{pmatrix} \tag{3.1.6}$$

$$\bar{u}^{A'}_{M'} = \begin{pmatrix} I & -\bar{\vartheta}^{\dot{\alpha}} \\ 0 & I \end{pmatrix} \tag{3.1.7}$$

These matrices have the following finite superconformal transformations (indices are suppressed in matrix notation below):

$$\bar{z}' = g_0 \bar{z}, \quad z' = z g_0^{-1}; \quad g_0 = \begin{pmatrix} a & b \\ c & d \end{pmatrix}, \quad g_0^{-1} = \begin{pmatrix} \tilde{d} & -\tilde{b} \\ -\tilde{c} & \tilde{a} \end{pmatrix} \tag{3.1.8}$$

$$\Rightarrow w' = (aw+b)(cw+d)^{-1}, \quad u' = (w\tilde{c}+\tilde{d})^{-1} u, \quad \bar{u}' = \bar{u}(cw+d)^{-1} \tag{3.1.9}$$

We can also construct symmetry invariants as differentials or finite differences:

$$\begin{aligned} {z_A}^{\mathcal{M}} d{\bar{z}_{\mathcal{M}}}^{A'} &= {u_A}^M \left(d{w_M}^{M'}\right) {\bar{u}_{M'}}^{A'}, \\ {z_{2A}}^{\mathcal{M}} {\bar{z}_{1\mathcal{M}}}^{A'} &= {u_{2A}}^M \left(w_1 - w_2\right)_M{}^{M'} {\bar{u}_{1M'}}^{A'}. \end{aligned} \tag{3.1.10}$$

3.1.2 Covariant Derivatives

It is easier to derive the symmetry generators ($G = g\partial_g$) and covariant derivatives ($D = \partial_g g$) from the infinitesimal forms of the transformations given above

and in matrix form, they read:

$$G_w = \partial_w, \quad G_u = w\partial_w + u\partial_u, \quad G_{\bar{u}} = \partial_w w + \partial_{\bar{u}}\bar{u} \tag{3.1.11}$$

$$D_w = \bar{u}\partial_w u, \quad D_u = \partial_u u, \quad D_{\bar{u}} = \bar{u}\partial_{\bar{u}} \tag{3.1.12}$$

This defines the 'projective representation', which is not quite useful for the construction of a 'simple' $\mathcal{N} = 2$ SYM action. For that, we need what is called a 'reflective representation' in which the D's are 'switched' with G's. The explicit forms of covariant derivatives for all the coordinates in both representations are given in Table 3.1. (These are similar to those seen in Table 2.1 but in this chapter we use a different convention so some i's are missing.)

D's	Projective ($\breve{\Pi}$)	Reflective (Я)
d_x	∂_x	∂_x
d_θ	$\partial_\theta - \bar{\vartheta}\partial_x$	∂_θ
$\bar{d}_\theta$	$\partial_{\bar{\theta}} + \partial_x\vartheta$	$\partial_{\bar{\theta}}$
d_y	$\partial_y - \bar{\vartheta}\partial_{\bar{\theta}} - \vartheta\partial_\theta - \bar{\vartheta}\partial_x\vartheta$	∂_y
d_ϑ	∂_ϑ	$\partial_\vartheta + y\partial_\theta + \bar{\theta}\partial_x$
$\bar{d}_\vartheta$	$\partial_{\bar{\vartheta}}$	$\partial_{\bar{\vartheta}} + y\partial_{\bar{\theta}} + \partial_x\theta$

Table 3.1: Covariant derivatives in two different representations.

All the D-commutators can be read directly from Table 3.1 and are same in both the representations except the first one below, which is non-trivial only in Я:

$$\{d_{1\vartheta}, \bar{d}_{2\vartheta}\} = y_{12}d_x \tag{3.1.13}$$

$$\{d_{1\theta}, \bar{d}_{2\vartheta}\} = d_x = \{\bar{d}_{1\theta}, d_{2\vartheta}\} \tag{3.1.14}$$

$$[d_y, d_\vartheta] = d_\theta \quad \& \quad [d_y, \bar{d}_\vartheta] = \bar{d}_\theta \tag{3.1.15}$$

The subscript 'a' in $d_{a\vartheta}$'s labels different y's (to condense notation, it will also label ϑ's wherever required), $y_{12} \equiv y_1 - y_2$ and $d_\theta \equiv d_{a\theta}$. All these commutations lead to the following useful identities[2]:

$$d_{1\vartheta}d^4_{2\vartheta} = y_{12}d_{1\theta}d^4_{2\vartheta} \tag{3.1.16}$$

$$d^4_{1\vartheta}d^4_{2\vartheta} = y^2_{12}\left[\tfrac{1}{2}\Box + y_{12}d_{1\theta}d_x\bar{d}_{1\theta} + y^2_{12}d^4_{1\theta}\right]d^4_{2\vartheta} \tag{3.1.17}$$

$$\delta^8(\theta_{12})d^4_{1\vartheta}d^4_{2\vartheta}\delta^8(\theta_{21}) = y^4_{12}\delta^8(\theta_{12}) \tag{3.1.18}$$

$$d^4_\vartheta d^2_y d^4_\vartheta = \Box d^4_\vartheta \tag{3.1.19}$$

[2] $d^4_\theta = d^2_\theta\bar{d}^2_\theta$, $d^2_\theta = \frac{1}{2}C_{\beta\alpha}d^\alpha_\theta d^\beta_\theta$, and so on.

3.1.3 Hyperfields

We define a projective hyperfield Φ such that $d_\vartheta\Phi = \bar{d}_\vartheta\Phi = 0$. In $\check{\Pi}$, it just means that $\Phi \equiv \Phi(x, \theta, \bar{\theta}, y)$. This representation is useful for defining actions in projective hyperspace. In Я, the dependence on $(\vartheta \,\&\, \bar{\vartheta})$ is non-trivial and looks like: $\Phi \equiv \Phi(x + \vartheta\bar{\theta} + \theta\bar{\vartheta} - y\vartheta\bar{\vartheta}, \theta - y\vartheta, \bar{\theta} - y\bar{\vartheta}, y)$. This representation is more suited for writing actions in the 'full' hyperspace with $8\,\theta$'s.

The superconformal transformation of Φ with a (superscale) weight 'ω' can be deduced by requiring that $dw\,\Phi^{1/\omega}$ transforms as a scalar. The resulting transformations are:

$$dw' = dw[\,\mathrm{sdet}(cw + d)]^2, \quad \Phi(w') = [\,\mathrm{sdet}(cw + d)]^{-2\omega}\Phi(w) \tag{3.1.20}$$

This means that the Lagrangian should have $\omega = 1$ for the action to be superconformally invariant. An example of this will be the scalar hypermultiplet action.

Charge conjugate expressions of the coordinates can be derived in a way similar to the derivation of superconformal transformations:

$$\mathcal{C}\begin{pmatrix} y & \bar{\theta} \\ \theta & x \end{pmatrix}^\dagger = \begin{pmatrix} -\frac{1}{y} & \frac{\bar{\theta}}{y} \\ \frac{\theta}{y} & x - \frac{\theta\bar{\theta}}{y} \end{pmatrix} \tag{3.1.21}$$

$$\mathcal{C}(\vartheta)^\dagger = \vartheta - \frac{\theta}{y} \tag{3.1.22}$$

$$\mathcal{C}(\bar{\vartheta})^\dagger = \bar{\vartheta} + \frac{\bar{\theta}}{y} \tag{3.1.23}$$

The (bar) conjugate of the hyperfield Φ can be now defined as follows:

$$\bar{\Phi} \equiv \mathcal{C}(\Phi)^\dagger = y^{2\omega}[\Phi(\mathcal{C}w)]^\dagger \tag{3.1.24}$$

3.1.4 Internal Coordinate

Much of projective hyperspace can be understood by analogy to full $\mathcal{N} = 1$ superspace, as a consequence of both having 2 θ's and 2 $\bar{\theta}$'s. Then what we've left to understand is the treatment of the internal y-coordinate. The field strengths turn out to be Taylor expandable in y on-shell [53], so their charge conjugates must be Laurent expandable on-shell. Thus, it seems natural to use contour integration (as seen in the previous chapter, this is also a consistent thing to do):

$$\oint \frac{dy}{2\pi i}\frac{y^m}{y^n} = \delta_{m+1,n} \tag{3.1.25}$$

(The factor of $2\pi i$ will be suppressed in what follows.) This makes the y-space effectively compact, as expected for an internal symmetry. It is also a convenient way to constrain a generic hyperfield Φ's y-dependence:

$$\phi\left(y\left[0^{\uparrow}\right]\right) = \oint_{0,y} dy' \frac{1}{y'-y} \Phi\left(y'\left[0^{\uparrow}_{\downarrow}\right]\right) = \sum_{n=0}^{\infty} y^n \oint_0 dy' \frac{1}{y'^{n+1}} \Phi\left(y'\left[0^{\uparrow}_{\downarrow}\right]\right) \tag{3.1.26}$$

Here, $\phi(y)$ has only the non-negative powers of y encoded in the notation $\left[0^{\uparrow}\right]$. The coefficients of different powers of y in ϕ matches with the correct ones in $\Phi(y')$ which has all the powers of y denoted by $\left[0^{\uparrow}_{\downarrow}\right]$. Thus, the contour integral acts as an 'arctic' projector and ϕ is an arctic hyperfield, being regular at origin.

As for Feynman diagrams in Minkowski space, it is often more convenient, when defining how to integrate around poles (especially when there's more than one integral to evaluate), to move the poles rather than the contour. In this interpretation, instead of having a bunch of integrals over various contours, with the poles for integration over each variable lying on the contour of another variable, we have all integrals over the same contour, with all poles in various different positions near that contour. Let us make this idea concrete by defining the following 'arctic' (Π_R) and 'antarctic' (Π_N) projectors:

$$\Pi_R = \oint_{C_0} dy' \frac{1}{y'-y}\,, \qquad \Pi_N = \oint_{C_0} dy' \frac{1}{y-y'}\,, \tag{3.1.27}$$

where C_0 is a closed contour enclosing the origin. Applying the projector Π_R, we will need to calculate

$$\oint dy_1 \frac{1}{y_1-y_2} y_1^m\,.$$

Since there's a pole at $y_1 = y_2$, we avoid the singularity by moving the pole slightly inwards in the radial direction. This can be achieved by introducing the following $i\epsilon$-prescription

$$\frac{1}{y_{12}} \equiv \frac{1}{y_1 - y_2 + \epsilon(y_1+y_2)}\,,$$

at least for the case of any convex contour (e.g., a circular one) about the origin; otherwise, we need to invent a fancier notation. If $m \geq 0$, there is only the singularity at 0 enclosed by the contour and the integral simply gives y_2^m. If $m < 0$, the contour encloses both the singularities at 0 and y_2 so the integral

vanishes (because sum of residues). That is, only non-negative powers survive:

$$\oint dy_1 \frac{y_1^m}{y_1 - y_2} = \begin{cases} y^m & \text{if } m \geq 0 \\ 0 & \text{if } m < 0 \end{cases} .$$

Thus, the arctic projection of Φ reads

$$\phi\left(y_2\left[0^{\uparrow}\right]\right) = \int dy_1 \frac{1}{y_{12}} \Phi\left(y_1\left[0^{\uparrow}_{\downarrow}\right]\right). \tag{3.1.28}$$

Similarly, the 'antarctic' projector with the same $\epsilon-$prescription gives an antarctic hyperfield. Now, the pole is shifted radially outwards so if $m \geq 0$, there are no singularities enclosed by the contour and the integral vanishes. Only when $m < 0$ the residue becomes y_2^m, such that

$$\bar{\phi}\left(y_2\left[(-1)_{\downarrow}\right]\right) = \int dy_1 \frac{1}{y_{21}} \Phi\left(y_1\left[0^{\uparrow}_{\downarrow}\right]\right) \tag{3.1.29}$$

where, $[(-1)_{\downarrow}]$ denotes $\bar{\phi}$ contains only the negative powers of y. Thus, $\Pi_N + \Pi_R = 1$ as expected. In addition to these, we can construct other projectors by using appropriate powers of $\frac{y}{y'}$. Such a projector will be constructed in the next chapter to annihilate the non-positive powers of y in a given hyperfield.

Finally, we list some 'simple' identities that will be useful for proving gauge invariance of the vector action, deriving component action of $\mathcal{N} = 2$ SYM, deriving vector propagator and evaluating y-integrals in the Feynman diagrams:

$$\frac{1}{y_{ij} y_{jk}} = \frac{1}{y_{ik}} \left(\frac{1}{y_{ij}} + \frac{1}{y_{jk}}\right) \tag{3.1.30}$$

$$\frac{1}{y_{12}} + \frac{1}{y_{21}} = 2\pi i\, \delta(y_{12}) \tag{3.1.31}$$

$$\frac{y_1}{y_{12}} + \frac{y_2}{y_{21}} - 1 = \frac{y_1 + y_2}{2}\, 2\pi i\, \delta(y_{12}) \tag{3.1.32}$$

All these generalities now enable us to properly see them in action!

3.2 Massless Hypermultiplets

We start with writing the actions for various massless hypermultiplets and end with enumerating the Feynman rules, which allow us to do all the necessary calculations presented in the next section.

3.2.1 Actions

Scalar Hypermultiplet. For the scalar hypermultiplet, the requirement of Laurent expandability in y turns out to be too weak off-shell; we therefore require that it be Taylor expandable. This 'polarity' (arctic or antarctic) will be the analog of the 'chirality' of $\mathcal{N} = 1$ supersymmetry. Unlike the $\mathcal{N} = 1$ case, we now have an infinite number of auxiliary component fields because of the infinite Taylor expansion in y. The free action can be written in analogy to $\mathcal{N} = 1$ as:

$$\mathcal{S}_\Upsilon = -\int dx\, d^4\theta\, dy\, \bar{\Upsilon}\Upsilon. \tag{3.2.1}$$

For superconformal invariance and reality, the arctic hyperfield $\Upsilon\left[0^\uparrow\right]$ must have $\omega = \frac{1}{2}$. Its conjugate is an (almost) antarctic hyperfield $\bar{\Upsilon}\left[1_\downarrow\right] = y[\Upsilon(\mathcal{C}w)]^\dagger$. Note that the integral of Υ^2 or $\bar{\Upsilon}^2$ would give 0, just as for $\mathcal{N} = 1$, but now because of polarity rather than chirality. Also, since there is no analog to the chiral superpotential terms of $\mathcal{N} = 1$, there are no renormalizable self-interactions for this hypermultiplet. All its interactions will be through coupling to the vector hypermultiplet.

There is not much to say about the off-shell components: they are just the coefficients of Taylor expansion in y and the θ's. So we examine the field equations to see how only a finite number of components survive on-shell. A direct and easy way to accomplish that is to use reflective representation. Using the 4 extra ϑ's, we can write both the arctic and antarctic hyperfields in terms of an unconstrained (in both y and ϑ) hyperfield:

$$\Upsilon\left(y_2\left[0^\uparrow\right]\right) = d^4_{2\vartheta}\int dy_1 \frac{1}{y_{12}}\Phi\left(y_1\left[0^\uparrow_\downarrow\right]\right) \tag{3.2.2}$$

$$\bar{\Upsilon}\left(y_2\left[1_\downarrow\right]\right) = d^4_{2\vartheta}d^2_{y_2}\int dy_1 \frac{1}{y_{21}}\bar{\Phi}\left(y_1\left[0^\uparrow_\downarrow\right]\right) \tag{3.2.3}$$

The y-derivatives appear in (3.2.3) because: (1) the antarctic projection makes '-1' the highest power of y; (2) the y term in each $d_{2\vartheta}$ increases this to '3'; and (3) the two y-derivatives decrease this to the correct power of '1'. Unconstrained variation of the action with respect to $\bar{\Phi}$ (after using the d^4_ϑ to turn $\int d^4\theta$ into $\int d^8\theta$) then gives the field equations $d_y^2\Upsilon = 0$ (the arctic projection is redundant). On the other hand, variation with respect to Φ kills the antarctic pieces of $\bar{\Upsilon}$, which is the same as $d_y^2\bar{\Upsilon} = 0$. Due to superconformal invariance, the rest of the superconformal equations are also satisfied.

Thus, the on-shell component expansion of the scalar hypermultiplet reads[3]:

$$\Upsilon(x,\theta,\bar\theta,y) = (A+yB) + \theta\chi + \bar\theta\bar{\bar\chi} - \theta\partial B\bar\theta \tag{3.2.4}$$

$$\bar\Upsilon(x,\theta,\bar\theta,y) = y\Bigg[\bar A - \frac{\theta\partial\bar A\bar\theta}{y} + \frac{\theta^2\bar\theta^2\Box\bar A}{y^2} - \frac{\bar B}{y} + \frac{\theta^2\bar\theta^2\Box\bar B}{y^3} + \frac{\theta}{y}\left(\chi - \frac{\theta\partial\chi\bar\theta}{y}\right) + \frac{\bar\theta}{y}\left(\bar{\bar\chi} - \frac{\theta\partial\bar{\bar\chi}\bar\theta}{y}\right)\Bigg]. \tag{3.2.5}$$

From the last equation, we clearly see that the equations of motion for the complex scalars and the Weyl spinors are satisfied if $d_y^2\bar\Upsilon = 0$ applies.

Vector Hypermultiplet. Like the scalar hypermultiplet, we look for a description of the vector hypermultiplet in terms of a prepotential defined on projective hyperspace. Again in analogy to $\mathcal{N}=1$, this should be a real prepotential, rather than a polar one. Because it lacks the polarity restriction, and is thus Laurent expandable in y, it is called 'tropical'. Like the scalar hypermultiplet, it will have only a few powers of y surviving on-shell.

Just as for both $\mathcal{N}=0$ & 1, gauge symmetry is understood as a generalization of global symmetry, so we derive its form by coupling to matter. The straightforward generalization of the $\mathcal{N}=1$ coupling is then given by the action for the scalar hypermultiplet coupled to a vector hypermultiplet background:

$$\mathcal{S}_{\Upsilon-V} = -\int dx\, d^4\theta\, dy\, \bar\Upsilon e^V \Upsilon. \tag{3.2.6}$$

This coupling fixes the weight of V to be 0:

$$V'(w) = V(w'), \quad \bar V(w) \equiv [V(\mathcal{C}w)]^\dagger = V(w) \tag{3.2.7}$$

The gauge transformations are then

$$\Upsilon' = e^{-i\Lambda}\Upsilon, \quad \bar\Upsilon' = \bar\Upsilon e^{i\bar\Lambda}, \quad e^{V'} = e^{-i\bar\Lambda}e^V e^{i\Lambda} \tag{3.2.8}$$

where Λ is arctic like Υ, but has $\omega = 0$ like V. Thus, $\bar\Lambda$ has only non-positive powers of y, unlike $\bar\Upsilon$. Because of the $\frac{1}{y}$'s associated with conjugated coordinates, setting Λ to $\bar\Lambda$ would reduce Λ to a real constant, *i.e.*, the global symmetry.

With this gauge invariance, we can examine the on-shell component fields

[3] The $\theta\bar\theta-$term in Υ can be understood as a consequence of one of the superconformal field equations [53], which schematically reads: $\partial_x\partial_y + \partial_\theta\partial_{\bar\theta} = 0$.

of the vector hypermultiplet. Since Λ contains all non-negative powers of y, and $\bar{\Lambda}$ contains all non-positive powers, it might seem that everything can be gauged away, but again the additional $\frac{1}{y}$'s associated with charge conjugation modify things: The $\frac{1}{y}$ in $\mathcal{C}\theta$ increases the number of non-gauge components of V with increasing θ, while the $\frac{\theta\bar{\theta}}{y}$ in $\mathcal{C}x$ leads to an $x-$derivative gauge transformation, again in analogy with the $\mathcal{N}=1$ case. (We can also look at just what Λ gauges away, and then apply 'reality' to V.) The result is that, unlike the scalar hypermultiplet (but like the $\mathcal{N}=1$ vector multiplet), V has a finite number of auxiliary fields.

In a Wess-Zumino gauge,

$$V=\frac{1}{y}\Bigg[\left(\theta A\bar{\theta}+\theta^2\phi+\bar{\theta}^2\bar{\phi}\right)+\bar{\theta}^2\theta\left(\lambda+\frac{\tilde{\lambda}}{y}\right)+\theta^2\bar{\theta}\left(\bar{\lambda}+\frac{\bar{\tilde{\lambda}}}{y}\right)+\theta^2\bar{\theta}^2\left(\mathcal{D}+\frac{\mathcal{D}_0}{y}+\frac{\bar{\mathcal{D}}}{y^2}\right)\Bigg] \tag{3.2.9}$$

where the residual gauge invariance is the usual one for the vector A. We thus find, in addition to the expected physical vector (A), a complex scalar (ϕ) and SU(2) doublet of spinors ($\lambda\,\&\,\tilde{\lambda}$), there is an SU(2) triplet of auxiliary scalars ($\mathcal{D},\bar{\mathcal{D}}\,\&\,\mathcal{D}_0$). This same set of fields is found if the vector hypermultiplet is reduced to $\mathcal{N}=1$ supermultiplets, one vector supermultiplet plus one scalar supermultiplet. In the $\mathcal{N}=1$ case, the construction of the vector multiplet action depended on the fact that a spinor derivative could kill the chiral gauge parameter. In the $\mathcal{N}=2$ case, we have arctic and antarctic gauge parameters, and the only way to kill them is by antarctic or arctic projection. This leads to an action of the form

$$\mathcal{S}_V=\frac{\mathrm{tr}}{g^2}\int dx\,d^8\theta\sum_{n=2}^{\infty}\frac{(-1)^n}{n}\prod_{i=1}^{n}\int dy_i\frac{\left(e^{V_1}-1\right)...\left(e^{V_n}-1\right)}{y_{12}y_{23}...y_{n1}} \tag{3.2.10}$$

where $V_i\equiv V(x,\theta,\vartheta,y_i)$. This action is invariant under the following gauge transformation:

$$\delta\left(e^V\right)=i\left(e^V\Lambda-\bar{\Lambda}e^V\right)\Rightarrow\delta V=i\left[\frac{V}{2},\left((\Lambda+\bar{\Lambda})+\left[\coth\frac{V}{2},(\Lambda-\bar{\Lambda})\right]\right)\right]. \tag{3.2.11}$$

We can show that by varying $\mathcal{S}_V$ using

$$\delta\left(e^V-1\right)=-i\left[\left(\bar{\Lambda}-\Lambda\right)-\left\{\left(e^V-1\right)\Lambda-\bar{\Lambda}\left(e^V-1\right)\right\}\right],$$

which gives:

$$\delta\mathcal{S}_V \sim \text{tr}\int d^{12}X\sum_{n=2}^{\infty}(-1)^n\oint\prod_{i=1}^{n}dy_i\frac{\delta\left(e^{V_1}-1\right)\left(e^{V_2}-1\right)...\left(e^{V_n}-1\right)}{y_{12}y_{23}...y_{n1}}\,.$$

Collecting homogeneous variational part of n^{th} term and inhomogeneous part of $(n-1)^{th}$ term for $n\geq 3$ leads to:

$$\begin{aligned}\delta\mathcal{S}_V^{(n\geq 3)} \sim \oint &\frac{-\left[\Lambda_1\left(e^{V_1}-1\right)-\left(e^{V_1}-1\right)\bar{\Lambda}_1\right]\left(e^{V_2}-1\right)...\left(e^{V_{n-1}}-1\right)}{y_{12}y_{23}...y_{n-1,1}}\\ &-\frac{\left[\bar{\Lambda}_1-\Lambda_1\right]\left(e^{V_2}-1\right)...\left(e^{V_n}-1\right)}{y_{12}y_{23}...y_{n1}}\\ =\oint&\frac{-\Lambda_1\left(e^{V_1}-1\right)...\left(e^{V_{n-1}}-1\right)}{y_{12}y_{23}...y_{n-1,1}}+\frac{\bar{\Lambda}_1\left(e^{V_2}-1\right)...\left(e^{V_{n-1}}-1\right)\left(e^{V_1}-1\right)}{y_{12}y_{23}...y_{n-1,1}}\\ &-\frac{\left[\bar{\Lambda}_1-\Lambda_1\right]\left(e^{V_2}-1\right)...\left(e^{V_n}-1\right)}{y_{n2}y_{12}...y_{n-1,n}}-\frac{\left[\bar{\Lambda}_1-\Lambda_1\right]\left(e^{V_2}-1\right)...\left(e^{V_n}-1\right)}{y_{23}...y_{n1}y_{n2}}\,.\end{aligned}$$

Evaluating the four terms in the last line, we see half of them vanish:

$$\begin{aligned}\oint dy_1\frac{\bar{\Lambda}_1}{y_{12}}=\oint dy_1\frac{\bar{\Lambda}\left(\frac{1}{y_1}\right)}{y_1-y_2+\epsilon(y_1+y_2)}&=0\\ \text{Similarly,}\quad\oint dy_1\frac{\Lambda(y_1)}{y_1-y_2+\epsilon(y_1+y_2)}&=\Lambda(y_2)\\ \text{Also,}\quad\oint dy_1\frac{\bar{\Lambda}\left(\frac{1}{y_1}\right)}{y_n-y_1+\epsilon(y_n+y_1)}&=\bar{\Lambda}\left(\frac{1}{y_n}\right)\\ \text{And,}\quad\oint dy_1\frac{\Lambda(y_1)}{y_n-y_1+\epsilon(y_n+y_1)}&=0\,.\end{aligned}$$

Substituting these results back in $\delta\mathcal{S}_V$, we get:

$$\begin{aligned}\delta\mathcal{S}_V^{(n\geq 3)} \sim \int&\frac{-\Lambda_1\left(e^{V_1}-1\right)...\left(e^{V_{n-1}}-1\right)}{y_{12}...y_{n-1,1}}+\frac{\Lambda_2\left(e^{V_2}-1\right)...\left(e^{V_n}-1\right)}{y_{23}...y_{n-1,n}y_{n2}}\\ &+\frac{\bar{\Lambda}_1\left(e^{V_2}-1\right)...\left(e^{V_{n-1}}-1\right)\left(e^{V_1}-1\right)}{y_{12}...y_{n-1,1}}-\frac{\bar{\Lambda}_n\left(e^{V_2}-1\right)...\left(e^{V_n}-1\right)}{y_{23}...y_{n2}}=0\,.\end{aligned}$$

Finally, the homogeneous variational term when $n=2$ vanishes on its own as

follows:

$$\begin{aligned}\delta\mathcal{S}_V^{(n=2)} &\sim \mathrm{tr}\int d^8\theta \oint dy_1 dy_2 \frac{\left[\bar{\Lambda}_1 - \Lambda_1\right]\left(e^{V_2}-1\right)}{y_{12}y_{21}} \\ &= \mathrm{tr}\int d^4\theta \oint dy_1 dy_2 \frac{\left[\Lambda_1 - \bar{\Lambda}_1\right] d^4_{1\vartheta}\left(e^{V_2}-1\right)}{y_{12}^2} \\ &= \mathrm{tr}\int d^4\theta \oint dy_1 dy_2 \left[\Lambda_1 - \bar{\Lambda}_1\right]\left[\Box + \mathcal{O}\left(y_{12}\right)\right]\left(e^{V_2}-1\right) \\ &= 0\,.\end{aligned}$$

Superconformal invariance of the action might not be obvious, especially because of the non-locality. The first thing to note is that the full superspace volume element ($\int dx\, d^8\theta$) is superconformally invariant (because $sdet(g_0) = 1$). Next is to use the results for the superconformal transformations of dw_i and w_{ij}, read from (3.1.9) & (3.1.10), to find those for the coordinate y:

$$dy_i' = \frac{dy_i}{(w_i\tilde{c}+\tilde{d})(cw_i+d)} \tag{3.2.12}$$

$$y_{ij}' = \frac{y_{ij}}{(w_i\tilde{c}+\tilde{d})(cw_j+d)} \tag{3.2.13}$$

where, the factors (cw_i+d), etc denote the single matrix element corresponding to the y-coordinate. We also use the fact that the other w_{ij}'s vanish as the action is local in these coordinates. The similar transformation factors of dy_i's and y_{ij}'s then cancel due to the 'cyclic' nature of the denominator in SYM action proving its superconformal invariance.

Ghost Hypermultiplets. The introduction of ghosts follows the usual quantization procedure of BRST and is analogous to the case of $\mathcal{N}=1$ at least in the Fermi-Feynman gauge (see next section for more details):

$$\begin{aligned}\mathcal{S}_{bc} &= -\,\mathrm{tr}\int dx\, d^4\theta\, dy\,(y\,b+\bar{b})\left[\frac{V}{2},\left(\left(c+\frac{\bar{c}}{y}\right)+\left[\coth\frac{V}{2},\left(c-\frac{\bar{c}}{y}\right)\right]\right)\right] \\ &= -\,\mathrm{tr}\int dx\, d^4\theta\, dy\,\left[\bar{b}\,c+\bar{c}\,b+(y\,b+\bar{b})\frac{V}{2}\left(c+\frac{\bar{c}}{y}\right)\right. \\ &\qquad \left.+\frac{1}{3}(y\,b+\bar{b})\frac{V^2}{4}\left(c-\frac{\bar{c}}{y}\right)+\cdots\right]\end{aligned} \tag{3.2.14}$$

We can also choose a non-linear gauge like the Gervais-Neveu gauge in

which the ghost action would be simplified to:

$$\begin{aligned}\mathcal{S}_{bc} &= -\operatorname{tr}\int dx\, d^4\theta\, dy\, (y\, b+\bar{b})\left[e^V c-\frac{\bar{c}}{y}\, e^V\right]\\ &= -\operatorname{tr}\int dx\, d^4\theta\, dy\, \left[y\, b\, e^V c+\bar{c}\, e^V b+\bar{b}\, e^V c+\frac{1}{y}\bar{c}\, e^V \bar{b}\right]\end{aligned} \tag{3.2.15}$$

There does not seem to be any real advantage of this gauge apart from the absence of 'weird' numerical factors coming from the expansion of $\coth(x)$ in the case of Fermi-Feynman gauge. So we will use action (3.2.14) in all the calculations presented later.

3.2.2 Propagators

Scalar. We add source terms to the quadratic action of Υ and convert the $d^4\theta$ integral to $d^8\theta$ integral by rewriting Υ's using equations (3.2.2) & (3.2.3):

$$\begin{aligned}\mathcal{S}_{\Upsilon-J} &= -\int dx\, d^4\theta\, dy\, \left[\bar{\Upsilon}\Upsilon+\bar{J}\Upsilon+\bar{\Upsilon}J\right] \qquad (3.2.16)\\ &= -\int dx\, d^8\theta \int dy_1 \left[d^2_{y_1}\int dy_3 \frac{\bar{\Phi}_3}{y_{13}} d^4_{1\vartheta}\int dy_2 \frac{\Phi_2}{y_{21}}\right.\\ &\qquad \left. +\bar{J}_1\int dy_2\frac{\Phi_2}{y_{21}}+d^2_{y_1}\int dy_3\frac{\bar{\Phi}_3}{y_{13}}J_1\right]\end{aligned}$$

The sources $J\,\&\,\bar{J}$ are generic projective hyperfields with $\omega=\frac{1}{2}$. Now, the modified equations of motion of $\bar{\Upsilon}\,\&\,\Upsilon$ can be derived from above and (after some integration by parts and acting with $d^4_{1\vartheta}$) they read:

$$\begin{aligned}\int dy_1 \frac{d^4_{1\vartheta} d^2_{y_1}\Upsilon_1}{y_{13}} &= -\int dy_1 d^4_{1\vartheta} d^2_{y_1}\left(\frac{1}{y_{13}}\right) J_1\\ \Rightarrow \Box\Upsilon_3 &= -\, d^4_{3\vartheta}\int dy_1 \frac{2J_1}{y^3_{13}} \qquad (3.2.17)\\ \text{Similarly, } \Box\bar{\Upsilon}_2 &= -\, d^4_{2\vartheta}\int dy_1 \frac{2\bar{J}_1}{y^3_{21}} \qquad (3.2.18)\end{aligned}$$

Plugging the equations (3.2.17) & (3.2.18) back in action (3.2.16), we get:

$$\begin{aligned}\mathcal{S}_{\Upsilon-J} &= \frac{1}{2}\int dx\, d^8\theta\, dy_1 \left[\bar{J}_1 \frac{1}{\frac{1}{2}\Box}\int dy_2 \frac{J_2}{y_{21}^3} + \frac{1}{\frac{1}{2}\Box}\int dy_2 \frac{\bar{J}_2}{y_{12}^3} J_1\right] \\ &= \int dx\, d^8\theta\, dy_1\, dy_2 \left[\bar{J}_1 \frac{1}{y_{21}^3}\frac{1}{\frac{1}{2}\Box} J_2\right] \end{aligned} \tag{3.2.19}$$

This gives us the following scalar propagator:

$$\langle \Upsilon(1)\bar{\Upsilon}(2)\rangle = -\frac{d^4_{1\vartheta} d^4_{2\vartheta}}{y_{12}^3}\frac{1}{\frac{1}{2}\Box}\delta^8(\theta_{12})\delta(x_{12}). \tag{3.2.20}$$

Vector. Gauge fixing of the vector hypermultiplet action looks similar to the $\mathcal{N}=1$ case, in the same sense that the scalar hypermultiplet action does. The main modifications are that now $d^4\theta$ is projective, there is also dy, the ghosts and Nakanishi-Lautrup fields are projective arctic / antarctic fields instead of chiral / anti-chiral ones. The y-dependence of ghosts $c\,\&\,\bar{c}$ is $\left[0^{\uparrow}\right]$ & $[0_{\downarrow}]$; anti-ghosts $b\,\&\,\bar{b}$ is $\left[0^{\uparrow}\right]$ & $[2_{\downarrow}]$ and NL fields $B\,\&\,\bar{B}$ is $\left[0^{\uparrow}\right]$ & $[2_{\downarrow}]$. We redefine the conjugates so that their y-dependence is similar to $\bar{\Upsilon}$:

$$\bar{c}\,[0_{\downarrow}] \to \tfrac{1}{y}\bar{c}\,[1_{\downarrow}]\,;\; \bar{b}\,[2_{\downarrow}] \to y\,\bar{b}\,[1_{\downarrow}]\,;\; \bar{B}\,[2_{\downarrow}] \to y\,\bar{B}\,[1_{\downarrow}] \tag{3.2.21}$$

We choose the following gauge-fixing function:

$$V_{gf} = -\int dx\, d^4\theta\, dy\, (y\,b + \bar{b})V \tag{3.2.22}$$

$$\delta V_{gf} = -\int dx\, d^4\theta\, dy \left[(y\,B + \bar{B})V + (y\,b+\bar{b})\delta V\left(c, \frac{\bar{c}}{y}\right)\right] \tag{3.2.23}$$

The second term gives $\mathcal{S}_{bc}$ in Fermi-Feynman gauge[4] (3.2.14). The first term along with a gauge-averaging term (kinetic term for NL field) gives us the gauge-fixing action:

$$\mathcal{S}_{gf} = -\frac{\mathrm{tr}}{g^2}\int dx\, d^4\theta\, dy \left[\bar{B}\frac{1}{\Box}B + (y\,B+\bar{B})V\right] \tag{3.2.24}$$

$$\Rightarrow \mathcal{S}_{gf} = \frac{\mathrm{tr}}{2g^2}\int dx\, d^8\theta\, dy_1\, dy_2\, V_1 \left[\frac{y_1}{{y_{12}}^3} + \frac{y_2}{{y_{21}}^3}\right] V_2 \tag{3.2.25}$$

The final expression for $\mathcal{S}_{gf}$ follows from similar manipulations employed in deriving (3.2.19), *i.e.*, by integrating out B & $\bar{B}$ using their equations of mo-

[4] Choosing $\left(e^V - 1\right)$ instead of V in V_{gf} gives the ghost action (3.2.15).

tion. We now combine the terms quadratic in V from the above equation and (3.2.10) to get:

$$\begin{aligned}\mathcal{S}_V^{(2)}+\mathcal{S}_{gf}^{(2)} &= -\frac{\mathrm{tr}}{2g^2}\int dx\, d^4\theta\, dy_1\, dy_2\, V_1 \frac{1}{y_{12}^2}\left[1-\frac{y_1}{y_{12}}-\frac{y_2}{y_{21}}\right] d^4_{1\vartheta} V_2 \\ &= \frac{\mathrm{tr}}{2g^2}\int dx\, d^4\theta\, dy_1\, dy_2\, V_1 \frac{1}{y_{12}^2}\left[\frac{y_1+y_2}{2}\delta(y_{12})\right] y_{12}^2\left[\frac{1}{2}\Box+\mathcal{O}(y_{12})\right] V_2 \\ &= \frac{\mathrm{tr}}{2g^2}\int dx\, d^4\theta\, dy\, V\left(y\frac{\Box}{2}\right)V \end{aligned} \tag{3.2.26}$$

This gives the following vector propagator:

$$\langle V(1)V(2)\rangle = d^4_{1\vartheta}\frac{\delta(y_{12})}{y_1}\frac{1}{\frac{1}{2}\Box}\delta^8(\theta_{12})\delta(x_{12}). \tag{3.2.27}$$

Ghosts. The derivation of ghost propagators proceeds along similar lines to that of the scalar propagator and the results are:

$$\langle \bar{b}(1)c(2)\rangle = \langle \bar{c}(1)b(2)\rangle = \frac{d^4_{2\vartheta}d^4_{1\vartheta}}{y_{12}^3}\frac{1}{\frac{1}{2}\Box}\delta^8(\theta_{12})\delta(x_{12})\,, \tag{3.2.28}$$

$$\langle c(1)\bar{b}(2)\rangle = \langle b(1)\bar{c}(2)\rangle = -\frac{d^4_{1\vartheta}d^4_{2\vartheta}}{y_{21}^3}\frac{1}{\frac{1}{2}\Box}\delta^8(\theta_{12})\delta(x_{12}). \tag{3.2.29}$$

3.2.3 Vertices

Υ. The scalar hypermultiplet does not have any self-interactions. Only $\Upsilon-V$ vertices are possible as is evident from the actions written above (We use the group theoretical conventions and diagrams along the lines of [47, 48][5].):

$$\bar{\Upsilon}^i V^{j_1}\ldots V^{j_n}\Upsilon^k \;\rightarrow\; \int d^4\theta\int dy\left(\;\right)$$

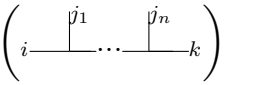

where, the group theory factor (shown in parentheses) is for adjoint representation.

[5] To summarize: The vector and ghost hyperfields are in the adjoint representation of gauge group and the scalar hyperfield is in some representation R: $V=V^aT_a$, $\Upsilon=\Upsilon^aT_a$, etc. The group generators (T_a) satisfy $[T_a,T_b]=if_{ab}{}^cT_c$ and in adjoint rep: $(T_a)_b{}^c=if_{ab}{}^c=$. The Dynkin index (c_A) is defined by: $\mathrm{tr}_A(T_aT_b)=f_{acd}f_b{}^{cd}=c_A\delta_{ab}$. In R, this trace generalizes to: $\mathrm{tr}_R(T_aT_b)=c_R\delta_{ab}$.

***V*.** Pure vector hypermultiplet vertices take the following form:

$$(V_1)^{m_1}...(V_n)^{m_n} \;\to\; \int d^8\theta\, dy_1 \,...\, dy_n \frac{1}{y_{12}...y_{n1}} \left(1 \text{---} \cdots \text{---} n \right)$$

The group theory factor shown above corresponds to the case of $m_1 = ... = m_n = 1$. For other cases, this factor depends on the number of V's rather than that of the independent y-coordinates. Apart from this subtlety, the factor is still similar to the simplest case but we will not consider diagrams containing such vertices (with $m_i > 1$) here.

(b, c). There are altogether four possibilities for ghost vertices and they differ in the accompanying y-integrals:

$$\begin{aligned}
b\, V^n\, c \;&\to\; \int d^4\theta \int dy\, y \\
\bar{c}\, V^n\, b \;&\to\; \int d^4\theta \int dy \\
\bar{b}\, V^n\, c \;&\to\; \int d^4\theta \int dy \\
\bar{c}\, V^n\, \bar{b} \;&\to\; \int d^4\theta \int dy\, \frac{1}{y}
\end{aligned}$$

Group theory factors for these ghost vertices are similar to those for the scalar vertices.

3.2.4 Feynman Rules

1. Basic set-up: Apply usual Feynman rules for drawing diagrams and writing expressions for them using the propagators and vertices derived above.

2. d-Algebra: Convert $d^4\theta$ integrals to $d^8\theta$ integrals by taking $d^4_{a\vartheta}$'s off the propagators. There should be at least two $d^4_{a\vartheta}$'s remaining for the diagram to not vanish. Remove the remaining $d^4_{a\vartheta}$'s using integration by parts (which implicitly assumes using the 'freed' $\delta^8(\theta_{12})$ to do one $d^8\theta$ integral) and keep using the identity (3.1.17) till only one $d^4_{a\vartheta}$ is left[6]. As far as computing divergences is concerned, this leads to a deceptively

[6] All this can be summarized by the formula: $n_\theta - \left(n_\delta - \frac{n_\vartheta}{2}\right) = \frac{1+n}{2}$; where, n_θ=no. of $\int d^8\theta$, n_δ=no. of $\delta^8(\theta)$, n_ϑ=no. of $d^4_{a\vartheta}$ and n=no. of times the identity (3.1.17) has to be applied, which means that a diagram vanishes if $n \leq 0$.

simple result for a 1-hoop diagram (or a particular 1-hoop in a multi-hoop diagram):

$$d^4_{a_1\vartheta}d^4_{a_2\vartheta}...d^4_{a_n\vartheta} = \tfrac{1}{2}(k^2)^{n-2}y^2_{a_1a_2}y^2_{a_2a_3}...y^2_{a_na_1}d^4_{a_n\theta}d^4_{a_n\vartheta} \tag{3.2.30}$$

where, k is the loop momentum and the second-to-last $\theta-$integral can be done by using this identity: $\delta^8(\theta_{12})d^4_\theta d^4_\vartheta \delta^8(\theta_{12}) = \delta^8(\theta_{12})$.

3. y-Calculus: Use some of the identities mentioned in Section 3.1.4 to do 'some' of the y-integrals. These can be set up by using the pictorial rules shown in Figure 3.1. Specifically, for evaluation of divergences, perform

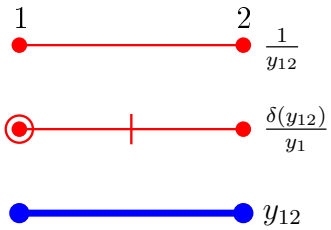

Figure 3.1: Rules for setting up y-integrals.

partial fractions to generate the cyclic y-denominator $(y_{12}y_{23}...y_{n1})$ of the SYM action. Then, performing the extra y-integrals is equivalent to just replacing the extra y's in the integrand by following these two rules: (a) Remove the factor $\int \frac{dy_a}{y_{a1}}$ after replacing all non-negative powers of y_a by y_1 and setting its negative powers to 0; (b) Remove the factor $\int \frac{dy_a}{y_{1a}}$ after replacing all negative powers of y_a by y_1 and setting other (non)-occurrences of y_a to 0.

4. Miscellaneous: Evaluate group theoretical factors and track down signs and symmetry factors. Finally, evaluate the integrals over loop momenta.

3.3 Calculations

3.3.1 1-hoop Examples

Scalar Self-energy. There are two diagrams with different propagators making the loop as shown in Figure 3.2.

1. $1\,V-$propagator: Remove d^4_ϑ from the vector propagator to get the $d^8\theta$ measure. This leaves no d_ϑ's to kill the $\delta^8(\theta_{12})$, so this diagram vanishes. Such tadpole diagrams (even multi-hoop diagrams containing these as

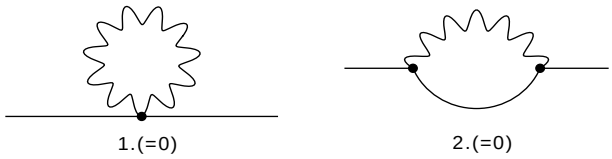

Figure 3.2: Scalar self-energy diagrams at 1-hoop.

sub-diagrams) always vanish, so we will not consider these anymore in what follows.

2. $1\,V\,-\,\&\,1\,\Upsilon-$propagators: Remove two d^4_ϑ's from these propagators to complete the two $d^4\theta$ measures. This means there are not enough (in fact, only 4) d_ϑ's left to kill one of the $\delta^8(\theta_{12})$, so this diagram also vanishes.

This means that the scalar hyperfield is not renormalized which is obvious from the fact that its action is over only the projective hyperspace but the Feynman diagrams give contributions over full hyperspace. In other words, scalar hypermultiplet action (coupled to vector hypermultiplet, as shown below) is not renormalized at any loop order.

$\bar{\Upsilon}\,V\,\Upsilon$. There are four diagrams in this case as shown in Figure 3.3. Two of these diagrams vanish because of d-algebra similar to the self-energy case. The other two are evaluated below:

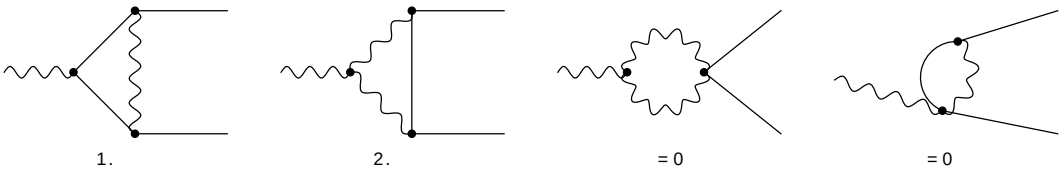

Figure 3.3: $\bar{\Upsilon}\,V\,\Upsilon$ diagrams at 1-hoop.

1. $1\,V\,-\,\&\,2\,\Upsilon-$propagators: This diagram has enough (8, at last) d_θ's to kill one of the $\delta^8(\theta_{12})$ functions so that two $\theta-$integrals can now be done. However, this generates only a $y^4_{12}-$factor without any momentum factors in the numerator, which makes this diagram power-counting finite and the explicit finite result reads:

$$-\frac{c_A}{2}\int\frac{d^4k}{(2\pi)^4}\frac{1}{\frac{1}{2}k^2\frac{1}{2}(k+p_2)^2\frac{1}{2}(k-p_1)^2}\int d^8\theta\int\frac{dy_{1,2}}{y_2}\frac{\bar{\Upsilon}_2(p_2)V_1(p_1)\Upsilon_2(p_3)}{y_{12}\,y_{21}} \tag{3.3.1}$$

where, p_i's are the external momenta.

2. $2V - \&1\,\Upsilon-$propagators: Applying similar maneuvers as above, we conclude that this diagram is also finite:

$$-\mathcal{A}_3(p_2,-p_1)\times\frac{c_A}{2}\int d^8\theta\int\frac{dy_{1,2,3}}{y_2\,y_3}\frac{\bar{\Upsilon}_2(p_2)V_1(p_1)\Upsilon_3(p_3)}{y_{12}\,y_{31}} \tag{3.3.2}$$

where, $\mathcal{A}_3(p_2,-p_1)$ is just the momentum integral of (3.3.1).

In fact, all hoop diagrams for any $\bar{\Upsilon}\,V^n\,\Upsilon$ vertices are finite because of the non-cancellation of 'sufficient' momentum factors in the denominator.

$\bar{\Upsilon}\,\Upsilon\,\bar{\Upsilon}\,\Upsilon$. Such a vertex does not appear in the action and hence, the 1-hoop diagrams (Figure 3.4) contributing to this vertex can not be divergent.

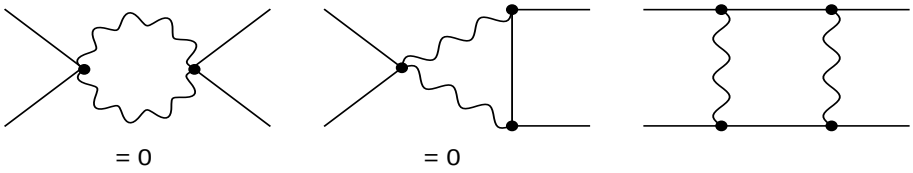

Figure 3.4: $\bar{\Upsilon}\,\Upsilon\,\bar{\Upsilon}\,\Upsilon$ diagrams at 1-hoop.

Out of the three diagrams, two vanish due to d-algebra and the remaining box-diagram can be evaluated in a straightforward manner to give a finite result:

$$\begin{aligned}\sim\int\frac{d^4k}{(2\pi)^4}\frac{1}{\frac{1}{2}k^2\frac{1}{2}(k+p_2)^2\frac{1}{2}(k+p_2+p_3)^2\frac{1}{2}(k-p_1)^2}\times\\ \times\int d^8\theta\int\frac{dy_{1,2}}{y_1y_2}\frac{\bar{\Upsilon}_1(p_1)\Upsilon_1(p_2)\bar{\Upsilon}_2(p_3)\Upsilon_2(p_4)}{y_{12}\,y_{21}}\,.\end{aligned} \tag{3.3.3}$$

Vector Self-energy. There are three classes of diagrams contributing to the self-energy corrections with different hyperfields (vector, ghosts or scalar) running inside the loop as shown in Figure 3.5:

1. $V-$propagators: There are a couple of diagrams (not shown explicitly in Figure 3.5) which have at least one $V_1^2V_2$-type vertex and they vanish trivially due to the presence of expressions like $y^3\delta(y)$ or $y^4\delta(y)^2$. This is a generic feature of 1-hoop (at least) diagrams containing such vertices and these will not be considered here anymore.

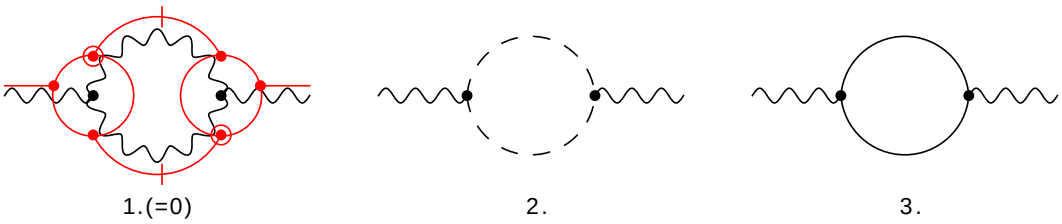

Figure 3.5: Vector self-energy diagrams at 1-hoop.

The diagram which has both vertices of $V_1V_2V_3$-type (shown explicitly in Figure 3.5.1) also vanishes but in a different way. After doing the d-algebra and integrating the two $\delta(y)$'s, we are left with the following y-integrals:

$$\begin{aligned}
&\int dy_{1,2,a,b} \frac{V_1V_2\, y_{ab}\, y_{ba}}{y_a\, y_b\, y_{1b}\, y_{a1}\, y_{2a}\, y_{b2}} \\
&= \int dy_{1,2} \frac{V_1V_2}{y_{12}y_{21}} \int dy_{a,b} \left(\frac{1}{y_{a1}} + \frac{1}{y_{2a}}\right)\left(\frac{1}{y_{1b}} + \frac{1}{y_{b2}}\right)\left(2 - \frac{y_a}{y_b} - \frac{y_b}{y_a}\right) \\
&= \int dy_{1,2} \frac{V_1V_2}{y_{12}y_{21}} \left(2 - \frac{y_1}{y_1} - \frac{y_2}{y_2}\right) = 0.
\end{aligned}$$

2. $(b,c)-$propagators: There are four diagrams with different combinations of ghost propagators and vertices. All of them combine to give (after relevant d-algebra)[7]:

$$\begin{aligned}
&\mathcal{A}_2(p) \times 2\frac{1}{2} c_A \frac{g^2}{4} \int d^8\theta \int dy_{1,2} \frac{V_1V_2}{y_{12}\, y_{21}} \left(1 + \frac{y_1}{y_2} + \frac{y_2}{y_1} + 1\right) \\
&= \mathcal{A}_2(p) \times \frac{c_A}{4} g^2 \int d^8\theta \int dy_{1,2} \frac{V_1V_2}{y_{12}\, y_{21}} \left(\frac{-y_{12}\, y_{21} + 4y_1y_2}{y_1y_2}\right) \\
&= \mathcal{A}_2(p) \times c_A\, g^2 \int d^8\theta \int dy_{1,2} \frac{V_1V_2}{y_{12}\, y_{21}}. \qquad (3.3.4)
\end{aligned}$$

The last line follows entirely from the second term in parentheses of the previous line. This is because the first term with no y_{12}'s in the integrand vanishes since $d^8\theta$ kills such projective integrands. Also, $\mathcal{A}_2(p)$ is the divergent integral and is evaluated using dimensional regularization to

[7] $V \to gV$ in rest of these calculations.

give:

$$\mathcal{A}_2(p) = \int \frac{d^D k}{(2\pi)^D} \frac{1}{\frac{1}{2}k^2 \frac{1}{2}(k+p)^2} = \frac{1}{4\pi^2}\left[\frac{1}{\epsilon} - \gamma_E - \ln\left(\frac{p^2}{\mu^2}\right)\right],$$

where $\frac{1}{\epsilon} = \frac{2}{4-D}$.

3. $\Upsilon-$propagators: The calculation for this single diagram is similar to that of the ghost which gives:

$$-\mathcal{A}_2(p) \times c_R\, g^2 \int d^8\theta \int dy_{1,2} \frac{V_1 V_2}{y_{12}\, y_{21}}. \tag{3.3.5}$$

$V_1\, V_2\, V_3$. Similar to the vector self-energy case, three classes of diagrams contribute in this case also as shown in Figure 3.6. We give only the final results after doing the d-algebra and y-calculus in what follows.

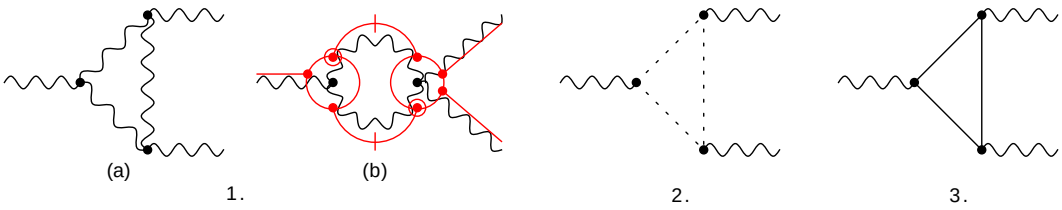

Figure 3.6: $V_1\, V_2\, V_3$ diagrams at 1-hoop.

1. $V-$propagators: There are two diagrams in this class and both are non-zero. We use the notation $\left\updownarrow \frac{y_i}{y_j} \right\updownarrow$ to denote the sum of permutations of $\frac{y_i}{y_j}-$factors over all possible values of i, e.g. $\left\updownarrow \frac{y_1}{y_2} \right\updownarrow = \left(\frac{y_1}{y_2} + \frac{y_2}{y_3} + \frac{y_3}{y_1}\right)$.

   (a) $(VVV)^3$ vertices: The full (divergent and finite) contribution of this diagram reads:

$$-\frac{c_A}{2} g^3 \int d^8\theta \int dy_{1,2,3} \frac{V_1 V_2 V_3}{y_{12}\, y_{23}\, y_{31}} \left[\mathcal{A}_2(p_3)\left(-3 + \left\updownarrow \frac{y_1}{y_2} \right\updownarrow\right) + \right.$$
$$\left. + p_2^2\, \mathcal{A}_3(p_2, -p_1)\left(1 + \left\updownarrow \frac{y_1}{y_2} - \frac{1}{3}\left(\frac{y_{31}}{y_1}\right)^2 \right\updownarrow\right)\right] \tag{3.3.6}$$

   (b) $(VVVV) - (VVV)$ vertices: The (wavy line) diagram looks like contributing only to the $V_1 V_2^2$ vertex term in the action but due to

the 4−point vertex, this diagram also contributes to $V_1V_2V_3$ vertex as shown explicitly by the 'y-dependence' in Figure 3.6.1.(b). We will be giving the results for diagrams with all (external) V's at distinct y's only since the results for other diagrams follow from those of the self-energy case. This particular diagram gives a very simple contribution similar to the self-energy case:

$$-\mathcal{A}_2(p_3)\times\frac{1}{2}\frac{c_A}{2}g^3\int d^8\theta\int dy_{1,2,3}\frac{V_1V_2V_3}{y_{12}\,y_{23}\,y_{31}}\left(3-\Big\updownarrow\frac{y_1}{y_2}\Big\updownarrow\right) \tag{3.3.7}$$

2. (b,c)−propagators: There are eight diagrams with different combinations of ghost propagators and vertices. All of them combine to give the following part containing the divergence:

$$\begin{aligned}&\mathcal{A}_2(p_3)\times 2\frac{c_A}{2}\frac{g^3}{8}\int d^8\theta\int dy_{1,2,3}\frac{V_1V_2V_3}{y_{12}\,y_{23}\,y_{31}}\left(1+\Big\updownarrow\frac{y_1}{y_2}+\frac{y_1}{y_3}\Big\updownarrow+1\right)\\ =&\,\mathcal{A}_2(p_3)\times\frac{c_A}{8}g^3\int d^8\theta\int dy_{1,2,3}\frac{V_1V_2V_3}{y_{12}\,y_{23}\,y_{31}}2\left(1+\Big\updownarrow\frac{y_1}{y_2}\Big\updownarrow-\frac{y_{12}\,y_{23}\,y_{31}}{2\,y_1\,y_2\,y_3}\right)\end{aligned} \tag{3.3.8}$$

where the last term in the parentheses does not contribute as in the case of self-energy diagram but the last term does contribute in the remaining finite part given below:

$$\begin{aligned}p_2^2\,\mathcal{A}_3(p_2,-p_1)\times\frac{c_A}{4}g^3\int d^8\theta\int dy_{1,2,3}\frac{V_1V_2V_3}{y_{12}\,y_{23}\,y_{31}}\frac{1}{3}\Big\updownarrow\left(\frac{y_{12}}{y_{31}}\right)^2\Big\updownarrow\times\\ \times\left(1+\Big\updownarrow\frac{y_1}{y_2}\Big\updownarrow-\frac{y_{12}\,y_{23}\,y_{31}}{2\,y_1\,y_2\,y_3}\right)\end{aligned} \tag{3.3.9}$$

3. Υ−propagators: The calculation for this single diagram is again straightforward and gives as expected:

$$-c_R\,g^3\int d^8\theta\int dy_{1,2,3}\frac{V_1V_2V_3}{y_{12}\,y_{23}\,y_{31}}\left[\mathcal{A}_2(p_3)+p_2^2\,\mathcal{A}_3(p_2,-p_1)\frac{1}{3}\Big\updownarrow\left(\frac{y_{12}}{y_{31}}\right)^2\Big\updownarrow\right]. \tag{3.3.10}$$

$\boldsymbol{V_1\,V_2\,V_3\,V_4}$**.** The calculations in this case are similar to the earlier ones except for an increase in the number of y-integrals to be evaluated. Before we proceed further, we make a group theoretical comment. None of the 4−point

diagrams generate terms proportional to

$$f_{ipq}f_{jqr}f_{krs}f_{lsp}V_1^iV_2^jV_3^kV_4^l \equiv G_{ijkl}V_1^iV_2^jV_3^kV_4^l\,,$$

which do not appear in the SYM action[8]. This was, however, not the case when similar calculations were done using $\mathcal{N}=1$ supergraph rules in [45, 46] and a nonlinear (cubic) wavefunction renormalization (proportional to $GVVV$) was required to keep the effective action renormalizable as predicted in [43, 44].

We do not encounter this feature because of the 'antisymmetry' of the y_{ab} factors, which enforces the Jacobi identity leading (in this particular case) to this useful identity:

$$G_{ijkl} - G_{ijlk} = \frac{c_A}{2}f_{ijp}f_{klp} \equiv \frac{c_A}{2}$$

Hence, all the 4−point diagrams end up producing the V^4 term present in the SYM action and the usual renormalization procedure is applicable. (One more reason is that *'gV' is not renormalized* as explained later.) Now, we enumerate the complete results for the usual three classes of diagrams shown in Figure 3.7:

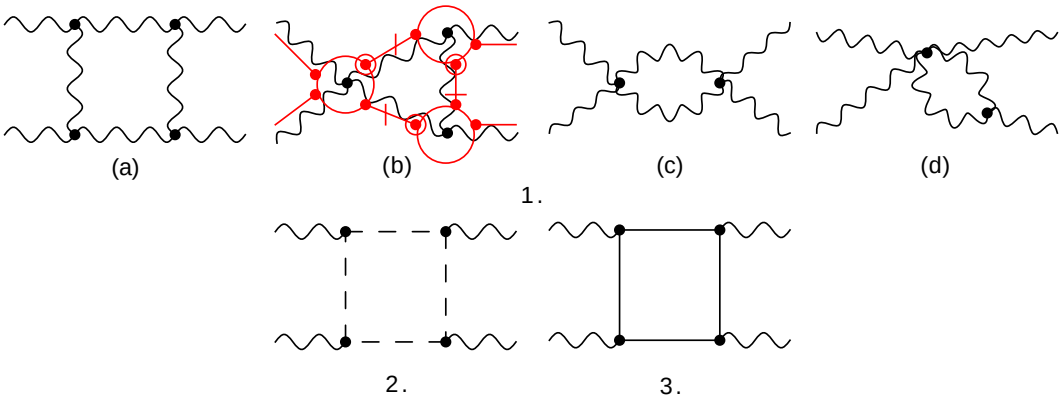

Figure 3.7: $V_1\,V_2\,V_3\,V_4$ diagrams at 1-hoop.

1. V−propagators: There are four non-zero diagrams in this class. After doing the relevant algebra and including the permutations of $\frac{y_i}{y_j}$−factors, we get:

[8]Recall from Section 3.2.3 that the V^4 term appearing in the action is proportional to $f_{ijp}f_{klp}V_1^iV_2^jV_3^kV_4^l$.

(a) $(VVV)^4$ vertices:

$$
\begin{aligned}
&-\frac{c_A}{2}g^4\int d^8\theta\int dy_{1,2,3,4}\frac{V_1V_2V_3V_4}{y_{12}\,y_{23}\,y_{34}\,y_{41}}\Bigg[\big(\mathcal{A}_2(p_4)-p_2^2\mathcal{A}_3(-p_3,p_4)\big)\times\\
&\times\left(\frac{1}{2}\Big\uparrow\frac{y_1}{y_2}+\frac{y_1}{y_4}\Big\uparrow-\Big\uparrow\frac{y_1}{y_3}\Big\uparrow\right)+\mathcal{A}_3(-p_3,p_4)\times\\
&\Bigg\{p_1^2\left(\frac{1}{4}\Big\uparrow 3\frac{y_1}{y_2}-2\frac{y_1}{y_3}-\frac{y_3^2}{y_1^2}-\frac{y_3^2}{y_1\,y_4}+\frac{y_3^3}{y_1^2\,y_4}\Big\uparrow\right)+\\
&+p_2^2\left(-2+\frac{1}{4}\Big\uparrow 4\frac{y_1}{y_2}-3\frac{y_1}{y_3}+\frac{y_3\,y_4}{y_1^2}-\frac{y_4^2}{y_1^2}+\frac{y_4^2}{y_1\,y_2}\Big\uparrow\right)+\\
&+2p_1\cdot p_2\left(2-\frac{1}{4}\Big\uparrow 4\frac{y_1}{y_2}-\frac{y_1}{y_3}+\frac{y_3^2}{y_1^2}-\frac{y_3^2}{y_1\,y_4}-\frac{y_3\,y_4}{y_1^2}\Big\uparrow\right)\Bigg\}+\\
&+p_1^2(p_1+p_2)^2\mathcal{A}_4(p_2,p_2+p_3,-p_1)\times\\
&\times\left(-4+\frac{1}{4}\Big\uparrow 5\frac{y_1}{y_2}+2\frac{y_1}{y_3}-\frac{y_3^2}{y_1^2}-\frac{3y_3^2}{y_1\,y_4}+\frac{y_3^3}{y_1^2\,y_4}\Big\uparrow\right)\Bigg]
\end{aligned}
\tag{3.3.11}
$$

(b) $(VVVV)-(VVV)^2$ vertices:

$$
\begin{aligned}
&-\frac{c_A}{2}g^4\int d^8\theta\int dy_{1,2,3,4}\frac{V_1V_2V_3V_4}{y_{12}\,y_{23}\,y_{34}\,y_{41}}\Bigg[\mathcal{A}_2(p_4)\left(-8+2\Big\uparrow\frac{y_1}{y_3}\Big\uparrow\right)+\\
&+p_3^2\,\mathcal{A}_3(-p_3,p_4)\Big\uparrow\frac{1}{y_{12}}\left(3y_{41}+\frac{y_{23}y_1}{y_3}+\frac{y_{12}y_3}{y_4}-\frac{y_{41}y_4}{y_2}+\frac{y_{41}y_4^2}{y_2^2}\right)\Big\uparrow\Bigg]
\end{aligned}
\tag{3.3.12}
$$

(c) $(VVVV)^2$ vertices:

$$
-\mathcal{A}_2(p_4)\times\frac{1}{2}\frac{c_A}{2}g^4\int d^8\theta\int dy_{1,2,3,4}\frac{V_1V_2V_3V_4}{y_{12}\,y_{23}\,y_{34}\,y_{41}}\left(4-\frac{1}{2}\Big\uparrow\frac{y_1}{y_2}+\frac{y_1}{y_4}\Big\uparrow\right)
\tag{3.3.13}
$$

(d) $(VVVVV)-(VVV)$ vertices:

$$
-\mathcal{A}_2(p_4)\times\frac{1}{2}c_Ag^4\int d^8\theta\int dy_{1,2,3,4}\frac{V_1V_2V_3V_4}{y_{12}\,y_{23}\,y_{34}\,y_{41}}\left(4-\Big\uparrow\frac{y_1}{y_3}\Big\uparrow\right)
\tag{3.3.14}
$$

2. $(b,c)-$propagators: There are sixteen diagrams that combine to give

(after dropping the term with a projective integrand):

$$\frac{c_A}{16}g^4\int d^8\theta\int dy_{1,2,3,4}\frac{V_1V_2V_3V_4}{y_{12}\,y_{23}\,y_{34}\,y_{41}}\Bigg[\big(\mathcal{A}_2(p_4)-p_2^2\mathcal{A}_3(-p_3,p_4)\big)\times$$
$$\times\left(2\Big\uparrow\frac{y_1}{y_2}+\frac{y_1}{y_4}\Big\uparrow\right)+\Bigg\{\mathcal{A}_3(-p_3,p_4)\frac{1}{4}\left(p_1^2\Big\uparrow\left(\frac{y_{24}}{y_{41}}\right)^2\Big\uparrow+\right.$$
$$+p_2^2\Big\uparrow\left(\frac{y_{13}}{y_{41}}\right)^2\Big\uparrow-2p_1\cdot p_2\Big\uparrow\frac{y_{23}}{y_{14}}+\frac{y_{12}}{y_{41}}\frac{y_{34}}{y_{41}}\Big\uparrow\Bigg)+$$
$$\left.+p_1^2(p_1+p_2)^2\mathcal{A}_4(p_2,p_2+p_3,-p_1)\frac{1}{4}\Big\uparrow\left(\frac{y_{12}}{y_{41}}\right)^2\Big\uparrow\right\}\times$$
$$\times\left(2\Big\uparrow\frac{y_1}{y_2}+\frac{y_1}{y_4}\Big\uparrow+\frac{y_{12}\,y_{23}\,y_{34}\,y_{41}}{y_1\,y_2\,y_3\,y_4}\right)\Bigg] \tag{3.3.15}$$

3. $\Upsilon-$propagators: Without doing any new calculations, we can write the result, which is similar to (3.3.15):

$$-c_R\,g^4\int d^8\theta\int dy_{1,2,3,4}\frac{V_1V_2V_3V_4}{y_{12}\,y_{23}\,y_{34}\,y_{41}}\Bigg[\big(\mathcal{A}_2(p_4)-p_2^2\mathcal{A}_3(-p_3,p_4)\big)+$$
$$+\mathcal{A}_3(-p_3,p_4)\frac{1}{4}\left(p_1^2\Big\uparrow\left(\frac{y_{24}}{y_{41}}\right)^2\Big\uparrow+p_2^2\Big\uparrow\left(\frac{y_{13}}{y_{41}}\right)^2\Big\uparrow-\right.$$
$$\left.-2p_1\cdot p_2\Big\uparrow\frac{y_{23}}{y_{14}}+\frac{y_{12}}{y_{41}}\frac{y_{34}}{y_{41}}\Big\uparrow\right)+$$
$$+p_1^2(p_1+p_2)^2\mathcal{A}_4(p_2,p_2+p_3,-p_1)\frac{1}{4}\Big\uparrow\left(\frac{y_{12}}{y_{41}}\right)^2\Big\uparrow\Bigg]. \tag{3.3.16}$$

3.3.2 1-hoop β-function

The divergences proportional to the terms in the vector hypermultiplet's action are absorbed via wavefunction (V) and coupling constant (g) renormalization following the usual well-known procedure.

$$\mathrm{Z-factor\,for}\,V:\quad V_R=\sqrt{Z_V}V\Rightarrow Z_V^{(1)}=Z_2^{(1)} \tag{3.3.17}$$

$$\mathrm{Z-factor\,for}\,g:\quad g_R=Z_g g\mu^\epsilon\Rightarrow Z_g^{(1)}=Z_3^{(1)}\left(Z_V^{(1)}\right)^{-3/2} \tag{3.3.18}$$

where, the $Z_n^{(1)}$'s are the $Z-$factors for corresponding $n-$point vertex terms in the action, *i.e.*, $\mathcal{S}(V_R^n) = Z_n \mathcal{S}(V^n)$. To figure these out, we combine the divergent term of $\mathcal{A}_2$ occurring in all $n-$point functions. The result is:

$$\begin{aligned}
2-\text{point}\,((3.3.4)\,\&\,(3.3.5)): &\quad \frac{(c_A-c_R)g^2}{4\pi^2\epsilon}\int d^8\theta \int dy_{1,2}\frac{V_1V_2}{y_{12}\,y_{21}};\\
3-\text{point}\,((3.3.6)-(3.3.10)): &\quad \frac{(c_A-c_R)g^3}{4\pi^2\epsilon}\int d^8\theta \int dy_{1,2,3}\frac{V_1V_2V_3}{y_{12}\,y_{23}\,y_{31}};\\
4-\text{point}\,((3.3.11)-(3.3.16)): &\quad \frac{(c_A-c_R)g^4}{4\pi^2\epsilon}\int d^8\theta \int dy_{1,2,3,4}\frac{V_1V_2V_3V_4}{y_{12}\,y_{23}\,y_{34}\,y_{41}}.\\
\Rightarrow \text{Z}-\text{factors for Vertices}: &\quad Z_2^{(1)}=Z_3^{(1)}=Z_4^{(1)}=1+\frac{(c_A-c_R)g^2}{4\pi^2\epsilon}
\end{aligned} \tag{3.3.19}$$

Finally, plugging (3.3.19) in (3.3.17) & (3.3.18), we get:

$$Z_V^{(1)} = 1+\frac{(c_A-c_R)g^2}{4\pi^2\epsilon}; \tag{3.3.20}$$

$$Z_g^{(1)} = 1-\frac{(c_A-c_R)g^2}{8\pi^2\epsilon}. \tag{3.3.21}$$

Using the coupling constant renormalization factor, the 1-loop β-function for $\mathcal{N}=2$ SYM coupled to matter in representation R is easily calculated:

$$\beta^{(1)}_{\mathcal{N}=2} = g^3\frac{\partial\left(\epsilon Z_g^{(1)}\right)}{\partial g^2} = -\frac{(c_A-c_R)g^3}{8\pi^2}\left(=-\frac{(2N-c_R)g^3}{8\pi^2}\quad \text{for SU}(N)\right). \tag{3.3.22}$$

For $\mathcal{N}=4$ SYM, it is trivial to see that the β-function vanishes at 1-loop since the scalar hypermultiplet is in adjoint representation (so $c_R=c_A$) implying

$$\beta^{(1)}_{\mathcal{N}=4}=0.$$

3.3.3 2-hoops Finiteness

We recall that any $n-$point function involving external scalar hyperfields (including ghosts) can not be divergent and hence the hyperfields b, c & Υ and other terms in actions (3.2.6) & (3.2.14) are not renormalized. Thus, we need to calculate just the vector self-energy corrections to compute the β-function at two-hoops. We can read off the Z_g-factor from $g\,\bar{b}\,V c$ (or $g\bar{\Upsilon}V\Upsilon$ in case of $\mathcal{N}=4$ SYM) vertex at 2-hoops (which is true even in the case of 1-hoop as

can be easily checked.):

$$Z_g^{(2)} = \left(Z_V^{(2)}\right)^{-\frac{1}{2}}. \tag{3.3.23}$$

In other words, gV is not renormalized which means that the vector hyperfield V can not have any non-linear renormalization since the coupling constant g is always linearly renormalized. This is the same result as in the background field formalism as far as renormalization is concerned.

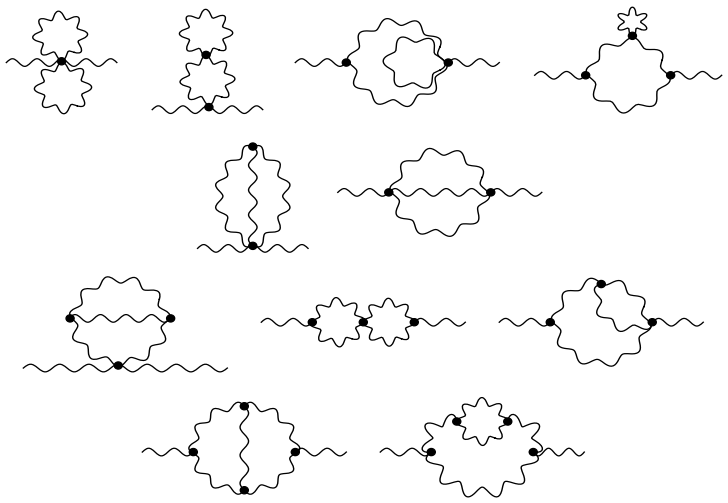

Figure 3.8: Vector self-energy diagrams at 2-hoops with only $V-$propagators.

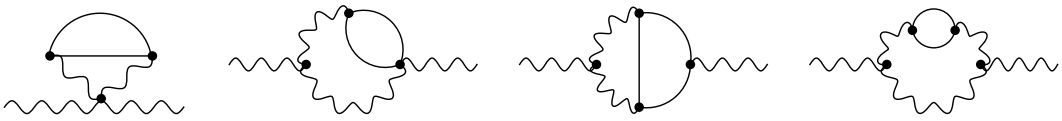

Figure 3.9: Vector self-energy diagrams at 2-hoops including b, c & Υ-propagators.

There are a lot of diagrams to consider at 2-loops (at first sight) but their evaluation is not any more difficult than those at 1-loop. Firstly, we consider the 11 diagrams shown in Figure 3.8 which have only vector propagators. The first two rows in the figure show diagrams that vanish due to d-algebra, *i.e.*, insufficient number of $d^4_{a\vartheta}$'s. The remaining 5 diagrams require some y-calculus and we find that none of their divergent terms survive and only the last two of them have finite terms. The vanishing of divergences for these two diagrams is shown in the Appendix A.

Secondly, there are a lot more diagrams having ghost and scalar propagators but only 4 classes of such diagrams (Figure 3.9) need to be examined in

'detail'. The rest of such diagrams vanish either due to the d-algebra or emergence of $y\delta(y)$ (even $y^2\delta(y)$) factor (mainly in diagrams having only $\bar{b}Vc-$type vertices). Again, after doing some y-calculus we see that these four classes of diagrams also do not have any divergences. Thus, there are no divergent vector self-energy corrections at 2-hoops, *i.e.*, $Z_V^{(2)}=1$ and hence for both $\mathcal{N}=2$ SYM coupled to matter in any representation and $\mathcal{N}=4$ SYM,

$$\beta^{(2)} \sim \partial_{g^2}\left(Z_g^{(2)}\right) = 0\,.$$

3.4 Massive Scalar Hypermultiplet

Introducing central charges in superalgebras leads to the possibility of having massive multiplets as 'short' as the massless ones. The central charges in 4D, $\mathcal{N}=2$ superspace have been dealt directly in both projective [15, 32] and harmonic [17, 20, 54] hyperspaces.

Having dealt with massless scalar and vector hypermultiplets, for the sake of completeness, we now extend such an analysis to the massive case. In the next section, we review the projective hyperspace with central charges. Then we discuss the massive scalar hypermultiplet in detail from the 4D perspective. Next, we show that the dimensional reduction of a massless hypermultiplet from 6D reproduces all the 4D results rather trivially. Finally, we present a simple 1-hoop calculation using Feynman rules similar to the massless case.

3.4.1 Projective Hyperspace with Central Charges

The centrally extended algebra of covariant derivatives then reads[9]:

$$\{d_{\theta,\alpha}, \bar{d}_{\vartheta,\dot{\beta}}\} = \partial_{\alpha\dot{\beta}} \tag{3.4.1}$$
$$\{d_{\theta,\alpha}, d_{\vartheta,\beta}\} = \bar{m}C_{\alpha\beta} \tag{3.4.2}$$
$$\{\bar{d}_{\theta,\dot{\alpha}}, \bar{d}_{\vartheta,\dot{\beta}}\} = -mC_{\dot{\alpha}\dot{\beta}} \tag{3.4.3}$$
$$[d_{\vartheta,\alpha}, d_y] = -d_{\theta,\alpha} \tag{3.4.4}$$
$$[\bar{d}_{\vartheta,\dot{\alpha}}, d_y] = -\bar{d}_{\theta,\dot{\alpha}} \tag{3.4.5}$$

Such an algebra can be incorporated in the superspace by introducing additional bosonic coordinates corresponding to the central charges. Then, requiring a trivial dependence of the hyperfields on these coordinates leads to a volume element same as the one when $m=0$. However, this generates explicit appearances of θ's in the Lagrangian (for example, [20]).

[9] m is in general complex but for our purposes, its imaginary part plays no role.

There are two alternative manifestly covariant approaches to deal with non-zero m. One (simplest) approach is the dimensional reduction of $d = 6, \mathcal{N} = 1$ massless multiplets to $d = 4$, $\mathcal{N} = 2$ massive ones. Since six-dimensional projective superspace exists [55] and is similar to the projective hyperspace in 4D, the main results can be written down just by inspection. We will show that this is the case in Section 3.4.3, where we will compare the results derived via another approach.

In this second approach, we work in $d = 4$ and turn d's into covariant derivatives: $\mathcal{D} = d + A$, where A is an Abelian connection that has acquired a vev, *i.e.*, $A \propto m$. This avoids the explicit θ's in the Lagrangian that are now hidden inside the connections [32, 54]. So, the starting point for the simplest example of a massive hypermultiplet is a massless scalar hypermultiplet coupled to a U(1) vector hypermultiplet.

Having said that, let us repeat here the relevant information about massless hypermultiplets. The following is valid in both 4D & 6D with a few obvious changes, some of which will be pointed out later. A massless scalar hypermultiplet represented by a complex 'arctic' projective hyperfield (Υ) has the following on-shell expansion containing complex scalars $A\,\&\,B$ and Weyl spinors $\chi\,\&\,\tilde{\chi}$:

$$\Upsilon = (A + yB) + \left(\theta\chi + \bar{\theta}\bar{\tilde{\chi}}\right) + \theta\partial B\bar{\theta} \tag{3.4.6}$$

and their corresponding equations of motion follow from $d_y^2\bar{\Upsilon}(\Upsilon) = 0$, which in turn follow from the action:

$$\mathcal{S}_\Upsilon = -\int dx d^4\theta dy \bar{\Upsilon}\Upsilon. \tag{3.4.7}$$

The vector hypermultiplet is represented by a real 'tropical' projective hyperfield (V) and since we are mainly interested in the vevs of Abelian connections, we give below only the vev structure of V (read from the full expression for V in Wess-Zumino gauge (3.2.9)) to which the connections will eventually get related:

$$V = \tfrac{1}{y}\left(\theta^2\bar{m} - \bar{\theta}^2 m\right). \tag{3.4.8}$$

Finally, the coupling of these two hypermultiplets is simply given by:

$$\mathcal{S}_{\Upsilon-V} = -\int dx d^4\theta dy \bar{\Upsilon} e^V \Upsilon. \tag{3.4.9}$$

These are all the massless ingredients we need to construct the massive scalar hypermultiplet.

3.4.2 4D Approach

Action. From the arguments above, it follows that we should be able to represent a massive scalar hypermultiplet by a complex projective hyperfield $\hat{\Upsilon}$ whose quadratic action should be equivalent to (3.4.9):

$$\mathcal{S}_{\hat{\Upsilon}} = -\int dx d^4\theta dy \bar{\hat{\Upsilon}}\hat{\Upsilon} = -\int dx d^4\theta dy \bar{\Upsilon} e^V \Upsilon. \tag{3.4.10}$$

The equations of motion for $\hat{\Upsilon}\,\&\,\Upsilon$ can be derived in a way similar to the massless case and they read

$$d_y^2 \bar{\hat{\Upsilon}} = \mathcal{D}_y^2 \bar{\Upsilon} = \int \frac{dy_2}{y_{12}} \bar{\Upsilon}_2 e^{V_2} = 0. \tag{3.4.11}$$

We know the massive equations of motion (Klein-Gordon and Dirac equations) for the component fields and the expression for vev of V (3.4.8), so it is a simple algebraic exercise to get the (new) on-shell form of Υ:

$$\Upsilon = (A + yB) + \left(\theta\chi + \bar{\theta}\bar{\tilde{\chi}}\right) + \left(\theta^2 m - \bar{\theta}^2 \bar{m}\right) B + \theta\partial B\bar{\theta}. \tag{3.4.12}$$

This form (obviously) gives the correct massless limit (3.4.6) when $m = 0$. Plugging this expression in the action gives the usual kinetic terms for the component fields and the mass terms have an expected appearance:

$$\sim \int dx \left(m\chi\chi + \bar{m}\bar{\tilde{\chi}}\bar{\tilde{\chi}}\right) + m\bar{m}\left(\bar{A}A + \bar{B}B\right).$$

It is important to note that if we had naïvely used the (3.4.6) in above calculation, we would have gotten a wrong sign for B's mass term! This small calculation makes it clear that we now have a correct representation for the massive scalar hypermultiplet. Thus, we can assign[10] $\hat{\Upsilon} = e^{V_+}\Upsilon$ and $\bar{\hat{\Upsilon}} = \bar{\Upsilon}e^{V_-}$ such that their on-shell y-dependence remains the same as that of the massless hyperfields, *i.e.*, $\left[0^{\uparrow}\right]$ & $[1_{\downarrow}]$, respectively.

Moreover, in this case we can also figure out what $\mathcal{D}$'s look like explicitly.

[10] $V = V_+[0^{\uparrow}] + V_-[0_{\downarrow}]$.

Comparing the two forms of equations in (3.4.11) (with $\bar{\Upsilon}$), we get:

$$\mathcal{D}_y^2\bar{\Upsilon} = \partial_y^2\bar{\Upsilon} - \frac{2\left(\theta^2\bar{m} - \bar{\theta}^2 m\right)}{y^2}\left(\partial_y\bar{\Upsilon} - \frac{\bar{\Upsilon}}{y}\right) - \frac{2\,\theta^2\bar{\theta}^2 m\bar{m}}{y^4}\bar{\Upsilon} \tag{3.4.13}$$

$$\Rightarrow \mathcal{D}_y = \partial_y + A_y = \partial_y - \frac{\left(\theta^2\bar{m} - \bar{\theta}^2 m\right)}{y^2} \tag{3.4.14}$$

$$\Rightarrow A_y = d_y \int dy' \frac{V'}{(y-y')}. \tag{3.4.15}$$

We can also find the expressions for other connections using equations (3.4.4) & (3.4.5) in the gauge $A_\vartheta = \bar{A}_\vartheta = 0$:

$$A_\theta = -d_\vartheta A_y = \frac{\bar{m}\theta}{y} \quad \& \quad \bar{A}_\theta = -\bar{d}_\vartheta A_y = \frac{-m\bar{\theta}}{y}. \tag{3.4.16}$$

These obviously satisfy the equations (3.4.2) & (3.4.3) as can be easily checked using the expressions $d_\vartheta = \partial_\vartheta + y\partial_\theta + \bar{\theta}\partial_x$ and $\bar{d}_\vartheta = \bar{\partial}_\vartheta + y\bar{\partial}_\theta + \partial_x\theta$ in reflective representation. This completes the basic construction of a massive scalar hyperfield.

The coupling of this massive hypermultiplet to a non-Abelian vector is a straightforward generalization similar to the massless case:

$$\mathcal{S}_{\hat{\Upsilon}-\hat{V}} = -\int dx d^4\theta dy \bar{\hat{\Upsilon}} e^{\hat{V}} \hat{\Upsilon}. \tag{3.4.17}$$

Note that having a central charge in the superalgebra does not make the vector hypermultiplet massive! This is because $\int d^2\theta d^2\vartheta\, W^2 \xrightarrow{m\neq 0} \int d^2\theta d^2\vartheta (W+m)^2 = \int d^2\theta d^2\vartheta\, W^2$. The equality holds because $\int d^2\theta d^2\vartheta\, W$ is a total spacetime derivative due to the Bianchi identity $d_\theta^2 W = \bar{d}_\theta^2 \overline{W}$.

Propagator. The quantization of (3.4.10) is almost identical to that of the massless case. First, we need to rewrite the massive scalar hyperfield in terms of a generic unconstrained hyperfield:

$$\hat{\Upsilon}(y_2)\left[0^\uparrow\right] = d_{2\vartheta}^4 \int dy_1 \frac{1}{y_{12}} \Phi(y_1)\left[0^\uparrow_\downarrow\right]$$

$$\text{and,} \quad \bar{\hat{\Upsilon}}(y_2)\left[1_\downarrow\right] = d_{2\vartheta}^4 d_{y_2}^2 \int dy_1 \frac{1}{y_{21}} \bar{\Phi}(y_1)\left[0^\uparrow_\downarrow\right].$$

Then, we add source terms to the action and convert the $d^4\theta$ integral to $d^8\theta$ integral by rewriting $\hat{\Upsilon}$ using above relations:

$$\mathcal{S}_{\hat{\Upsilon}-\hat{J}} = -\int dx\, d^8\theta \int dy_1 \left[d^2_{y_1} \int dy_3 \frac{\bar{\Phi}_3}{y_{13}} d^4_{1\vartheta} \int dy_2 \frac{\Phi_2}{y_{21}} + \right. \\ \left. + \bar{\hat{J}}_1 \int dy_2 \frac{\Phi_2}{y_{21}} + d^2_{y_1} \int dy_3 \frac{\bar{\Phi}_3}{y_{13}} \hat{J}_1 \right] \tag{3.4.18}$$

where the sources $\hat{J}$ & $\bar{\hat{J}}$ are generic projective hyperfields. The equation of motion for $\hat{\Upsilon}$ with the source reads:

$$d^4_{1\vartheta} \int dy_1 \frac{d^2_{y_1} \hat{\Upsilon}_1}{y_{13}} = -d^4_{1\vartheta} \int dy_1 d^2_{y_1} \left(\frac{1}{y_{13}} \right) \hat{J}_1. \tag{3.4.19}$$

The difference with respect to the massless case arises at this stage due to the presence of central charges in the superalgebra, which gives the following modified identity:

$$d^4_\vartheta d^2_y d^4_\vartheta = (\Box - 2m\bar{m})\, d^4_\vartheta.$$

Using this identity in (3.4.19) leads us to the following equations:

$$(\Box - 2m\bar{m})\, \hat{\Upsilon}_3 = -\, d^4_{3\vartheta} \int dy_1 \frac{2\hat{J}_1}{y^3_{13}} \tag{3.4.20}$$

$$\text{Similarly, } (\Box - 2m\bar{m})\, \bar{\hat{\Upsilon}}_2 = -\, d^4_{2\vartheta} \int dy_1 \frac{2\bar{\hat{J}}_1}{y^3_{21}}. \tag{3.4.21}$$

Plugging these equations back in action (3.4.18), we get:

$$\mathcal{S}_{\hat{\Upsilon}-\hat{J}} = \int dx\, d^8\theta\, dy_1\, dy_2 \left[\bar{\hat{J}}_1 \frac{1}{y^3_{21}} \frac{1}{\frac{1}{2}(\Box - 2m\bar{m})} \hat{J}_2 \right]. \tag{3.4.22}$$

This leads to the expected change in the massless propagator to give us the massive propagator:

$$\left\langle \hat{\Upsilon}(1) \bar{\hat{\Upsilon}}(2) \right\rangle = -\frac{d^4_{1\vartheta} d^4_{2\vartheta}}{y^3_{12}} \frac{1}{\frac{1}{2}\Box - m\bar{m}} \delta^8(\theta_{12}) \delta(x_{12}). \tag{3.4.23}$$

Vertices. As in the massless case, there are no self-interacting renormalizable vertices for massive scalar hypermultiplet. The interactions appear purely with the coupling to a vector as seen in action (3.4.17). That means the ver-

tices look similar to the massless case:

$$\bar{\hat{\Upsilon}}^i \hat{V}^{j_1} ... \hat{V}^{j_n} \hat{\Upsilon}^k \rightarrow \int d^4\theta \int dy \left(i \overset{j_1}{\vert} \cdots \overset{j_n}{\vert} k \right)$$

where, the group theory factor shown in parentheses is for adjoint representation.

3.4.3 6D Approach

We now explain the simpler method for obtaining a massive scalar hypermultiplet in $d = 4$ via dimensional reduction of a six-dimensional massless scalar multiplet [55]. First of all, we dimensionally reduce the bosonic coordinates from 6D $\left(X^{M=0...5}\right)$ to 4D $(x^{\mu=0...3})$ by defining a complex coordinate:

$$z(\bar{z}) = \frac{1}{\sqrt{2}} \left[X^4 + (-)iX^5\right] \quad \Rightarrow \quad \partial(\bar{\partial}) \equiv \partial_z(\partial_{\bar{z}}) = \frac{1}{\sqrt{2}} \left[\partial_4 - (+)i\partial_5\right] \tag{3.4.24}$$

and demanding that the corresponding momenta equal the 4D central charges:

$$p = -i\partial = m \quad \& \quad \bar{p} = -i\bar{\partial} = \bar{m}.$$

The 6D d'Alambertian then reduces to:

$$\Box_{\underline{6}} = \partial^M \partial_M = \partial^\mu \partial_\mu + 2\partial\bar{\partial} = \Box_{\underline{4}} - 2m\bar{m}. \tag{3.4.25}$$

Secondly, we reduce the fermionic coordinates in 6D, which are represented by Weyl spinors of SU*(4) to 4D coordinates, which are represented by dotted and undotted Weyl spinors of SL(2,C):

$$\Theta^{\tilde{\alpha}} = \begin{pmatrix} \theta^\alpha \\ \bar{\theta}^{\dot{\alpha}} \end{pmatrix} \tag{3.4.26}$$

with similar relation holding true for ϑ's. The charge conjugation for Θ works as follows:

$$\bar{\Theta}^{\tilde{\alpha}} \equiv C^{\tilde{\alpha}}{}_{\dot{\tilde{\beta}}} \bar{\Theta}^{\dot{\tilde{\beta}}} = \begin{pmatrix} \theta^\alpha \\ -\bar{\theta}^{\dot{\alpha}} \end{pmatrix}. \tag{3.4.27}$$

The $d = 6$, $\mathcal{N} = (1, 0)$ algebra of supercovariant derivatives is equivalent to the $d = 4$, $\mathcal{N} = 2$ algebra in equations (3.4.1)-(3.4.3), after the dimensional reduction. Furthermore, we can express a vector using just spinorial indices in 6D too:

$$V_{\tilde{\alpha}\tilde{\beta}} = \frac{1}{2} \begin{pmatrix} \bar{v}\, C_{\alpha\beta} & v_{\alpha\dot{\beta}} \\ v_{\dot{\alpha}\beta} & v\, C_{\dot{\alpha}\dot{\beta}} \end{pmatrix} \tag{3.4.28}$$

where $v\,(\bar{v}) \sim -i\,[V_4 + (-)iV_5]$.

We are now ready to deal with the 6D massless multiplets. As in $d = 4$, the massless scalar hypermultiplet is represented by a projective arctic hyperfield $\Upsilon_{\underline{6}}$. Using the (bi)spinor matrices defined above, we can reduce the $\Upsilon_{\underline{6}}$ (3.4.6) to 'massive' hypermultiplet in 4D:

$$\begin{aligned} \Upsilon_{\underline{6}} &= (A + yB) + \Theta\Xi + \bar{\Theta}^{\tilde{\alpha}}\partial_{\tilde{\alpha}\tilde{\beta}}B\Theta^{\tilde{\beta}} \\ \Rightarrow \Upsilon_{\underline{4}} &= (A + yB) + \left(\theta\chi + \bar{\theta}\bar{\tilde{\chi}}\right) + \left(\bar{\theta}^{\dot{\alpha}}\partial_{\alpha\dot{\alpha}}B\theta^{\alpha} + \theta^2 mB - \bar{\theta}^2\bar{m}B\right), \end{aligned} \tag{3.4.29}$$

which is the same as in (3.4.12). A vector hypermultiplet in $d = 6$ is again represented by a projective tropical hyperfield $V_{\underline{6}}$ and its lowest $\Theta-$component (in Wess-Zumino gauge) looks like:

$$V_{\underline{6}} = \frac{\bar{\Theta}^{\tilde{\alpha}}A_{\tilde{\alpha}\tilde{\beta}}\Theta^{\tilde{\beta}}}{y} \Rightarrow V_{\underline{4}} = \frac{1}{y}\left(\bar{\theta}^{\dot{\alpha}}A_{\alpha\dot{\alpha}}\theta^{\alpha} + \theta^2\bar{\phi} - \bar{\theta}^2\phi\right). \tag{3.4.30}$$

If the scalar field ϕ develops a vev, then the above equation is identical to (3.4.8). Moreover, the action of $\Upsilon_{\underline{6}}$ coupled to $V_{\underline{6}}$ is given by (3.4.9) so the 6D hyperfield's reduction to 4D reproduces the same massive action derived in Section 3.4.2.

Now the propagator for $\Upsilon_{\underline{6}}$ is similar to that of the massless scalar hypermultiplet in 4D and the reduction to massive case is straightforward owing to (3.4.25):

$$\begin{aligned} \left\langle \Upsilon_{\underline{6}}(1)\bar{\Upsilon}_{\underline{6}}(2)\right\rangle &= -\frac{d^4_{1\vartheta}d^4_{2\vartheta}\delta^8(\Theta_{12})}{y^3_{12}}\frac{\delta(X_{12})}{\frac{1}{2}\Box_{\underline{6}}} \\ \Rightarrow \left\langle \Upsilon_{\underline{4}}(1)\bar{\Upsilon}_{\underline{4}}(2)\right\rangle \equiv \left\langle \hat{\Upsilon}(1)\bar{\hat{\Upsilon}}(2)\right\rangle &= -\frac{d^4_{1\vartheta}d^4_{2\vartheta}\delta^8(\theta_{12})}{y^3_{12}}\frac{\delta(x_{12})}{\frac{1}{2}\Box_{\underline{4}} - m\bar{m}}, \end{aligned} \tag{3.4.31}$$

which is equivalent to (3.4.23) derived from the 4D perspective.

3.4.4 Sample Calculation

The Feynman rules are almost the same as those for the massless case. The only difference is the following modified identity:

$$d^4_{1\vartheta}d^4_{2\vartheta}d^4_{1\vartheta} = y^2_{12}\left[\left(\tfrac{1}{2}\Box - m\bar{m}\right) + y_{21}\left(\bar{d}_{2\theta}d_x d_{2\theta} + md^2_{2\theta} - \bar{m}\bar{d}^2_{2\theta}\right) + y^2_{12}d^4_{2\theta}\right]d^4_{1\vartheta} \tag{3.4.32}$$

The non-renormalization theorem for massless scalar hypermultiplet holds for the massive case also for straightforward reasons.

One-hoop correction to vector 2−point function (Figure 3.10) due to the

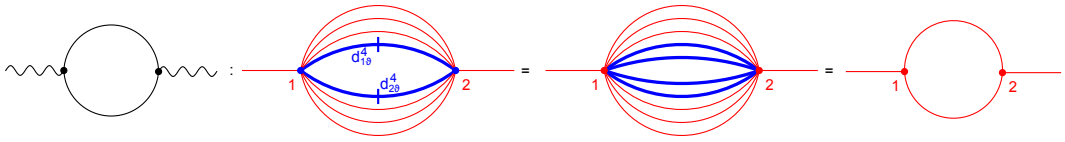

Figure 3.10: One-hoop massive scalar example with d-algebra and y-calculus shown. [A blue (thick) line with a cut represents a $\delta^8(\theta_{12})$.]

coupling to a massive scalar is simple to calculate and looks same (modulo the momentum integral) as the massless case:

$$-\hat{\mathcal{A}}_2(p;m) \times c_R\, g^2 \int d^8\theta \int dy_{1,2} \frac{\hat{V}_1 \hat{V}_2}{y_{12}\, y_{21}}. \tag{3.4.33}$$

The momentum integral is a standard integral and evaluates to (with $D = 4 - 2\epsilon$):

$$\begin{aligned}\hat{\mathcal{A}}_2 &= \int \frac{d^D k}{(2\pi)^D} \frac{1}{\left(\frac{1}{2}k^2 - m\bar{m}\right)\left(\frac{1}{2}(k+p)^2 - m\bar{m}\right)} \\ &= \frac{1}{4\pi^2}\left[\frac{1}{\epsilon} - \gamma_E + 2 - \ln\left(\frac{2m\bar{m}}{\mu^2}\right) - \sqrt{1 + \frac{8m\bar{m}}{p^2}}\, \ln\left(\frac{1 + p/\sqrt{p^2 + 8m\bar{m}}}{1 - p/\sqrt{p^2 + 8m\bar{m}}}\right)\right].\end{aligned}$$

3.5 Background Field Formalism

The construction of background field formalism for $\mathcal{N} = 2$ SYM in projective hyperspace is an interesting problem. Such a formalism is desirable for any (non-)supersymmetric theory as it simplifies (loop) calculations and even intermediate steps respect gauge covariance. A major obstacle in solving this problem for the $\mathcal{N} = 2$ case seems to be the lack of knowledge relating the gauge connections to the tropical hyperfield V, which describes the SYM multiplet for all practical purposes.

We note that the closely related $\mathcal{N} = 2$ harmonic superspace doesn't encounter this issue as the hyperfield, $V^{(++)}$ describing the SYM multiplet is itself a connection, $A_{\bar{y}}$. In fact, background field formalism in harmonic superspace has quite a straightforward construction [40, 56]. Although the construction has some subtleties, it has been refined in a series of papers along with relevant calculations [39, 41, 42, 57–60].

In this section, we solve the problem of constructing the background field formalism in projective superspace without the need for knowing the connections explicitly in terms of V. This is possible by choosing the background

fields to be in a 'real' representation ($A_y = 0$) and the quantum fields to be in the 'analytic' representation ($A_\vartheta = 0$). This is reminiscent of the quantum-chiral but background-real representation used in $\mathcal{N} = 1$ superspace [61]. What this does is make the effective action independent of A_y and dependent on background fields (like A_ϑ) with 'dimension' greater than 0 (since the lowest one is a spinor). Non-existence of 0-dimension background fields (like A_y) is a crucial requirement for the non-renormalization theorems to hold as discussed in [51]. This directly leads to a proof of finiteness beyond 1-loop. (A different approach for proof of finiteness has been discussed in [62].)

The coupling of quantum fields to background fields comes through the former's projective constraint alone, which simplifies the vertex structure a lot. The calculations are also simplified at 1-hoop as most y-integrals turn out to be trivial since the background fields have trivial y-dependence. This means that the y-integration effectively vanishes from the effective action and as expected from the supergraph rules, only one θ-integration survives at the end of the calculations. We also work in Fermi-Feynman gauge so there are no IR issues to worry about while evaluating the super-Feynman graphs.

Another important aspect is the ghost structure of the theory in this background gauge. Apart from the expected Faddeev-Popov (fermionic b, c) and Nielsen-Kallosh (bosonic E) ghosts, we require two more extra ghosts, namely real bosonic X and complex fermionic R. This is in contrast to $\mathcal{N} = 1$ SYM but very similar to the harmonic treatment of $\mathcal{N} = 2$ theory. Heuristically, we can even see that such a field content would give a vanishing β-function for $\mathcal{N} = 4$: $V + [\Upsilon + (b, c) + E] + X + R = 1 + [1 + (-2) + 1] + 1 + (-2) = 0$. However, we will see that the loop contributions of V and extra ghosts have spurious divergences arising due to multiple $\delta(y)$'s. These are very similar to the 'coinciding harmonic' singularities in the harmonic case, which manifest themselves at 1-loop level via the subtleties regarding regularization of similar looking determinants. However, in our case, we do not encounter such striking similarities. Only the divergences turn out to be similar, leading to a cancellation between the vector hyperfield's contribution and that of the extra ghosts. The finite pieces in the effective action are contributed by these extra ghosts only.

This section is mostly built on the ordinary projective superspace construction of SYM already detailed in this chapter. We also continue using the 6D notation explained above to simplify some useful identities involving background covariant derivatives and moreover, the results carry over to $d = 6$, $\mathcal{N} = 1$ SYM in a trivial manner with this notation.

3.5.1 Background – Quantum Splitting

The gauge covariant derivatives, $\nabla = d + A$, describing $\mathcal{N} = 2$ SYM satisfy the following (anti-) commutation relations:

$$\{\nabla_{a\alpha}, \nabla_{b\beta}\} = -iC_{ab}\nabla_{\alpha\beta}\,, \tag{3.5.1}$$

$$[\nabla_{a\alpha}, \nabla_{\beta\gamma}] = -\epsilon_{\alpha\beta\gamma\delta}W_a^{\delta}\,, \tag{3.5.2}$$

$$\{\nabla_{a\alpha}, W_b^{\beta}\} = \mathcal{D}_{ab}\delta_{\alpha}^{\beta} - \tfrac{i}{2}C_{ab}f_{\alpha}^{\beta}\,, \tag{3.5.3}$$

$$[\nabla_{\alpha\beta}, \nabla^{\gamma\delta}] = f_{\alpha}^{[\gamma}\delta_{\beta}^{\delta]}\,, \tag{3.5.4}$$

$$[\nabla_{\vartheta\alpha}, \nabla_y] = \nabla_{\theta\alpha}\,, \quad [\nabla_{\theta\alpha}, \nabla_y] = 0\,, \tag{3.5.5}$$

where the SU(2) index $a = (\vartheta, \theta)$, $C_{\vartheta\theta} = i$, W_a^{α} and f_{α}^{β} are the field strengths, and $\mathcal{D}_{ab}$ are the triplet of auxiliary scalars. The 4D scalar chiral field strength, $W \sim -i\,(\nabla_4 - i\nabla_5)$ is related to the spinor field strength via appropriate spinor derivatives. We solve the commutation relation for ∇_ϑ by writing $\nabla_\vartheta = e^{\Omega}d_\vartheta e^{-\Omega}$, where Ω is an unconstrained complex hyperfield. We can do a background splitting of Ω (similar to $\mathcal{N} = 1$ superspace) such that

$$\nabla_\vartheta = e^{\Omega_Q}\mathcal{D}_\vartheta e^{-\Omega_Q}\,, \tag{3.5.6}$$

with $\mathcal{D}_\vartheta$ being the background covariant derivative. We can now choose 'real' representation for the background derivatives independently such that $\mathcal{A}_y = 0 \Rightarrow \mathcal{D}_y = d_y$. This simplifies the y-dependence of the connections:

$$d_y\mathcal{A}_\theta = 0\,; \quad d_y\mathcal{A}_\vartheta = -\mathcal{A}_\theta \qquad \Rightarrow \mathcal{A}_\vartheta = \mathcal{A}_\vartheta^{(0)} - y\mathcal{A}_\theta\,.$$

Since these connections have simple y-dependence, the y-integrals in the effective action can be trivially done. Moreover, the quantum part of the full covariant derivatives then can be chosen to be in 'analytic' representation, *i.e.*, $A_y \neq 0$ and $A_\vartheta = 0$.

The projective (analytic) constraint on hyperfields 'lifts' to $\nabla_\vartheta\Upsilon = 0$ so we can now define a background projective hyperfield $\mathring{\Upsilon}(\equiv \mathring{\Upsilon}_B + \mathring{\Upsilon}_Q)$ as $\Upsilon = e^{\Omega_Q}\mathring{\Upsilon}$ such that $\mathcal{D}_\vartheta\mathring{\Upsilon} = 0$. Then, the scalar hypermultiplet's action reads:

$$\mathcal{S}_\Upsilon = -\int dw\,\bar{\Upsilon}\Upsilon = -\int dw\,\bar{\mathring{\Upsilon}}e^{\bar{\Omega}_Q}e^{\Omega_Q}\mathring{\Upsilon} \equiv -\int dw\,\bar{\mathring{\Upsilon}}e^{V}\mathring{\Upsilon}\,. \tag{3.5.7}$$

The vector hyperfield V's action looks the same as in the ordinary case; the difference being that the V appearing below is only the quantum piece and

is background projective:

$$\mathcal{S}_V = \frac{\mathrm{tr}}{g^2}\int dx\, d^8\theta \sum_{n=2}^{\infty}\frac{(-1)^n}{n}\left(\prod_{i=1}^{n}\int dy_i\right)\frac{\left(e^{V_1}-1\right)\cdots\left(e^{V_n}-1\right)}{y_{12}\, y_{23}\cdots y_{n1}}\,. \tag{3.5.8}$$

We know from the discussion in previous chapter that this action should give an expression for A_y and hence the 'analytic' representation for quantum hyperfields is a consistent choice. The background dependence of V comes through the projective constraint and the background covariant derivatives only. The following identities will be useful in showing that and deriving other results in the following sections:

$$\nabla^4_\vartheta\left(\tfrac{1}{2}d_y^2\right)\nabla^4_\vartheta = \tfrac{1}{2}\widehat{\Box}\,\nabla^4_\vartheta = \left[\tfrac{1}{2}\Box - W^\alpha_\vartheta\nabla_{\theta,\alpha} + \mathcal{D}_{\vartheta\vartheta}d_y + \mathcal{D}_{\theta\vartheta}\right]\nabla^4_\vartheta\,, \tag{3.5.9}$$

$$\begin{aligned}\nabla^4_{1\vartheta}\nabla^4_{2\vartheta} = \big[&y_{12}\mathcal{D}_{\vartheta\vartheta} + \tfrac{1}{2}y_{12}^2\check{\Box} + \tfrac{1}{2}y_{12}^3\left(\nabla_{\theta,\alpha}\nabla^{\alpha\beta}\nabla_{\theta,\beta}\right.\\ &\left.+W^\alpha_\theta\nabla_{\theta,\alpha} + 2\mathcal{D}_{\theta\theta}\right) + y_{12}^4\nabla^4_{2\theta}\big]\nabla^4_{2\vartheta}\,,\end{aligned} \tag{3.5.10}$$

where $\Box = \frac{1}{2}\nabla_{\alpha\beta}\nabla^{\alpha\beta}$ is the gauge-covariant d'Alembertian and $\check{\Box} = \widehat{\Box} - 2\mathcal{D}_{\vartheta\vartheta}d_y$. As the quantum connections do not appear explicitly in the calculations, we will drop the usage of curly fonts to denote the background fields (as has been done above) and also the subscript '$_\vartheta$' on W^α_ϑ from now on.

3.5.2 Quantum

The quantization procedure in the background gauge proceeds similar to the ordinary case. The ordinary derivatives are now background-covariant derivatives so $\Box$ gets replaced by $\widehat{\Box}$ (or $\check{\Box}$) everywhere. Moreover, we need extra ghosts for the theory to be consistent in this formalism as we elaborate further in the following subsections.

Scalar and Vector. The scalar hypermultiplet is background projective but the structure of its action is still the same as in the ordinary case. That means the kinetic operator appearing in the equations of motion is d_y^2, *i.e.*, $d_y^2\Upsilon = 0$ still holds. So the derivation of the propagator performed earlier goes through after employing these changes: $d_\vartheta \to \nabla_\vartheta$ and $\Box \to \widehat{\Box}$:

$$\langle\bar{\Upsilon}(1)\Upsilon(2)\rangle = -\frac{\nabla^4_{1\vartheta}\nabla^4_{2\vartheta}}{y_{12}^3}\frac{1}{\frac{1}{2}\widehat{\Box}}\delta^8(\theta_{12})\delta(x_{12})\,. \tag{3.5.11}$$

The gauge-fixing for the vector hypermultiplet leading to Faddeev-Popov (FP) ghosts is still similar to the ordinary case and we just quote the results

with suitable modifications:

$$\mathcal{S}_{gf} = -\frac{\mathrm{tr}}{2\alpha\, g^2}\int dx\, d^8\theta\, dy_1\, dy_2\, V_1\left[\frac{y_1}{y_{21}^3}+\frac{y_2}{y_{12}^3}\right]V_2\,; \tag{3.5.12}$$

$$\mathcal{S}_{FP} = -\mathrm{tr}\int dx\, d^4\theta\, dy\,\left[\bar{b}\,c+\bar{c}\,b+(y\,b+\bar{b})\frac{V}{2}\left(c+\frac{\bar{c}}{y}\right)+...\right]. \tag{3.5.13}$$

The propagators for the FP ghosts are similar to the scalar hypermultiplet and will be written down later.

We will always work in Fermi-Feynman gauge ($\alpha = 1$) but let us derive the propagator for V with arbitrary α as this technique will be useful later. We first combine the terms quadratic in V from the above equation and the vector hypermultiplet action to get

$$\begin{aligned}\mathcal{S}_V^{(2)}+\mathcal{S}_{gf}^{(2)} &= -\frac{\mathrm{tr}}{2g^2}\int dx\, d^4\theta\, dy_1\, dy_2\, V_1\frac{1}{y_{12}^2}\left[1+\frac{1}{\alpha}\left(\frac{y_1}{y_{21}}+\frac{y_2}{y_{12}}\right)\right]\nabla_{1\vartheta}^4 V_2\\ &= -\frac{\mathrm{tr}}{2g^2}\int dx\, d^4\theta\, dy_{1,2}\, V_1\left[1+\frac{-1+y_1\delta(y_{12})}{\alpha}\right]\left(\frac{1}{2}\check{\Box}+\cdots\right)V_2\,.\end{aligned} \tag{3.5.14}$$

Then, we add a generic real source J to the quadratic gauge-fixed vector action:

$$\begin{aligned}\mathcal{S}_{V-J} &= -\frac{\mathrm{tr}}{g^2}\int dx\, d^8\theta\left\{\int dy_{1,2}\, V_1\left[1+\frac{1}{\alpha}\left(\frac{y_1}{y_{21}}+\frac{y_2}{y_{12}}\right)\right]\frac{V_2}{2y_{12}^2}-\int dy_2\, J_2V_2\right\}\\ &= -\frac{\mathrm{tr}}{g^2}\int dx\, d^4\theta\left\{\int dy_{1,2}\, V_1\left[1+\frac{-1+y_1\delta(y_{12})}{\alpha}\right]\frac{\nabla_{1\vartheta}^4V_2}{2y_{12}^2}-\int dy_2\,\mathcal{J}_2V_2\right\}\end{aligned} \tag{3.5.15}$$

Here, $\mathcal{J}$ is now defined to be (background) projective. Now, equation of motion for V reads

$$\int dy_1 V_1\left[1+\frac{-1+y_1\delta(y_{12})}{\alpha}\right]\frac{\nabla_{2\vartheta}^4}{y_{12}^2} = \mathcal{J}_2\,, \tag{3.5.16}$$

which we can solve to write V in terms of $\mathcal{J}$. This amounts to inverting the kinetic operator for V as we will see. Assuming the following ansatz for V:

$$V_1 = \int dy_0\,\frac{p+q\,\delta(y_{01})}{y_{01}^2}\frac{1}{\left(\frac{1}{2}\check{\Box}\right)^2}\mathcal{J}_0\nabla_{1\vartheta}^4 \tag{3.5.17}$$

and demanding it satisfy (3.5.16), we are led to $p = \frac{(1-\alpha)}{y_0\, y_1}$ & $q = \frac{\alpha}{y_0}$ because

$$\int dy_1 \left[\frac{(1-\alpha)+\alpha y_1 \delta(y_{01})}{y_0\, y_1}\right]\left[1+\frac{-1+y_1\delta(y_{12})}{\alpha}\right] = \delta(y_{02})\,.$$

Plugging (3.5.16) and (3.5.17) in the action (3.5.15), we get

$$\mathcal{S}_{V-J} = \frac{\mathrm{tr}}{2g^2}\int dx\, d^4\theta\, dy_{1,2}\, \mathcal{J}_1 \nabla^4_{1\vartheta} \frac{(1-\alpha)+\alpha y_2\,\delta(y_{12})}{y_1 y_2\, y_{12}^2} \frac{1}{\left(\frac{1}{2}\check{\Box}\right)^2}\mathcal{J}_2\,,$$

which leads to the required propagator, first derived (for the ordinary case) in [33]

$$\langle V(1)V(2)\rangle = \nabla^4_{1\vartheta}\nabla^4_{2\vartheta}\frac{(1-\alpha)+\alpha y_2\,\delta(y_{12})}{y_1 y_2\, y_{12}^2}\frac{1}{\left(\frac{1}{2}\check{\Box}\right)^2}\delta^8(\theta_{12})\delta(x_{12})\,. \tag{3.5.18}$$

This expression simplifies for $\alpha = 1$ to

$$\langle V(1)V(2)\rangle = \nabla^4_{1\vartheta}\frac{\delta(y_{12})}{y_1}\frac{1}{\frac{1}{2}\check{\Box}}\delta^8(\theta_{12})\delta(x_{12})\,, \tag{3.5.19}$$

as does the quadratic part of the vector action

$$\mathcal{S}_V^{(2)} = -\frac{\mathrm{tr}}{2g^2}\int dw\, V\left(\frac{1}{2}y\check{\Box}\right)V\,. \tag{3.5.20}$$

1-loop. In background field gauge, the gauge fixing function leads to additional ghosts apart from the FP ghosts, which contribute to the 1-loop calculations. To see that, consider the effective action Γ defined by the following functional:

$$e^{i\Gamma} = \int \mathcal{D}V\,\mathcal{D}b\,\mathcal{D}c\,\mathcal{D}f\, e^{i(\mathcal{S}_{SYM}(V)+\mathcal{S}_{FP}(V,b,c)+\mathcal{S}_{avg}(f))}\Delta(V)\delta\left(f-V\right), \tag{3.5.21}$$

where $\Delta(V)$ is found by the normalization condition $\int \mathcal{D}f\,\Delta(V)e^{i\mathcal{S}_{avg}(f)} = 1$. It gives

$$\begin{aligned}\Delta^{-1} &= \int \mathcal{D}f\, e^{-i\frac{\mathrm{tr}}{2}\int dx\, d^8\theta\, dy_{1,2} f_1 \frac{1}{2}\left(\frac{y_1}{y_{21}^3}+\frac{y_2}{y_{12}^3}\right)f_2}\\ &= \int \mathcal{D}f\, e^{-i\frac{\mathrm{tr}}{2}\int dx_{1,2}\, d^8\theta_{1,2}\, dy_{1,2} f_1 \mathcal{Y}_{12} f_2} = \frac{1}{\sqrt{\det(\mathcal{Y}_{12})}}\,.\end{aligned} \tag{3.5.22}$$

So (3.5.21) simplifies to

$$e^{i\Gamma} = \int \mathcal{D}V\, \mathcal{D}b\, \mathcal{D}c\, e^{i\left(\mathcal{S}_{SYM}(V)+\mathcal{S}_{gf}(V)+\mathcal{S}_{FP}(V,b,c)\right)} \sqrt{\det(\mathcal{Y}_{12})}\,.$$

We can rewrite the last factor as

$$\frac{1}{\det \mathcal{Y}_{12}} = \int \mathcal{D}\rho\, \mathcal{D}\chi\, e^{i\mathcal{S}_{\rho\chi}} = \int \mathcal{D}\rho\, \mathcal{D}\chi\, e^{i\mathrm{tr}\int dw_1 dw_2 \rho_1 \mathcal{Y}_{12}\chi_2} \tag{3.5.23}$$

where (ρ, χ) are unconstrained hyperfields. Proceeding similar to the harmonic case [56], we redefine $\chi \to d_y^2\chi$ and introduce Nielsen-Kallosh (NK) ghost E to account for the resulting Jacobian. This means the 1-loop contribution for $\mathcal{N}=2$ SYM coupled to matter simplifies to:

$$i\Gamma = -\tfrac{1}{2}\ln \det_{V}(y\check{\Box}) + \tfrac{1}{2}\ln \det_{(\rho,\chi)}\left(\mathcal{Y}_{12}\, d_y^2\right) + \ln \det_{FP} d_y^2 - \tfrac{1}{2}\ln \det_{NK} d_y^2 - \tfrac{1}{2}\ln \det_{\Upsilon} d_y^2. \tag{3.5.24}$$

For $\mathcal{N}=4$, the scalar hypermultiplet is in adjoint representation and its contribution will cancel the joint FP and NK ghosts contributions. The remaining two terms have spurious divergences due to multiple $\delta(y)$'s but their joint contribution has to be finite, which will turn out to be the case as we develop this section further.

To incorporate the effect of (ρ, χ) fields directly in the path integral, we choose to introduce a real scalar X and a complex fermion R as follows:

$$\sqrt{\det\left(\mathcal{Y}_{12}\, d_y^2\right)} = \int \mathcal{D}X\, \mathcal{D}R\, \mathcal{D}\bar{R}\, e^{i(\mathcal{S}_X+\mathcal{S}_R)}, \tag{3.5.25}$$

where

$$\mathcal{S}_X = \frac{\mathrm{tr}}{2}\int dw_1 dw_2 X_1 \mathcal{Y}_{12} d_{y_2}^2 X_2\,; \qquad \mathcal{S}_R = \frac{\mathrm{tr}}{2}\int dw_1 dw_2 \bar{R}_1 \mathcal{Y}_{12} d_{y_2}^2 R_2\,. \tag{3.5.26}$$

So the background field requires 3 Fermionic ghosts (b, c, R) and 2 Bosonic ghosts (E, X) and the full quantum action for $\mathcal{N}=2$ SYM coupled to matter reads:

$$\mathcal{S}_{\mathcal{N}=2} = [\mathcal{S}_{SYM}(V)+\mathcal{S}_{gf}(V)]+\mathcal{S}_{FP}(V,b,c)+\mathcal{S}_{NK}(V,E)+\mathcal{S}_{XR}(V,X,R)+\mathcal{S}_{\Upsilon}(V,\Upsilon).$$

Ghosts. The FP and NK ghosts are background projective hyperfields. The actions for these ghosts look the same as those in the case of non-background gauge. The action for FP ghosts is given in equation (3.5.13) and that for NK ghost is similar to the scalar hypermultiplet's action. That means their

propagators are straightforward generalizations and read

$$\langle \bar{b}(1)c(2)\rangle = \frac{\nabla^4_{1\vartheta}\nabla^4_{2\vartheta}}{y_{12}^3}\frac{1}{\frac{1}{2}\widehat{\Box}}\delta^8(\theta_{12})\delta(x_{12})\,, \tag{3.5.27}$$

$$\langle \bar{E}(1)E(2)\rangle = \frac{\nabla^4_{1\vartheta}\nabla^4_{2\vartheta}}{y_{12}^3}\frac{1}{\frac{1}{2}\widehat{\Box}}\delta^8(\theta_{12})\delta(x_{12})\,. \tag{3.5.28}$$

Now, we focus on the new ingredient of the background field formalism: the eXtRa ghosts. In the same vein as the vector hypermultiplet, we can simplify the actions of these ghosts. Let us just concentrate on the scalar ghost action as the fermionic ghost can be treated similarly:

$$\begin{aligned}\mathcal{S}_X &= -\frac{\mathrm{tr}}{4}\int dx d^8\theta \oint dy_{1,2}\, X_1\left[\left(\frac{y_1}{y_{21}^3}+\frac{y_2}{y_{12}^3}\right)d^2_{y_2}\right]X_2\\ &= -\frac{\mathrm{tr}}{4}\int dx d^4\theta \oint dy_{1,2}\, X_1\left[\left(\frac{y_1}{y_{21}}+\frac{y_2}{y_{12}}\right)\frac{1}{y_{12}^2}\widehat{\Box}\right]X_2\\ &= -\frac{\mathrm{tr}}{4}\int dx d^4\theta \oint dy_{1,2}\, X_1\left[\frac{-1+y_1\delta\left(y_{12}\right)}{y_{12}^2}\widehat{\Box}\right]X_2\,.\end{aligned}$$

The X propagator can then be derived in a similar way as the vector propagator with arbitrary α. Lets add a source term to the action for X ghost:

$$\begin{aligned}\mathcal{S}_{X-J} &= -\frac{\mathrm{tr}}{4}\int dx\, d^8\theta\, dy_{1,2}\, X_1\left[\left(\frac{y_1}{y_{21}^3}+\frac{y_2}{y_{12}^3}\right)d^2_{y_2}\right]X_2 + \mathrm{tr}\int dx\, d^8\theta\, dy_2\, J_2X_2\\ &= -\frac{\mathrm{tr}}{4}\int dx\, d^4\theta\, dy_{1,2}\, X_1\left(\frac{-1+y_1\delta(y_{12})}{y_{12}^2}\right)\widehat{\Box}X_2 + \mathrm{tr}\int dx\, d^4\theta\, dy_2\, \mathcal{J}_2X_2\,.\end{aligned}$$

The equation of motion for X now reads

$$\int dy_1 X_1\left(\frac{-1+y_1\delta(y_{12})}{y_{12}^2}\right)\widehat{\Box} = 2\mathcal{J}_2\,. \tag{3.5.29}$$

Adopting an ansatz for X (similar to what was done for V before),

$$X_1 = d^4_{1\vartheta}\int dy_0\,[p+q\delta(y_{01})]\,\frac{1}{\frac{1}{2}\widehat{\Box}^2}2\mathcal{J}_0\,,$$

we find that $p=0$ and $q=\frac{1}{y_0}$ satisfy (3.5.29). Collecting all the results, the

action reduces to

$$\mathcal{S}_{X-J} = \frac{\mathrm{tr}}{2}\int dx\, d^4\theta\, dy_{1,2}\, \mathcal{J}_1 \nabla^4_{1\vartheta} \frac{\delta(y_{12})}{y_1} \frac{1}{\left(\frac{1}{2}\widehat{\Box}\right)^2} \mathcal{J}_2\,,$$

which leads to the required propagator

$$\langle X(1)X(2)\rangle = \nabla^4_{1\vartheta}\nabla^4_{2\vartheta} \frac{\delta(y_{12})}{y_1} \frac{1}{\left(\frac{1}{2}\widehat{\Box}\right)^2} \delta^8(\theta_{12})\delta(x_{12}). \tag{3.5.30}$$

The propagator for the fermionic R ghost has a similar expression.

3.5.3 Feynman Rules

Given this new construction of the background field formalism for $\mathcal{N}=2$ SYM, we can now employ it to calculate contributions to the effective action coming from different hypermultiplets. The general rules for constructing diagrams in the background field formalism are similar to the ordinary case discussed earlier. However, as expected in this formalism, the quantum propagators form the internal lines of the loops and the external lines correspond to the background fields.

The $\check{\Box}$ and $\widehat{\Box}$ operators in the propagators need to be expanded around $\Box_0$ (the connection-independent part of $\Box$), which will generate the vertices with the vector connection and background fields. For the extra ghosts, we can further simplify the naïve rules by noticing that the vertices have $\frac{1}{y_{12}^2}$-factor and the propagator will generate such a factor in the numerator due to the presence of $\nabla^4_{1\vartheta}\nabla^4_{2\vartheta}$. Thus, we can remove them from the very start and work with the revised propagator and vertex for the purpose of calculating diagrams. Let us now collect all the relevant Feynman rules below.

$$\begin{aligned}
\text{Scalar propagator:} &\quad \frac{\nabla^4_{1\vartheta}\nabla^4_{2\vartheta}}{y_{12}^3}\frac{\delta^8(\theta_{12})}{\frac{1}{2}k^2}\\
\text{Vector propagator:} &\quad \nabla^4_{1\vartheta}\frac{\delta(y_{12})}{y_1}\frac{\delta^8(\theta_{12})}{\frac{1}{2}k^2}\\
\text{FP \& NK ghosts propagator:} &\quad \frac{\nabla^4_{1\vartheta}\nabla^4_{2\vartheta}}{y_{12}^3}\frac{\delta^8(\theta_{12})}{\frac{1}{2}k^2}\\
\text{XR ghosts propagator:} &\quad \nabla^4_{1\vartheta}\frac{\delta(y_{12})}{y_1}\frac{\delta^8(\theta_{12})}{\frac{1}{2}k^2}\\
\text{Scalar, FP \& NK vertex:} &\quad \int d^4\theta\, dy\, (\widehat{\Box}-\Box_0) \quad \left(\text{use}\int d^4\theta\nabla^4_\vartheta = \int d^8\theta\right)
\end{aligned}$$

$$\text{Vector vertex (background):} \quad \int d^4\theta\, dy\, y\, (\check{\Box} - \Box_0)$$

$$\text{Vector vertex (quantum):} \quad \int d^8\theta\, dy_{1,\ldots,n} \frac{(-1)^n}{y_{12}y_{23}\ldots y_{n1}}$$

$$\text{XR ghosts vertex:} \quad \int d^4\theta \int dy_{1,2}\, [-1 + y_1\delta\,(y_{12})]\, (\widehat{\Box} - \Box_0)$$

3.5.4 Examples

Scalar. The one-loop contribution from the scalar hypermultiplet to the effective action can not be written in a fully gauge covariant form with a projective measure. Thus, the diagrammatic calculation required to get this contribution (which includes the UV-divergent piece too) is not accessible via the formalism constructed here. We note that such an issue appears in the $\mathcal{N} = 1$ background formalism too when the scalar multiplets in complex representation are considered. The calculations cannot be performed covariantly and explicit gauge fields appear in addition to the connections.

Vector. The contribution to one-loop $n-$point diagrams from vector hypermultiplet running in the loop would be given by the following:

$$\begin{aligned}
\Gamma_n^{(V)} \sim & \int d^4k \int d^4\theta_{1,\ldots,n} \int dy_{1,\ldots,n} \nabla^4_{1\vartheta}\delta^8(\theta_{12}) \frac{\delta(y_{12})}{y_1} \frac{1}{k_1^2}\, y_1\, (W^\alpha(1)\nabla_{\theta,\alpha} + \ldots) \ldots \\
& \nabla^4_{n\vartheta}\delta^8(\theta_{n1}) \frac{\delta(y_{n1})}{y_n} \frac{1}{k_n^2}\, y_n\, (W^\alpha(n)\nabla_{\theta,\alpha} + \ldots) \\
\sim & \int d^4k \int d^8\theta_{1,\ldots,n-1} d^4\theta_n \int dy_{1,n} \delta^8(\theta_{12})\delta(y_{1n}) \frac{1}{k_1^2}\, (W^\alpha(1)\nabla_{\theta,\alpha} + \ldots) \ldots \\
& \nabla^4_{n\vartheta}\delta^8(\theta_{n1})\delta(y_{n1}) \frac{1}{k_n^2}\, (W^\alpha(n)\nabla_{\theta,\alpha} + \ldots)\,, \qquad (3.5.31)
\end{aligned}$$

where the numerical subscript on k denotes the external momenta dependence. As usual, to kill the extra $\delta^8(\theta)$-function, at least four ∇_θ should be available from the vertices and so $\Gamma_2^{(V)} = \Gamma_3^{(V)} = 0$. The first non-vanishing contribution

is from the 4−point diagram:

$$\begin{aligned}\Gamma_4^{(V)} &= \frac{3\,c_A}{2}\int dy_{1,4}\delta(y_{14})\delta(y_{41})\int d^8\theta_1 d^4\theta_4\,\hat{\mathcal{A}}_4\,\delta^8(\theta_{14})\times\\ &\quad\times\left(\prod_{i=1}^{4}\frac{1}{2}W^\alpha(i)\nabla_{\theta,\alpha}\right)\nabla^4_{4\vartheta}\delta^8(\theta_{41})\\ &= \frac{3\,c_A}{32}\oint\frac{dy_1}{2\epsilon\,y_1}\int d^8\theta_1 d^4\theta_4\,\hat{\mathcal{A}}_4\,\delta^8(\theta_{14})\times\\ &\quad\times\left(W^\alpha(1)W^\beta(2)W^\gamma(3)W^\delta(4)\,\epsilon_{\alpha\beta\gamma\delta}\nabla^4_\theta\right)\nabla^4_{4\vartheta}\delta^8(\theta_{41})\\ &= \frac{3\,c_A}{32}\oint\frac{dy_1}{2\epsilon\,y_1}\int d^4\theta\,\hat{\mathcal{A}}_4\,\epsilon_{\alpha\beta\gamma\delta}W^\alpha(1)W^\beta(2)W^\gamma(3)W^\delta(4)\,,\end{aligned}\tag{3.5.32}$$

where, $\hat{\mathcal{A}}_4\sim\int dk\frac{16}{(k_1^2)\,(k_2^2)\,(k_3^2)\,(k_4^2)}$.

Too many $\delta(y)$'s lead to spurious $\frac{1}{\epsilon}$ singularity, similar to 'coinciding harmonic' singularities in the harmonic case. These will cancel when we take into account the (X,R) ghosts.

Extra Ghosts. Their combined contribution to one-loop n−point diagrams reads:

$$\begin{aligned}\Gamma_n^{(X,R)} &\sim -\int d^4k\,d^4\theta_{1,\ldots,n}\,d^2y_{1,\ldots,n}\nabla^4_{1\vartheta}\delta^8(\theta_{12})\frac{\delta(y_{1a,2a})}{y_{1a}}\frac{1}{k_1^2}\,[(-1+y_{1a}\delta(y_{1a,1b}))]\times\\ &\quad\times(W^\alpha(1)\nabla_{\theta,\alpha}+\ldots)\ldots\nabla^4_{n\vartheta}\delta^8(\theta_{n1})\frac{\delta(y_{nb,1b})}{y_{nb}}\frac{1}{k_n^2}\times\\ &\quad\times[(-1+y_{na}\delta(y_{na,nb}))]\,(W^\alpha(n)\nabla_{\theta,\alpha}+\ldots)\\ &\sim -\int d^4k\,d^4\theta_n\,dy_{1a,\ldots,1b}\nabla^4_{1b\vartheta}\delta^8(\theta_{n1})\frac{(-1+y_{1a}\delta(y_{1a,2b}))}{y_{1a}}\frac{1}{k_1^2}\\ &\quad(W^\alpha(1)\nabla_{\theta,\alpha}+\ldots)\ldots\frac{(-1+y_{na}\delta(y_{nb,1b}))}{y_{1b}}\frac{1}{k_n^2}\,(W^\alpha(n)\nabla_{\theta,\alpha}+\ldots)\,.\end{aligned}\tag{3.5.33}$$

Again, the first non-vanishing contribution is from $n=4$ that has the same $\delta(y)^2$ singularity structure as the vector in (3.5.32) leading to a cancellation,

in addition to the following finite part:

$$\Gamma_4 = -\frac{3\,c_A}{32}\int dy_{1,2,3,4}\left(\frac{1}{y_1y_2y_3y_4} - \frac{\delta(y_{12})}{y_2y_3y_4} + ...\right)\times$$
$$\times \int d^4\theta\,\hat{\mathcal{A}}_4\,\epsilon_{\alpha\beta\gamma\delta}W^\alpha(1)W^\beta(2)W^\gamma(3)W^\delta(4)$$
$$= \frac{3\,c_A}{32}\int d^4\theta\,\hat{\mathcal{A}}_4\,\epsilon_{\alpha\beta\gamma\delta}\left(W^\alpha(1)W^\beta(2)W^\gamma(3)W^\delta(4)\right)|_{y=0}\,. \qquad (3.5.34)$$

The last line follows because only y-independent pieces of W's can survive the y-integrals. (This result also holds for the 6D theory with d^6k for the momentum integral but in 4D it can be re-expressed as an integral over the full superspace of the usual chiral and antichiral field strengths.) Till here, we have treated W's as fields depending on individual external momenta and (3.5.34) is the complete 4−point effective action. Assuming them to be momentum independent, we can further simplify this expression in case of the U(1) gauge group and perform the integral over loop momentum to get

$$\hat{\mathcal{A}}_4 = \frac{16}{24}\frac{1}{(4\pi)^2}\frac{1}{\left(W\overline{W}\right)^2},$$

where we used the reduction to 4D for $\Box_0 \to \Box_0 - 2W\overline{W}$. Using this and the fact that W^α is related to $\mathcal{D}^\alpha_\vartheta W$ $\left(\&\,\mathcal{D}^{\dot\alpha}_\vartheta\overline{W}\right)$, we get the same non-holomorphic 4−point contribution (with the full superspace measure $\int d^8\theta$) to $\mathcal{N}=4$ SYM action rather directly when compared to the calculation done in [34] (for similar calculations in harmonic hyperspace see, for example, [42]).

2-loops. We can also see that there are no UV divergences at two-loops. The proof is similar to that given in the ordinary case, *i.e.*, absence of sufficient ∇^4_ϑ's. Only 3 diagrams shown in Figure 3.11 are supposed to contribute at 2-loops. All of them will vanish due to the d-algebra unless we get at least 4 ∇_θ's from the expansion of the propagators. This, as we have seen before, brings in 4 more $\Box$'s making these 2-loop diagrams convergent.

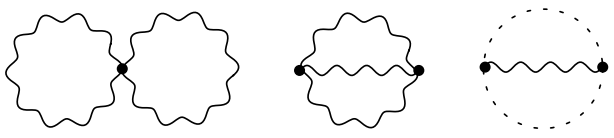

Figure 3.11: Diagrams contributing to SYM effective action at 2-loops with external background lines being suppressed.

Furthermore, we note that the arguments of [51] apply in our case since there is no background connection A_y, there cannot be any divergences at 2 or more loops from just power counting. This situation is different than harmonic where such '0-dimensional' connections are present and arguments similar to the one given above involving number of ∇_ϑ's have to be used and at higher loops they can be quite involved [60].

3.6 Discussion

We investigated one and two-loop(s) diagrams for $\mathcal{N}=2$ massless vector and scalar hypermultiplets directly in projective hyperspace for the cases of 2, 3 & 4−point functions. We found that the effective action receives only 1-loop divergent corrections, which have the same form as the classical action. We also calculated all the 1-hoop finite pieces of the diagrams. Some of them are similar to the classical action modulo the momentum factors whereas others have extra y-factors, whose 'non-linearity' prevents any simplification of the results. In spite of that, we derived the well-known result that the $\mathcal{N}=2$ SYM coupled to matter is 2-loops finite. These calculations also enable us to show that $\mathcal{N}=4$ SYM is finite at one and two-loop(s).

Similar calculations can be done with the harmonic hyperspace Feynman rules and the procedure is not that different or difficult. However, the repeated use of harmonic derivatives (d_y & $d_{\bar{y}}$) to simplify the SU(2) invariant harmonics in order to do the SU(2) integrals is definitely cumbersome compared to 'evaluating' some contour integrals on a complex plane in the projective hyperspace as we further demonstrate in the Appendix A.

We presented a reformulation of the massive scalar hypermultiplet that makes it more transparent at the component level from both 4D and 6D perspectives. The diagrammatic Feynman rules are similar to the massless case and hence no extra effort is needed to evaluate diagrams with massive scalar lines.

Our results like the linear wavefunction renormalization and the nonrenormalization of 'gV' have the same simplicity as expected from a background field formalism. In fact, we also formulated the background field formalism for projective hyperspace. The crucial ingredient was to recognize that different representations for background and quantum pieces of the hypermultiplets are required. Choosing real representation for the background fields allowed non-renormalization theorems to be applicable here as the lowest-dimensional fields available were spinors. The usual choice of analytic representation for the quantum fields allowed us to make a simple extension of the existing 'ordinary' super-Feynman rules to the background covariant rules.

Moreover, there are extra ghosts required (apart from FP and NK ghosts) to evaluate the full SYM effective action. These extra ghosts also appear in the harmonic case but in projective case, they cancel the spurious 'harmonic' divergences coming from vector hypermultiplet in a straightforward manner and the resultant finite pieces are as expected for $\mathcal{N} = 4$. The UV divergent parts come only from the usual (FP and NK) ghosts and scalar hypermultiplet. However, their contribution can not be directly calculated in the formalism developed here for reasons mentioned in Section 3.5.4. We also gave a diagrammatic 2-loops argument for finiteness of $\mathcal{N} = 2$ SYM coupled with matter. This is easily supplanted by the power counting argument of [51] in general, which directly leads to a proof for finiteness beyond 1-loop.

For $\mathcal{N} = 1$ background formalism, there exist improved rules as showcased in [63–65] and our hope is that such techniques could be applied to what we have developed in this paper. That would lead to a further simplification of the higher-loop calculations while also allowing explicit inclusion of the scalar hypermultiplet's 1-loop contribution.

Note the similarity of the 4−point result (3.5.34) to the case of $\mathcal{N} = 4$ superspace [66, 67]: There $\mathcal{N} = 4$ projective superspace (or maybe some harmonic analog) is the only convenient way to express this result (with a scalar field strength). This suggests the possibility that in the $\mathcal{N} = 4$ case, where there is only the vector multiplet, all the supergraph rules might be formulated most conveniently in projective superspace.

There is also an $\mathcal{N} = 3$ harmonic formulation of $\mathcal{N} = 4$ Yang-Mills [68, 69], but no amplitudes have been calculated with it. It is possible that the corresponding projective formulation is already $\mathcal{N} = 4$: The number of θ's (and x's) is already the same, and the combination of field equations (since there are an infinite number of auxiliary fields) with gauge condition might reduce the $\mathcal{N} = 3$ harmonic's 6 R-coordinates to the $\mathcal{N} = 4$ projective's 4. The $\mathcal{N} = 3$ action is curiously simpler than the $\mathcal{N} = 2$; this also suggests the existence of a simpler $\mathcal{N} = 2$ action.

Chapter 4

Applying Projective Superspace

Since the work of Seiberg and Witten [70, 71], the structure of $\mathcal{N} = 2$ theories in four dimensions has been extensively explored, leading to important insights into the dynamics of gauge theories. A recent area of progress in this field is the study of the Coulomb branch moduli space of $\mathcal{N} = 2$ theories on $\mathbb{R}^3 \times S^1$, first analyzed in [72]. It has received renewed attention due its relation to the Kontsevich-Soibelman (KS) wall-crossing formula [73] for $\mathcal{N} = 2$ theories in the work by Gaiotto, Moore, and Neitzke (GMN) [74]. As described by GMN, the KS formula ensures the continuity of the metric on the moduli space. Alternatively, demanding continuity of the metric provides a physical proof of the wall-crossing formula. The central idea in [74] was to find an efficient description of the moduli space metric and its corrections due to BPS instantons. Such a description was given in terms of the holomorphic Darboux coordinates (η_e, η_m) by making crucial use of twistor techniques. One of the important results of their work is that the magnetic coordinate η_m is given in terms of the electric coordinate η_e.

One of the goals of this chapter is to use the formalism of projective hyperspace to present a simple derivation and generalization of this formula for any hyperkähler manifold described by $\mathcal{O}(2p)$ multiplets. Our analysis is based on the projective Legendre transform, which dualizes the $\mathcal{O}(2p)$ hypermultiplet η_e to the arctic hypermultiplet Υ. We will see that η_m turns out to be the imaginary part of $y^{p-1}\Upsilon$ and Υ is related to the projective Lagrangian (f) for η_e by this Legendre transform. Such an expression can also be obtained from gluing conditions for the Darboux coordinates, as done in [75–78] (see [79] for a recent review and references therein). Our derivation, however, is based on requiring the consistency of the Legendre transform by imposing the condition that Υ is regular at $y = 0$.

In the specific case of the periodic Taub-NUT metric, by Poisson resummation of the usual projective Lagrangian describing the $\mathcal{O}(2)$ hypermultiplet, we

recover the relation given in [74]. A natural generalization of f to incorporate mutually nonlocal corrections leads to the integral TBA equation. We then consider the doubly-periodic Taub-NUT metric, deriving an expression for the Darboux coordinates. This metric was recently studied in [80] to describe the electric corrections to the moduli space of five-dimensional SYM on $\mathbb{R}^3 \times T^2$.

4.1 Preliminaries

In this section, we review some elements of $\mathcal{N} = 2$ projective superspace [14,16] which hasn't been introduced in the previous chapters and the construction of hyperkähler metrics [81]. A recent review of essential aspects of the relation between projective superspace and hyperkähler manifolds can be found in [82].

4.1.1 Projective Hypermultiplets

From the previous chapter we know that the projective hyperfields satisfy the following constraints:

$$d_\vartheta \Upsilon = \bar{d}_\vartheta \Upsilon = 0\,. \tag{4.1.1}$$

So far we have discussed only the arctic and antarctic hypermultiplets. In fact, there are more multiplets characterized by their (further) restricted y-dependence. We shall need the real $\mathcal{O}(2p)$ hypermultiplet apart from the already discussed (ant)arctic hypermultiplets. The $\mathcal{O}(2p)$ are polynomials in y, with its powers ranging from $-p$ to p, and real under the bar conjugation. In particular, the $\mathcal{O}(2)$ multiplet is defined by

$$\eta_e = \frac{a}{y} + \theta_e - \bar{a}y\,. \tag{4.1.2}$$

It follows from (4.1.1) that a and θ_e are $\mathcal{N} = 1$ chiral and real linear superfields, respectively.

4.1.2 Hyperkähler Manifolds

Here we review the construction of hyperkähler metrics in projective superspace [15,81–83]. Given an arbitrary analytic function $f(\eta_e; y)$, one defines the function (we will continue suppressing the $2\pi i$ factor in the integral measure)

$$F(a, \bar{a}, \theta_e) \equiv \oint_C \frac{dy}{y} f(\eta_e; y)\,, \tag{4.1.3}$$

where C is an appropriately chosen contour, which typically depends on the choice of f (referred to as the projective Lagrangian henceforth). The Legendre transform of F serves as the Kähler potential K for a hyperkähler manifold, *i.e.*,

$$K(a,\bar{a},v+\bar{v}) = F(a,\bar{a},\theta_e) - (v+\bar{v})\,\theta_e\,, \qquad F_{\theta_e} = v+\bar{v}\,, \tag{4.1.4}$$

where v is an $\mathcal{N}=1$ chiral superfield. Note that Kähler metrics described in this way automatically have an isometry, associated to shifts of $\mathrm{Im}(v)$. The resulting metric is of the Gibbons-Hawking form

$$ds^2 = \frac{1}{V(x)}\left(d\theta_m + A\right)^2 + V(x)d\vec{x}\cdot d\vec{x}\,, \tag{4.1.5}$$

where $a = x^1 + ix^2$, $\theta_e = x^3$ and $dV = \star dA$, with

$$V = \oint_C \frac{dy'}{y'}\frac{\partial^2 f}{\partial \eta_e'^2}\,, \qquad A = \frac{1}{2}\oint_C \frac{dy'}{y'}\left(\frac{1}{y'}da + y'd\bar{a}\right)\frac{\partial^2 f}{\partial \eta_e'^2}\,. \tag{4.1.6}$$

An important class of metrics are A_{N-1} ALE metrics and can be described in this way by taking

$$f(\eta_e) = \sum_k (\eta_e - \eta_k)\log(\eta_e - \eta_k)\,, \tag{4.1.7}$$

where η_k are constant $\mathcal{O}(2)$ multiplets simply giving the position $\vec{x}_k$ of N mass points. For this Lagrangian, the contour in (4.1.3) is an 8-shaped contour $\tilde{C}$ enclosing the two roots of $\eta_e - \eta_k = 0$. Indeed, using (4.1.7) in (4.1.6) gives the harmonic function

$$V = \sum_k \oint_{\tilde{C}} \frac{dy}{y}\frac{1}{\eta_e - \eta_k} = 2\sum_k \frac{1}{|\vec{x} - \vec{x}_k|} \tag{4.1.8}$$

and the corresponding A. Taking an infinite superposition of mass points along θ_e, *i.e.*, taking $\eta_k = k$ and $N \to \infty$, the metric becomes periodic along this direction[1]. This metric (commonly referred to as the Ooguri-Vafa metric) was discussed by Ooguri and Vafa in [84] and Seiberg and Shenker in [85]. Following the terminology of [86], we will refer to it as the periodic Taub-NUT (PTN) metric. We will refer to a PTN metric which is periodic along two directions as the doubly-periodic Taub-NUT (dPTN) metric.

[1] Strictly speaking, V is logarithmically divergent and must be properly regularized. It should be understood that this has been done in what follows.

A hyperkähler manifold has three Kähler forms $\omega^{(2,0)}, \omega^{(1,1)}$ and $\omega^{(0,2)}$, which can be conveniently organized into

$$\varpi = \omega^{(2,0)} + \omega^{(1,1)} y - \omega^{(0,2)} y^2 \,. \tag{4.1.9}$$

This combination can be further written as:

$$\varpi = i y \, d\eta_e \wedge d\eta_m \,, \tag{4.1.10}$$

with

$$d\eta_e = \frac{da}{y} + d\theta_e - y d\bar{a} \,, \quad d\eta_m = d\theta_m + iA + \frac{iV}{2}\left(\frac{1}{y} da + y d\bar{a}\right). \tag{4.1.11}$$

Since the symplectic form ϖ takes the canonical form in (4.1.10), the set (η_e, η_m) are referred to as Darboux coordinates. The main purpose of the coming sections is to find an explicit expression for η_m in terms of $f(\eta_e; y)$.

4.1.3 Duality and Symplectic Form

One can alternatively describe these hyperkähler manifolds in terms of an arctic superfield Υ, rather than in terms of an $\mathcal{O}(2)$, by a duality relating these two multiplets [31, 83]. In terms of $\mathcal{N} = 1$ components, this is based on the Legendre transform (4.1.4) exchanging a real linear superfield by a chiral superfield. It is similarly described in terms of projective superfields as follows: One relaxes the condition of η_e being an $\mathcal{O}(2)$ multiplet, imposing this through a Lagrange multiplier $\Upsilon + \bar{\Upsilon}$. Integrating out Υ leads to the original description in terms of η_e, while integrating out η_e leads to a dual description in terms of Υ. That is, one defines

$$\tilde{f}(\Upsilon + \bar{\Upsilon}; y) = f(\eta_e; y) - (\Upsilon + \bar{\Upsilon})\eta_e \,, \tag{4.1.12}$$

with the standard Legendre transform relations

$$\frac{\partial f}{\partial \eta_e} = \Upsilon + \bar{\Upsilon} \,, \qquad \frac{\partial \tilde{f}}{\partial \Upsilon} = -\eta_e \,. \tag{4.1.13}$$

The main advantage of this setup (for our purposes) is that one can define a holomorphic symplectic two-form [82] that captures the essential aspects of the hyperkähler geometry (see also [87, 88] for related results). This is based on the observation that arctic superfields have infinitely many unconstrained $\mathcal{N} = 1$ fields Υ_i, for $i \geq 2$, which must be integrated out. These equations of

motion imply that

$$\tilde{\Upsilon} \equiv y\frac{\partial \tilde{f}}{\partial \Upsilon} = -y\eta_e \tag{4.1.14}$$

is also an arctic superfield. Thus, one can define a 2-form ϖ by

$$\varpi = d\Upsilon \wedge d\tilde{\Upsilon} = \omega^{(2,0)} + \omega^{(1,1)}y - \omega^{(0,2)}y^2\,. \tag{4.1.15}$$

In other words, Υ and $\tilde{\Upsilon}$ are (by construction) Darboux coordinates for the holomorphic symplectic form ϖ. Note that they are regular at $y = 0$, while $(\bar{\Upsilon}, \bar{\tilde{\Upsilon}})$ are regular at $y = \infty$, and

$$\varpi = -y^2\overline{\varpi} = -y^2 d\bar{\Upsilon} \wedge d\bar{\tilde{\Upsilon}}. \tag{4.1.16}$$

Thus, up to the twisting factor y^2, there is a symplectomorphism relating north pole and south pole coordinates and the generating function is precisely $\tilde{f}(\Upsilon + \bar{\Upsilon})$, giving a geometric interpretation to the $\mathcal{N} = 2$ projective Lagrangian.

4.2 Darboux Coordinates

As seen in Section 4.1.3, the projective Legendre transform provides an expression for a set of Darboux coordinates, namely $(\Upsilon, \tilde{\Upsilon})$. The coordinate $\tilde{\Upsilon}$ is given by (4.1.14) whereas only the real part (under bar conjugation) of Υ is determined by (4.1.13), *i.e.*,

$$\Upsilon = \frac{1}{2}\frac{\partial f}{\partial \eta_e} + i\eta_m\,, \tag{4.2.1}$$

where we have introduced $\eta_m = \bar{\eta}_m$ as the (undetermined) imaginary part of Υ. The crucial observation [89] is that Υ is actually completely determined by a consistency requirement on the whole construction. Recall that the constraint of η_e being an $\mathcal{O}(2)$ multiplet was imposed through a Lagrange multiplier, assuming that Υ was an arctic superfield. However, the first term on the r.h.s. of (4.2.1) contains negative powers of y and therefore, the consistency requirement is that these should be canceled by η_m. This η_m is precisely the magnetic coordinate we are after, since we find from (4.1.14) and (4.2.1) that

$$\varpi = d\Upsilon \wedge d\tilde{\Upsilon} = iy\, d\eta_e \wedge d\eta_m \tag{4.2.2}$$

coincides with (4.1.10). To determine η_m, we use the antarctic projector

$$\Pi_N \equiv \oint_{C_0} dy' \frac{1}{y-y'}\,, \qquad \Pi_N^2 = \Pi_N\,, \qquad \Pi_N \bar{\Pi}_N = 0\,, \tag{4.2.3}$$

where C_0 is a closed contour around the origin (see previous chapter for details). This projector annihilates the non-negative powers of y. Thus, the consistency requirement is simply

$$\Pi_N \Upsilon = 0\,. \tag{4.2.4}$$

It is easy to see that

$$\eta_m = \theta_m + \left(i\Pi_N - i\bar{\Pi}_N\right)\frac{1}{2}\frac{\partial f}{\partial \eta_e}\,, \tag{4.2.5}$$

with $\theta_m = \bar{\theta}_m$, solves the consistency condition[2]. We can rewrite (4.2.5) in a more familiar form. From (4.2.3), we see that the projectors combine into

$$i\Pi_N - i\bar{\Pi}_N = i\oint_{C_0} \frac{dy'}{y'}\frac{y+y'}{y-y'} \tag{4.2.6}$$

and hence

$$\eta_m = \theta_m + \frac{i}{2}\oint_{C_0} \frac{dy'}{y'}\frac{y+y'}{y-y'}\frac{\partial f}{\partial \eta'_e}\,, \tag{4.2.7}$$

recovering the expression obtained in [75–78]. The derivation of this expression, by ensuring and making manifest the condition that Υ is arctic, is one of the main results in this chapter. This condition is enforced by the projector $(y+y')(y-y')^{-1}$ and will be extended below to include $\mathcal{O}(2p)$ multiplets.

We can easily check that from (4.2.7) we recover the expression (4.1.11)

[2]Indeed, from (4.2.1), (4.2.5), and using the properties in (4.2.3), we see that

$$\Pi_N\Upsilon = \Pi_N\left(\frac{1}{2}\frac{\partial f}{\partial\eta_e} + i\left[\theta_m + \left(i\Pi_N - i\bar{\Pi}_N\right)\frac{1}{2}\frac{\partial f}{\partial\eta_e}\right]\right) = \Pi_N\left(\frac{1}{2}\frac{\partial f}{\partial\eta_e}\right) - \Pi_N\left(\frac{1}{2}\frac{\partial f}{\partial\eta_e}\right) = 0\,.$$

for Gibbons-Hawking metrics. Acting with d on η_m, we have

$$\begin{aligned} d\eta_m &= d\theta_m + \frac{i}{2}\oint_{C_0}\frac{dy'}{y'}\frac{y+y'}{y-y'}\frac{\partial^2 f}{\partial\eta_e'^2}\left(d\eta_e' - d\eta_e\right) \\ &= d\theta_m + \frac{i}{2}\oint_{C_0}\frac{dy'}{y'}\left[\left(\frac{1}{y}+\frac{1}{y'}\right)da + (y+y')d\bar{a}\right]\frac{\partial^2 f}{\partial\eta_e'^2} \\ &= d\theta_m + iA + \frac{iV}{2}\left(\frac{1}{y}da + y\,d\bar{a}\right) . \end{aligned} \tag{4.2.8}$$

In the first line, we have added a term proportional to $d\eta_e$, which gives no contribution to the symplectic form (4.2.2). In the last line, we have used the definitions (4.1.6), assuming that the contour giving the Kähler potential is C_0.

Although the derivation of (4.2.7) requires a contour enclosing only a singularity at the origin, note that choosing the contour to be the one defining the Kähler potential gives the correct symplectic form. This expression provides a systematic way of constructing Darboux coordinates for any hyperkähler manifold described by an $\mathcal{O}(2)$ multiplet η_e and projective Lagrangian f. We will use this in the following sectionss to describe instanton corrections to moduli spaces of SYM theories.

Semiflat Geometry and the *c*-map. It is clear from (4.2.7) that, unlike η_e, the magnetic coordinate η_m will not be an $\mathcal{O}(2)$ in general, this depending on the singularity structure of $f(\eta_e; y)$. A special case however is when the rigid c-map [90–93] (see Appendix B) can be applied. According to the c-map,

$$f^{sf}(\eta_e; y) = -i\left(\frac{\mathcal{F}\left(y\eta_e\right)}{y^2} - \overline{\mathcal{F}}\left(-\frac{\eta_e}{y}\right)y^2\right) , \tag{4.2.9}$$

where $\mathcal{F}(W)$ is the $\mathcal{N}=2$ holomorphic prepotential. The c-map gives the contribution from naïve dimensional reduction, without taking into account the effect of BPS particles. Thus, one expects η_m to be given by an $\mathcal{O}(2)$. However, by the direct substitution of (4.2.9) in (4.2.7), we see that this is not the case. This is resolved by recalling that the Darboux coordinates are defined up to terms that vanish in the symplectic form. In fact, we can add

such a term to the definition of η_m that does lead to an $\mathcal{O}(2)$, namely[3]

$$\begin{aligned}\Upsilon &= \frac{1}{2}\frac{\partial f^{sf}}{\partial \eta_e} + i\left[\eta_m^{sf} - \frac{1}{2}\left(\frac{\mathcal{F}'}{y} - \bar{\mathcal{F}}' y\right)\right] \\ &= -\frac{i\mathcal{F}'(y\eta_e)}{y} + i\eta_m^{sf}\,. \end{aligned} \tag{4.2.10}$$

From the fact that $\mathcal{F}'(y\eta_e) = \mathcal{F}'(a + \theta_e y - \bar{a}y^2)$ is regular at the origin, the condition that Υ in (4.2.10) is arctic is simply solved by

$$\eta_m^{sf} = \frac{\mathcal{F}'(a)}{y} + \theta_m - \bar{\mathcal{F}}'(\bar{a})\, y\,. \tag{4.2.11}$$

Therefore, naïve electric-magnetic duality $a \to a_D = \mathcal{F}'(a)$ holds. In general, dyonic multiplets have the form $\eta_\gamma^{sf} = \frac{Z_\gamma}{y} + \theta_\gamma - \bar{Z}_\gamma\, y$, where the central charge is $Z_\gamma = n_e a + n_m a_D$ with n_e and n_m being the electric and magnetic charges, respectively. Once BPS instanton corrections are included, the magnetic coordinate is no longer an $\mathcal{O}(2)$ since the total Lagrangian is

$$f = f^{sf} + f^{inst}\,,$$

where f^{inst} is not of the form (4.2.9). Thus, the full magnetic coordinate is given in general by

$$\eta_m = \eta_m^{sf} + \frac{i}{2}\oint_{C_0} \frac{dy'}{y'}\frac{y+y'}{y-y'}\frac{\partial f^{inst}}{\partial \eta_e'}\,, \tag{4.2.12}$$

where η_m^{sf} is given by (4.2.11).

Generalization to $\mathcal{O}(2p)$ Hypermultiplets. Our construction so far includes only hyperkähler manifolds described by $\mathcal{O}(2)$ multiplets, but it can be easily extended to the case of $\mathcal{O}(2p)$ multiplets by a generalization of the Legendre transform relating Υ to an $\mathcal{O}(2p)$ multiplet η_e [31] . Additional factors of y have to be introduced in the Legendre transform to impose the corresponding constraint on η_e, namely

$$\tilde{f} = f - \left(y^{p-1}\Upsilon + (-y)^{-(p-1)}\,\bar{\Upsilon}\right)\eta_e \tag{4.2.13}$$

[3] This observation is based on [89].

with the relations

$$\frac{\partial f}{\partial \eta_e} = y^{p-1}\Upsilon + (-y)^{-(p-1)}\,\bar{\Upsilon}\,, \qquad \tilde{\Upsilon} \equiv y\frac{\partial \tilde{f}}{\partial \Upsilon} = -y^p \eta_e\,. \tag{4.2.14}$$

Thus, we now have

$$y^{p-1}\Upsilon = \frac{1}{2}\frac{\partial f}{\partial \eta_e} + i\eta_m\,, \tag{4.2.15}$$

and the symplectic form is still given by

$$\varpi = d\Upsilon \wedge d\tilde{\Upsilon} = iy\, d\eta_e \wedge d\eta_m\,.$$

The magnetic coordinate η_m will again be determined by the requirement that the resulting superfield Υ is arctic. From (4.2.14) it follows that $\frac{\partial f}{\partial \eta_e}$ contains powers y^n with $|n| \geq (p-1)$ only. Thus, η_m in (4.2.15) is required to cancel the powers y^n with $n < -(p-1)$ of $\frac{\partial f}{\partial \eta_e}$ and we cannot add a y-independent term, contrary to the $\mathcal{O}(2)$ case. Using the corresponding projectors, we then find

$$\eta_m = \frac{i}{2}\oint_{C_0} \frac{dy'}{y'}\frac{1}{y-y'}\left[y\left(\frac{y}{y'}\right)^{p-1} + y'\left(\frac{y'}{y}\right)^{p-1}\right]\frac{\partial f}{\partial \eta'_e}\,. \tag{4.2.16}$$

The corresponding semiflat contribution can be determined using the c-map prescription for $\mathcal{O}(2p)$ multiplets given in [92].

A metric which is described, for example, by an $\mathcal{O}(4)$ multiplet is the Atiyah-Hitchin metric, characterizing the moduli space of two monopoles and the moduli space of three-dimensional SYM. It would be interesting to compare (4.2.16) to the Darboux coordinates given in [94,95]. In the remainder of the chapter, we will restrict ourselves to $\mathcal{O}(2)$ multiplets and apply our results to the study of moduli spaces of pure SYM theories with eight supercharges in $d = 4$ and $d = 5$.

4.3 $\mathcal{N} = 2$ SYM on $\mathbb{R}^3 \times S^1$

In this section, we apply our construction to the study of the Coulomb branch of pure $\mathcal{N} = 2$ SYM with gauge group $SU(2)$, first analyzed in [72]. The bosonic content of the four-dimensional theory consists of a complex scalar field a and a gauge field A_μ. Upon dimensional reduction on a circle S^1 of radius R (which we set to 1 in this section), the gauge field decomposes as $A_\mu \to (A_i, A_4)$, giving a three-dimensional photon and a real scalar field. Since in three dimensions the photon itself is dual to a scalar field, the moduli

space of supersymmetric vacua is four-dimensional. Furthermore, due to the amount of supersymmetry it is hyperkähler. It can be parameterized by the vev of the vector multiplet scalar field, a, in addition to the gauge-invariant electric and magnetic Wilson loops[4]

$$\theta_e \equiv \frac{1}{2\pi}\oint_{S^1_4} A_4\,, \qquad \theta_m \equiv \frac{1}{2\pi}\oint_{S^1_4} A_{D,4}\,. \tag{4.3.1}$$

Naïve dimensional reduction of the 4D SYM action results in a 3D sigma model with a target space metric of Gibbons-Hawking form, specified by the 'semiflat' potential $V^{sf} = \mathrm{Im}\tau$, where τ is the usual complexified 4D gauge coupling. However, the BPS particles from the four-dimensional theory can wrap the compactification circle S^1, generating instanton corrections to the semiflat metric in the compactified theory, which we discuss next.

4.3.1 Mutually Local Corrections

Following [74], we first focus on the case in which all the BPS particles are mutually local, by choosing a duality frame in which there are no magnetically charged particles. This leads to a shift isometry in θ_m and therefore the space is naturally described by the $\mathcal{O}(2)$ multiplet

$$\eta_e = \frac{a}{y} + \theta_e - \bar{a}y\,. \tag{4.3.2}$$

Integrating out a hypermultiplet of electric charge q (which we set to 1 here) leads to a Taub-NUT metric. Summing over the infinite tower of Kaluza-Klein momenta k along the S^1 turns it into the periodic Taub-NUT metric described in Section 4.1.2. Thus, the projective Lagrangian is given by

$$f(\eta_e) = \sum_{k=-\infty}^{\infty} (\eta_e - k)\log(\eta_e - k)\,. \tag{4.3.3}$$

Recall that here each term in the Lagrangian is to be integrated along an 8-figure contour around the roots of $\eta_e - k = 0$. To isolate instanton contributions, we perform a Poisson resummation, yielding[5] $f = f^{sf} + f^{inst}$, such

[4] We have normalized the angular variables $\theta_{e,m}$ to have period 1.

[5] Poisson resummation works as follows:

$$\sum_{n=-\infty}^{\infty} f(n) = \sum_{k=-\infty}^{\infty} \hat{f}(k)\,, \qquad \hat{f}(k) = \int_{-\infty}^{\infty} dx\, e^{-2\pi i k x} f(x)\,.$$

that

$$f^{sf} = -i\left(\eta_e^2 \log\left(\frac{y\eta_e}{\Lambda}\right) - \eta_e^2 \log\left(\frac{-\eta_e}{y\bar{\Lambda}}\right)\right), \tag{4.3.4}$$

$$f^{inst} = i\,s\sum_{n>0}\frac{1}{n^2}e^{in\eta_e}\theta(s) + i\,s\sum_{n<0}\frac{1}{n^2}e^{in\eta_e}\theta(-s), \tag{4.3.5}$$

where Λ is the UV cutoff, $s \equiv \text{sign}\,[\text{Im}\,(\eta_e)]$ and we have omitted the divergent $n = 0$ term. The semiflat Lagrangian f^{sf} has been included using the c-map prescription described previously, with the 1-loop prepotential $\mathcal{F}(W) \sim W^2 \log W^2$. The full magnetic coordinate is then given by (4.2.12). Note that since the Heaviside functions $\theta(\pm s)$ in f^{inst} contain y, they restrict the integration contour. Using the identity

$$\text{Im}\,(\eta_e) = (1+|y|^2)\text{Im}\left(\frac{a}{y}\right), \tag{4.3.6}$$

we see that $\theta(\pm s)$ imposes the BPS ray condition[6]

$$l_\pm = \left\{y : \text{sign}\left[\text{Im}\left(\frac{a}{y}\right)\right] = \pm 1\right\},$$

leading to

$$\oint_{C_0} f^{inst}(\eta_e) = i\int_{l_+}\text{Li}_2\left(e^{i\eta_e}\right) - i\int_{l_-}\text{Li}_2\left(e^{-i\eta_e}\right), \tag{4.3.7}$$

where we have used the series expansion for $\text{Li}_2(x) = \sum_{n=1}^{\infty}\frac{x^n}{n^2}$. Substituting (4.3.7) in (4.2.12) finally gives

$$\eta_m = \eta_m^{sf} + \frac{i}{2}\int_{l_+}\frac{dy'}{y'}\frac{y+y'}{y-y'}\ln\left(1-e^{i\eta_e}\right) - \frac{i}{2}\int_{l_-}\frac{dy'}{y'}\frac{y+y'}{y-y'}\ln\left(1-e^{-i\eta_e}\right), \tag{4.3.8}$$

where η_m^{sf} is given by (4.2.11). Thus, we have recovered GMN's result for the mutually local case. We now discuss the mutually nonlocal case.

4.3.2 Mutually Nonlocal Corrections

Inspired by the analytic and asymptotic properties of (4.3.8), an integral equation (of the form of a TBA equation) for the Darboux coordinates in the mutu-

[6] Our conventions in the definition of η_e differ by a factor i with those of GMN, and so does the definition of the BPS rays.

ally nonlocal case was derived in [74]. The natural proposal to include dyonic multiplets is that each BPS particle of charge γ contributes independently to the projective instanton Lagrangian, with a weight given by the multiplicity of each state $\Omega(\gamma';u)$, *i.e.*,

$$f^{inst} = i\sum_{\gamma'} \Omega(\gamma';u)\,\mathrm{Li}_2\left(\sigma(\gamma')e^{i\eta_{\gamma'}}\right)\,\theta(s_{\gamma'})\,. \tag{4.3.9}$$

Here $\gamma = (n_e, n_m)$ is a vector in the two-dimensional charge lattice with the antisymmetric product $\langle\gamma,\gamma'\rangle = n_e n'_m - n'_e n_m$, $\sigma(\gamma) = (-1)^{n_e\, n_m}$, and $s_\gamma = \mathrm{sign}\left[\mathrm{Im}\left(\frac{Z_\gamma}{y}\right)\right]$ that defines the BPS ray l_γ. The symplectic form is given by

$$\varpi = iy\, d\eta_\gamma \wedge d\tilde{\eta}_\gamma\,, \tag{4.3.10}$$

where $\tilde{\eta}_\gamma = \sum_{\gamma'\neq\gamma} \eta_{\gamma'}\langle\gamma',\gamma\rangle^{-1}$ is the dual Darboux coordinate. The straightforward extension of the results obtained for the mutually local case is

$$\eta_\gamma = \eta^{sf}_\gamma + \frac{i}{2}\sum_{\gamma'}\langle\gamma',\gamma\rangle \oint_{C_0}\frac{dy'}{y'}\frac{y+y'}{y-y'}\frac{\partial f^{inst}}{\partial\eta'_{\gamma'}}\,. \tag{4.3.11}$$

Inserting (4.3.9) above leads to

$$\eta_\gamma = \eta^{sf}_\gamma + \frac{i}{2}\sum_{\gamma'}\Omega(\gamma';u)\langle\gamma',\gamma\rangle\int_{l_{\gamma'}}\frac{dy'}{y'}\frac{y+y'}{y-y'}\ln\left(1-\sigma(\gamma')e^{i\eta'_{\gamma'}}\right)\,, \tag{4.3.12}$$

thus reproducing the TBA equation that determines the exact moduli space metric. Note that the Darboux coordinates played the central role in the analysis by GMN, being in some sense the fundamental objects. In the current setting, the fundamental object (which behaves additively and contains all the geometric information) is the projective Lagrangian f. The Darboux coordinates are determined by it through the integral equation (4.3.11).

4.4 $\mathcal{N} = 1$ SYM on $\mathbb{R}^3 \times T^2$

Minimally supersymmetric Yang-Mills in five dimensions has an interesting BPS spectrum, containing not only electrically charged particles, but also magnetically charged strings and dyonic instantons [96]. Since the theory is non-renormalizable by power-counting it should be viewed as a field theory with a cutoff. In this sense, one can still ask what are the quantum corrections to the moduli space. This was first studied in [97], where the exact Coulomb

branch metric was determined. More recently, the compactification of this theory on T^2 was studied in [80], giving an important first step in analyzing the Coulomb branch metric of the compactified theory. Since dimensional reduction of this theory to four dimensions leads to the theory discussed in the previous section, compactification of the five-dimensional theory on T^2 gives a (two-parameter) generalization of the moduli space studied above.

The bosonic content of this theory consists of a real scalar σ and the gauge field $A_{\hat{\mu}}$. Upon dimensional reduction to three dimensions, the gauge field reduces according to $A_{\hat{\mu}} \to (A_i, A_4, A_5)$, leading again to a four-dimensional moduli space. The two electric coordinates φ_1, φ_2 and the 'magnetic' coordinate λ are defined by

$$\varphi_1 \equiv \frac{1}{2\pi} \oint_{S^1_4} A_4 \,, \qquad \varphi_2 \equiv \frac{1}{2\pi} \oint_{S^1_5} A_5 \,, \qquad \lambda \equiv \int_{T^2} B \,, \tag{4.4.1}$$

where $B_{\hat{\mu}\hat{\nu}}$ is the (2-form) dual of the photon $A_{\hat{\mu}}$. Under large gauge transformations, these variables are periodic and parameterize a torus T^2. Due to the electric particles running around these two compactified dimensions, the Coulomb branch metric inherits the modular properties of the torus and has an isometry in λ. A full analysis of the moduli space must include the effect of dyonic instantons, as well as the mutually nonlocal effect of magnetic strings wrapping the whole T^2, which will break the isometry in λ. In this chapter, we focus only on the projective description of the electric corrections to the moduli space metric, hoping that this will help in incorporating the effect of magnetic strings as well.

4.4.1 Electric Corrections

Here we apply the methods of Section 4.2 to find the corrections to η_m, due to electric particles running along the two compact directions. It is clear that the metric in this case is simply the dPTN metric. For simplicity, we discuss first the projective description of this metric in the case of a rectangular torus and then for a generic torus with complex structure τ.

Rectangular Torus. Consider a rectangular torus with radii R_1, R_2 and complex structure $\tau = i\frac{R_1}{R_2}$. We define the doubly periodic $\mathcal{O}(2)$ multiplet by

$$\eta_e = \frac{\sigma R_2 + i\varphi_2}{2R_2 y} + \frac{\varphi_1}{R_1} - \frac{(\sigma R_2 - i\varphi_2)}{2R_2} y \,. \tag{4.4.2}$$

With this definition, the projective Lagrangian f for the dPTN metric has the form (4.1.7) with

$$\eta_k = \frac{1}{R_1} k_1 + \frac{i}{2R_2} \left(\frac{1}{y} + y \right) k_2 \equiv a_1 k_1 + a_2 k_2 \,. \tag{4.4.3}$$

For convenience, rather than concentrating on the calculation of f, in this section we will focus on the Gibbons-Hawking potential V, given by

$$V = \sum_{\vec{k}} \oint_{\tilde{C}} \frac{dy}{y} \frac{1}{\eta_e - a_1 k_1 - a_2 k_2} \,. \tag{4.4.4}$$

As before, $\tilde{C}$ is an 8−shaped contour enclosing the poles of the integrand for each $\vec{k}$, leading to a doubly periodic Gibbons-Hawking potential. This potential is linearly divergent and as in the PTN case should be understood to be properly regularized. We now perform a double Poisson resummation. Resumming over k_1 first gives

$$\begin{aligned} V &= V^{(0)} + V^{(1)} \,, \\ V^{(0)} &= -R_1 \oint_{C_0} \frac{dy}{y} \sum_{k_2} \log \left[y R_1 \left(\eta_e - a_2 k_2 \right) \right] + c.c. \,, \\ V^{(1)} &= -i R_1 \oint_{C_0} \frac{dy}{y} \sum_{k_2} \sum_{n_1 \neq 0} e^{i n_1 R_1 (\eta_e - a_2 k_2)} s \, \theta \left(n_1 s \right) \,, \end{aligned} \tag{4.4.5, 4.4.6}$$

where $s = \text{sign} \left[\text{Im} \left(\eta_e - a_2 k_2 \right) \right]$. Here $V^{(0)}$ is a superposition of shifted semiflat potentials of Section 4.3. We now show that it leads to the effective gauge coupling $\frac{1}{g_4(a)^2}$ due to the dimensional reduction from 5D to 4D [98], and it reduces (after Poisson resummation) to the semiflat potential in the $R_2 \to 0$ limit. Performing the integral around the origin in (4.4.5) gives

$$V^{(0)} = -R_1 \sum_{k_2} \log \left(\frac{\sigma R_2 + i(\varphi_2 - k_2)}{2R_2} \right) + c.c. = R_1 \sum_{n_2 \neq 0} \frac{1}{|n_2|} e^{-(R_2 |n_2 \sigma| - i n_2 \varphi_2)} \,, \tag{4.4.7}$$

where we performed a Poisson resummation for the second equality. This in fact matches the result in [98] (see also [80]). In the four-dimensional limit,

$$V^{(0)} \xrightarrow{R_2 \to 0} V^{sf}_{4D} = R_1 \left(\log a + \log \bar{a} \right) \,, \tag{4.4.8}$$

where $a = \frac{\sigma R_2 + i\varphi_2}{2R_2}$, which coincides with the potential derived from (4.3.4). The contribution to the magnetic coordinate is given by

$$\eta_m^{(0)} = \frac{\mathcal{F}'(a)}{y} + \frac{\lambda}{R_1} - \bar{\mathcal{F}}'(\bar{a})\, y\,, \tag{4.4.9}$$

where we have integrated (4.4.7) twice with respect to a to determine

$$\mathcal{F}(a) = \frac{1}{4R_2^2}\left[\mathrm{Li}_3\left(e^{2aR_2}\right)\theta(-\sigma) + \mathrm{Li}_3\left(e^{-2aR_2}\right)\theta(\sigma)\right]. \tag{4.4.10}$$

Now we turn to $V^{(1)}$, which in the $R_2 \to 0$ limit reduces to the instanton corrections in the four-dimensional theory. The contour in (4.4.6) splits into two rays $l_\pm$, and integration along these rays ensures that the limit $R_2 \to 0$ is well defined. In fact, in this limit the sum over k_2 is localized at $k_2 = 0$, *i.e.*,

$$V^{(1)} \xrightarrow{R_2\to 0} V_{4D}^{inst} = -iR_1 \oint_{C_0} \frac{dy}{y} \sum_{n_1\neq 0} e^{in_1 R_1 \eta_e} s\, \theta\left(n_1 s\right), \tag{4.4.11}$$

which is the Gibbons-Hawking potential one would get from (4.3.5). (One should rescale $a \to R_1 a$ in the four-dimensional case for comparison.)

For finite R_2, Poisson resumming (4.4.6) leads to[7]

$$V^{(1)} = -\oint_{C_0} \frac{dy}{y} \sum_{\substack{n_1\neq 0\\ n_2\in\mathbb{Z}}} \frac{e^{\frac{in_1\eta_e}{a_1}}}{a_2 n_1 - a_1 n_2}\,. \tag{4.4.12}$$

Note that after the double Poisson resummation, the contour in (4.4.12) remains a closed contour, enclosing only the essential singularity at the origin (and not the simple poles). By residue integration, we find

$$V^{(1)} = R_1 R_2 \sum_{\substack{n_1\neq 0\\ n_2\in\mathbb{Z}}} \frac{1}{\sqrt{n_1^2 R_1^2 + n_2^2 R_2^2}} e^{i(n_1\varphi_1 + n_2\varphi_2) - |\sigma|\sqrt{n_1^2 R_1^2 + n_2^2 R_2^2}}\,. \tag{4.4.13}$$

[7] Here we have dropped a term in the exponent

$$e^{in_1 R_1 \eta_e + i\,\mathrm{Im}(\eta_e)\frac{2R_1R_2|y|^2}{(1+|y|^2)\mathrm{Re}(y)}\left[\frac{n_2}{R_1} - \frac{in_1}{2R_2}\left(\frac{1}{y}+y\right)\right]},$$

because we choose the contour enclosing the origin along which $\mathrm{Im}(\eta_e) = \pm\epsilon$. In the limit $\epsilon \to 0$ this term does not contribute to the integral, which becomes simply an integral around the origin.

Combining the two contributions, we have

$$V = V^{(0)} + V^{(1)} = R_1 R_2 \sum_{\vec{n}\in\mathbb{Z}^{2'}} \frac{1}{\sqrt{n_1^2 R_1^2 + n_2^2 R_2^2}} e^{i(n_1\varphi_1 + n_2\varphi_2) - |\sigma|\sqrt{n_1^2 R_1^2 + n_2^2 R_2^2}}\,, \tag{4.4.14}$$

which matches the expression for U_{1-loop} in [80]. Integrating twice with respect to η_e (and dropping a possible linear term, which does not contribute to η_m), we find

$$f^{(1)} = \sum_{\substack{n_1\neq 0\\ n_2\in\mathbb{Z}}} \frac{a_1^2}{n_1^2\,(n_2 a_1 - n_1 a_2)}\, e^{\frac{i n_1 \eta_e}{a_1}}\,. \tag{4.4.15}$$

As explained in [80], the corrections due to $f^{(1)}$ to the Coulomb branch metric should coincide with the corrections to the hypermultiplet moduli space due to D1 instantons in type IIB theory. Indeed, we find that the projective Lagrangian $f^{(1)}$ matches with that given in [99]. Now, putting all the elements together, the magnetic coordinate for the dPTN metric finally reads

$$\eta_m = \eta_m^{(0)} + \frac{i}{2}\oint_{C_0} \frac{dy'}{y'}\,\frac{y+y'}{y-y'}\,\frac{\partial f^{(1)}}{\partial \eta_e'}\,. \tag{4.4.16}$$

In summary, the magnetic coordinate contains two parts: the $\eta_m^{(0)}$ part from the naïve 5D to 4D reduction, which becomes η_m^{sf} in the 4D limit, and the remaining part, which reduces to η_m^{inst}.

Generic Torus. To consider a generic torus with complex structure τ, we perform a modular transformation from the rectangular case. Under the $SL(2,\mathbb{Z})$ symmetry group of the torus, the complex structure $\tau = \tau_1 + i\tau_2$ and the coordinates transform as

$$\tau \to \frac{a\tau + b}{c\tau + d}\,, \qquad \begin{pmatrix} \varphi_2 \\ \varphi_1 \end{pmatrix} \to \begin{pmatrix} a & c \\ b & d \end{pmatrix} \begin{pmatrix} \varphi_2 \\ \varphi_1 \end{pmatrix}\,, \tag{4.4.17}$$

with $ad - bc = 1$.

The electric coordinate for a generic torus then becomes[8]

$$\eta_e = \frac{1}{2y}\left(\sigma + i\sqrt{\frac{\tau_2}{\mathcal{V}}}\varphi_2\right) + \frac{\varphi_1 + \tau_1\varphi_2}{\sqrt{\mathcal{V}\tau_2}} - \frac{1}{2}\left(\sigma - i\sqrt{\frac{\tau_2}{\mathcal{V}}}\varphi_2\right) y\,. \tag{4.4.18}$$

Here we also rescaled the φ_i's by the volume $\mathcal{V}$ of the torus. The Gibbons-Hawking potential is now given by (4.4.4) with

$$a_1 = \frac{1}{\sqrt{\mathcal{V}\,\tau_2}}\,, \qquad a_2 = \frac{1}{\sqrt{\mathcal{V}\tau_2}}\left[\tau_1 + i\tau_2\frac{1}{2}\left(\frac{1}{y} + y\right)\right]\,. \tag{4.4.19}$$

Upon Poisson resummation and contour integration, we find

$$V = \sqrt{\det g_{ij}} \sum_{\vec{n}\in\mathbb{Z}^{2'}} \frac{1}{\sqrt{n^i n^j g_{ij}}} e^{in^i\varphi_i - |\sigma|\sqrt{n^i n^j g_{ij}}}\,, \tag{4.4.20}$$

with the metric g on the torus given by

$$g_{ij} = \frac{\mathcal{V}}{\tau_2}\begin{pmatrix} 1 & -\tau_1 \\ -\tau_1 & |\tau|^2 \end{pmatrix}\,. \tag{4.4.21}$$

Finally, the magnetic coordinate is still given by (4.4.16), with the new definitions (4.4.18), (4.4.19), and the replacement $2a \to \left(\sigma + i\sqrt{\frac{\tau_2}{\mathcal{V}}}\varphi_2\right)$ in $\eta_m^{(0)}$.

4.4.2 Dyonic Instanton Corrections

Dyonic instantons are particle-like objects which are the uplift of 4-dimensional instantons to five dimensions. Due to the Chern-Simons term

$$\frac{\kappa}{24\pi^2} A \wedge F \wedge F\,, \tag{4.4.22}$$

they become electrically charged. Their central charge is given by

$$Z_I = \kappa\sigma|n_I| + \frac{|n_I|}{g_{5,0}^2}\,, \tag{4.4.23}$$

[8]For a generic torus with complex structure $\tau = \tau_1 + i\tau_2$, we perform the $SL(2,\mathbb{Z})$ transformation $\varphi \to M^T\varphi$, where M is given by

$$M = \frac{1}{\sqrt{\tau_2}}\begin{pmatrix} \tau_2 & \tau_1 \\ 0 & 1 \end{pmatrix}\,.$$

The metric transforms according to $g \to (M^{-1})^T g\, M^{-1}$, leading to (4.4.21).

where $g_{5,0}$ is the five-dimensional gauge coupling and n_I is the four-dimensional instanton number. Since these particles are electrically charged, they contribute corrections to the metric preserving the isometry. Hence, their effect is incorporated easily by replacing $a \to a + Z_I$ in the definition of the $\mathcal{O}(2)$ multiplet.

A more interesting contribution to the metric will come from magnetic corrections. These are now given by magnetic strings and incorporating their effect will be studied elsewhere.

4.5 Discussion

We have derived the expression for a set of Darboux coordinates on a hyperkähler manifold, parameterized by $\mathcal{O}(2p)$ projective superfields. Our derivation relies on the projective Legendre transform construction of such manifolds and can be understood as enforcing a consistency condition. The application of our results to the PTN metric leads to the expression for the magnetic coordinate derived by GMN, describing the mutually local corrections to the moduli space metric of $\mathcal{N} = 2$ SYM on $\mathbb{R}^3 \times S^1$. Mutually nonlocal corrections can also be incorporated into the projective Lagrangian, leading to the TBA equation studied by GMN.

We also applied this method to the study of electric corrections to the moduli space of five-dimensional SYM compactified on T^2, providing a projective superspace description of the metric discussed in [80] and the corresponding Darboux coordinates. There are two contributions: an $\mathcal{O}(2)$ part determined by the five-dimensional perturbative prepotential, which reduces to the semi-flat part in the 4D limit; and the corrections due to electric particles, which reduce to the instanton corrections of the 4D theory.

There are several open questions which could be addressed within this formalism. For example, it could shed new light on the three-dimensional limit of GMN (recently analyzed in [100]), corresponding to the Atiyah-Hitchin metric. Regarding the five-dimensional theory, corrections due to magnetic strings could be incorporated in a form analogous to what was done in (4.3.9) for the four-dimensional case, leading to an integral equation for the Darboux coordinates.

Apart from the Darboux coordinates, another important geometrical object is the hyperholomorphic connection (see for example [101, 102]) and it would be interesting to investigate its description using the $\Upsilon \leftrightarrow \eta$ duality. Finally, it would be quite interesting if this framework could yield any information about the six-dimensional SYM theory compactified on T^3, whose exact moduli space is K3.

Chapter 5

Quiver Chern-Simons Theories

Supersymmetric localization [103, 104] is a powerful method that makes exact computations in superconformal field theories (SCFTs) possible. This procedure reduces the infinite dimensional path integral to a finite dimensional integral, typically over the Coulomb branch. It has recently been used to obtain interesting results for field theories in various number of dimensions [104–109]. In particular, Kapustin, Willett and Yaakov [105] applied localization in three dimensions to calculate the exact partition function on S^3 for theories with $\mathcal{N} \geq 2$ supersymmetry. One of the outcomes of these calculations has been the proposal [110] that the free energy, defined by

$$F = -\log |Z_{S^3}| \,,$$

decreases along renormalization group (RG) flows, providing a good measure of the degrees of freedom in the field theory. On the other hand, many three-dimensional SCFTs can be realized as effective theories of coincident N M2-branes. Thus, localization is a tool that can be used to test predictions of the AdS/CFT correspondence [111–113]. One of the first and most remarkable results [114] was the evaluation of the free energy for $U(N)_k \times U(N)_{-k}$ Chern-Simons (CS) theory [115], matching the famous $N^{3/2}$ scaling of gravitational free energy predicted in [116].

A larger class of quiver Chern-Simons theories with $U(N)_{k_1} \times U(N)_{k_2} \times ... \times U(N)_{k_n}$ gauge groups, coupled to bifundamental matter forming a necklace-type quiver were considered in [110, 117–119]. It is believed that the M-theory description of these theories [120] arises as the near-horizon limit of a stack of N M2-branes placed at the tip of a Calabi-Yau cone with a tri-Sasaki Einstein

base Y. In the large N limit, the gravitational free energy is given by [114,117]

$$F = N^{3/2}\sqrt{\frac{2\pi^6}{27\,\mathrm{Vol}(Y)}} + o(N^{3/2})\,,$$

where $\mathrm{Vol}(Y)$ is the volume of the compact manifold Y whose geometry depends on the quiver data, in particular the CS levels. By evaluating the free energy F for the necklace quivers and matching it with the gravitational energy, an expression for $\mathrm{Vol}(Y)$ as a function of the CS levels was conjectured in [117]. This was corroborated in [121] by comparison with the explicit calculations of the volumes of toric Sasaki-Einstein manifolds [122] (see also [123] for a calculation in type-IIB supergravity).

These necklace quivers are actually an example of a more general class of quiver theories which have a nice large N limit, *i.e.*, long-range forces between eigenvalues in the matrix model cancel [124]. In fact, quiver theories for which this happens are in one-to-one correspondence with the extended ADE Dynkin diagrams with necklace quivers corresponding to the $\widehat{A}$-class.

In this chapter we focus on theories with $\widehat{D}_n$ quivers. The relevant tri-Sasaki Einstein manifold Y is the base of the hyperkähler cone $\mathbb{H}^{4n-8}///U(1)^{n-1}\times SU(2)^{n-3}$. By assuming a particular ordering of CS levels, we solve the matrix models for various values of n and propose an expression for $\mathrm{Vol}(Y)$ for arbitrary n. This expression is related to the area of a certain polygon as in the case of $\widehat{A}$-quivers. Then, we propose a general expression given by a rational function, which is valid for any ordering of the CS levels and is invariant under Seiberg duality. The numerator for such an expression was given in [124]. Here we give the denominator as well and show that the numerator of this expression can be expressed as a sum over certain graphs known as 'signed graphs'. Using a generalized matrix-tree formula, we show that this formula reduces to the polygon formula for a particular ordering of the CS levels. Although we do not discuss exceptional quivers in detail, we give the free energy for $\widehat{E}_6, \widehat{E}_7, \widehat{E}_8$ in Appendix C.3 for completeness.

5.1 $\widehat{ADE}$ Matrix Models

We will consider quiver Chern-Simons gauge theories involving products of unitary groups only, *i.e.*, $G = \otimes_a U(n_a N)$, coupled to bifundamental chiral superfields $(A_a,\, B_a)$. According to [105], the partition function of these theories on S^3 is localized on configurations where the auxiliary scalar fields σ_a in the $\mathcal{N} = 2$ vector multiplets are constant $N \times N$ matrices. Thus, evaluating the free energy amounts to solving a matrix model.

Matrix Model. We denote the eigenvalues of σ_a in each vector multiplet by $\lambda_{a,i}$, $i = 1, ..., N_a$. The partition function is then given by [105]

$$Z = \int \left(\prod_{a,i} d\lambda_{a,i} \right) L_v(\{\lambda_{a,i}\}) L_m(\{\lambda_{a,i}\}) = \int \left(\prod_{a,i} d\lambda_{a,i} \right) \exp\left[-F(\{\lambda_{a,i}\}) \right], \tag{5.1.1}$$

where the contribution from vector multiplets is

$$L_v = \prod_{a=1}^{d} \frac{1}{N_a!} \left(\prod_{i>j} 2\sinh[\pi(\lambda_{a,i} - \lambda_{a,j})] \right)^2 e^{\left(i\pi \sum_{a,j} k_a \lambda_{a,j}^2 \right)},$$

and from matter multiplets is

$$L_m = \prod_{(a,b)\in E} \prod_{i,j} \frac{1}{2\cosh[\pi(\lambda_{a,i} - \lambda_{b,j})]} \prod_c \left(\prod_i \frac{1}{2\cosh[\pi\lambda_{c,i}]} \right)^{n_c^f}.$$

The first product in L_m is due to bifundamental fields while the second one is due to fundamental flavor fields, where n_c^f is the number of pairs of flavor fields at the node labeled by the index c.

Large N Limit and $\widehat{ADE}$ Classification. Following [117,124], we assume that the eigenvalue distribution becomes dense in the large N limit, *i.e.*, $\lambda_{a,i} \to \lambda_a(x)$ with a certain density $\rho(x)$. In this limit the free energy becomes a 1-dimensional integral which we evaluate by saddle point approximation. We also assume that the eigenvalue distribution for a node with $N_a = n_a N$ is given by a collection of n_a curves in the complex plane labeled by $\lambda_{a,I}(x)$ with $I = 1, ..., n_a$ and write the ansatz

$$\lambda_{a,I}(x) = N^\alpha x + i\, y_{a,I}(x)\,. \tag{5.1.2}$$

The density $\rho(x)$ is assumed to be normalized, *i.e.*,

$$\int dx \rho(x) = 1\,, \tag{5.1.3}$$

which will be imposed through a Lagrange multiplier μ. As explained in [124], the leading order in N in the saddle point equation is proportional to the combination $2n_a - \sum_{b|(a,b)\in E} n_b$. The requirement that this term vanishes is equivalent to the quiver being in correspondence with simply laced extended Dynkin diagrams, leading to the ADE classification. To next order in N, the saddle

point equation contains a tree-level contribution and a 1-loop contribution. Assuming that $\sum_a n_a k_a = 0$, the requirement that these two contributions are balanced leads to $\alpha = 1/2$, which is ultimately responsible for the $N^{3/2}$ scaling of the free energy[1]. Finally, the Lagrangian to be extremized reads

$$F = N^{3/2} \int dx\, \rho(x) \Bigg[\pi n_F |x| + 2\pi x \sum_a \sum_{I=1}^{n_a} k_a y_{a,I}(x) + \frac{\rho(x)}{4\pi} \times \\ \times \left(\sum_{a=1}^{d} \sum_{I=1}^{n_a} \sum_{J=1}^{n_a} \arg\left(e^{2\pi i (y_{a,I} - y_{a,J} - \frac{1}{2})} \right)^2 - \sum_{(a,b)\in E} \sum_{I=1}^{n_a} \sum_{J=1}^{n_b} \arg\left(e^{2\pi i (y_{a,I} - y_{b,J})} \right)^2 \right) \Bigg] \\ - 2\pi\mu N^{3/2} \left(\int \rho(x)\, dx - 1 \right), \tag{5.1.4}$$

where $n_F \equiv \sum_a n_a^f n_a$. Evaluating the free energy on-shell gives

$$F = \frac{4\pi N^{3/2}}{3} \mu\,, \tag{5.1.5}$$

which can be understood as a virial theorem [121]. Thus, the free energy is determined by μ, which in turn is determined as a function of the CS levels from the normalization condition (5.1.3). Comparing (5.1.5) with the expression for gravitational free energy given in this chapter's introduction, we find that

$$\frac{\mathrm{Vol}(Y)}{\mathrm{Vol}(S^7)} = \frac{1}{8\,\mu^2}\,. \tag{5.1.6}$$

As mentioned earlier, theories with $\widehat{A}_{m-1}$ quiver diagrams have been extensively studied. Here, we wish to study theories with $\widehat{D}_n$ quivers as the one shown in Figure 5.1. For now we will set $n_a^f = 0$, but we will reintroduce flavors in Section 5.4.

It is convenient to relate the CS level $k_{(a)}$ at each node to a root α_a, by introducing a vector p and writing $k_{(a)} = \alpha_a \cdot p$. This way, the condition $\sum_a n_a k_a = 0$ is satisfied automatically. Choosing a basis for the roots of $\widehat{D}_n$ (see Appendix C.1 for conventions), we have

$$k_1 = -(p_1 + p_2)\,, \quad k_2 = p_1 - p_2\,, \quad k_3 = p_{n-1} - p_n\,, \quad k_4 = p_{n-1} + p_n\,, \\ k_i = p_{i-3} - p_{i-2}\,; \qquad i = 5, \ldots, n+1\,. \tag{5.1.7}$$

[1] Alternatively, one can assume that $\sum n_a k_a \neq 0$, and choose $\alpha = 1/3$, which leads to a massive IIA supergravity dual [110]. We will not consider this case here.

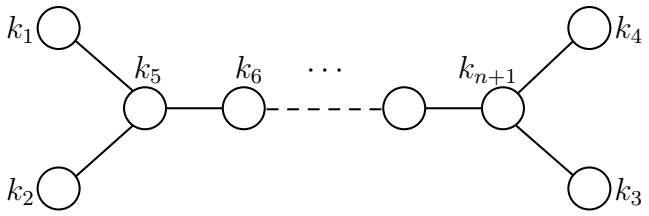

Figure 5.1: $\widehat{D}_n$ quiver diagram. Each node 'a' corresponds to a $U(n_a N)$ gauge group with CS level k_a, where n_a is the node's comark and we assume that $\sum_a n_a k_a = 0$.

In the next two sections we will solve the matrix models for various $\widehat{D}_n$ quivers and conjecture a general volume formula for arbitrary n.

5.2 Solving the Matrix Models

Here we describe the saddle point evaluation of the free energy (5.1.4). We show in detail the solution for $n = 5$, state the result for $n = 6$, and propose a general expression that we have checked for $n = 7, ..., 10$. Finally, we will relate this expression to the area of a certain polygon.

5.2.1 Explicit Solutions

Extremizing (5.1.4) (with respect to $y_{a,I}$ and ρ) requires an assumption on the branch of the arg functions. We will always take the principle value and therefore we assume that

$$|y_{a,I} - y_{a,J}| < 1\,; \qquad |y_{a,I} - y_{b,J}| < \frac{1}{2}\,, \quad \text{if } (a,b) \in E\,. \tag{5.2.1}$$

Based on numerical results [117, 124], we assume that the n_a curves for a given node initially coincide, *i.e.*, $|y_{a,I} - y_{a,J}| = 0$. Extremizing F under these assumptions, one finds that the solution is consistent only in a bounded region away from the origin. This is because as $|x|$ increases, the differences $|y_{a,I} - y_{b,J}|$ monotonically increase (or decrease), saturating one (or more) of the inequalities assumed in (5.2.1) at some point. The relation among the CS levels determines the sequence in which these inequalities saturate. This saturation will be maintained beyond this point, requiring the eigenvalue distribution involved either to bifurcate or develop a kink. As an example, consider the first plot in Figure 5.2 where we show the eigenvalue distributions

for the $\widehat{D}_5$ quiver[2]. It consists of seven regions determined by saturation of different inequalities. At the end of first region ($x = x_1$), one can see that $y_{1,1} - y_{5,2} = -1/2$ forcing $y_{5,1}$ and $y_{5,2}$ to bifurcate.

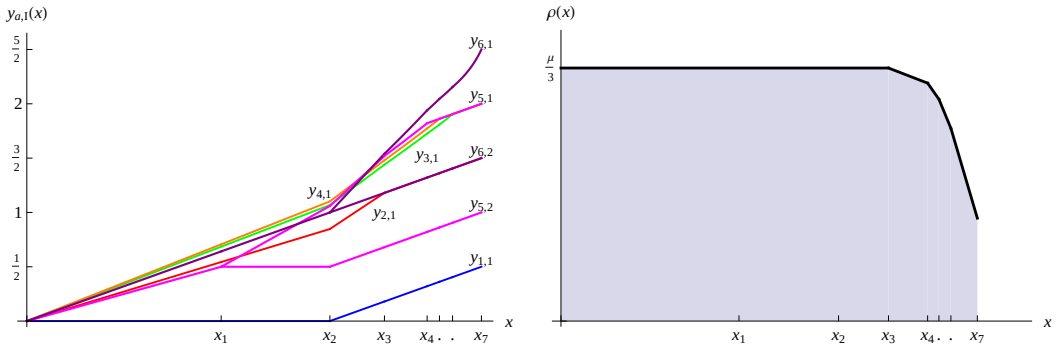

Figure 5.2: The eigenvalue distribution $y_{a,I}(x)$ (left) for all nodes and density $\rho(x)$ (right) for the $\widehat{D}_5$ quiver with CS levels: $(k_2, k_3, k_4, k_5, k_6) = (2, 2, 3, 4, 4)$.

After a saturation occurs, the total number of independent variables is reduced by one. Thus, at this point, we remove one variable from the Lagrangian, revise the inequalities and solve the equations of motion again until a new saturation is encountered. This process is iterated until all y_a's are related, determining a maximum of $(\sum_a n_a - 1)$ regions or until the eigenvalue distribution terminates, *i.e.*, $\rho(x) = 0$. Once the eigenvalue density $\rho(x)$ is determined in all regions, the value of μ (and therefore F) is found from the normalization condition (5.1.3).

The solution to the $\widehat{D}_4$ quiver consists of five regions and was solved in [124]. Assuming that $p_1 \geq p_2 \geq p_3 \geq p_4 \geq 0$, it was found that

$$\frac{1}{\mu^2} = -\frac{1}{4p_1} + \frac{2p_1 + 3p_2 - p_3}{(p_1 + p_2)^2} - \frac{1}{2(p_1 + p_2 + p_3 - p_4)} - \frac{1}{2(p_1 + p_2 + p_3 + p_4)}\,. \tag{5.2.2}$$

We now discuss the solution to the $\widehat{D}_5$ quiver, consisting of seven regions. We assume that $k_6 \geq k_5 \geq k_4 \geq k_3 \geq k_2 \geq 0$ with $k_1 = -(k_2 + k_3 + k_4 + 2k_5 + 2k_6)$ implying $p_1 \geq p_2 \geq p_3 \geq p_4 \geq p_5 \geq 0$. The solution is summarized in Table 5.1 and Figure 5.2 shows the eigenvalue distributions and density (further details are given in Appendix C.2). From the information given in

[2]We have used the freedom to add an arbitrary function to the $y_{a,I}$ to set $y_{1,1}(x) = 0$ in the first region and we solve explicitly only for $x \geq 0$ since the eigenvalue distributions and density are even functions of x.

R#	x_i	$\delta y(x=x_i)$	$\rho_i(x)$
1	$\frac{\mu}{3(k_2+k_3+k_4+2k_5+2k_6)}$	$y_{1,1}-y_{5,2}=-\frac{1}{2}$	$\frac{1}{3}\mu$
2	$\frac{4\mu}{6k_2+9k_3+9k_4+12k_5+18k_6}$	$y_{5,2}-y_{6,2}=-\frac{1}{2}$	$\frac{1}{3}\mu$
3	$\frac{2\mu}{3(2k_2+k_3+k_4+2k_5+2k_6)}$	$y_{2,1}-y_{6,2}=0$	$\frac{1}{3}\mu$
4	$\frac{2\mu}{2k_2+3(k_3+k_4+2k_5+2k_6)}$	$y_{5,1}-y_{6,2}=\frac{1}{2}$	$\frac{\mu}{2}+\frac{x}{4}(k_1-k_2)$
5	$\frac{2\mu}{2k_2+3k_3+5k_4+4k_5+6k_6}$	$y_{4,1}-y_{6,2}=\frac{1}{2}$	$\mu+xk_1$
6	$\frac{2\mu}{2k_2+5k_3+3k_4+4k_5+6k_6}$	$y_{3,1}-y_{6,2}=\frac{1}{2}$	$\frac{3\mu}{2}+\frac{x}{4}(6k_1-k_3-3k_4-2k_6)$
7	$\frac{2\mu}{2k_2+3k_3+3k_4+4k_5+6k_6}$	$y_{6,1}-y_{6,2}=1$	$2\mu+x(2k_1-k_3-k_4-k_6)$

Table 5.1: Key characteristics of the seven regions of $\widehat{D}_5$ matrix model: their boundaries, the saturated inequalities and the eigenvalue densities, assuming $k_6\geq k_5\geq k_4\geq k_3\geq k_2\geq 0$.

Table 5.1 and (5.1.3), we find

$$\begin{aligned}\frac{1}{\mu^2}=&-\frac{1}{2k_2+5k_3+3k_4+4k_5+6k_6}-\frac{1}{2k_2+3k_3+5k_4+4k_5+6k_6}\\&+\frac{4(k_3+k_4+3k_6-2k_1)}{(2k_2+3k_3+3k_4+4k_5+6k_6)^2}\\&-\frac{1}{9(2k_2+k_3+k_4+2k_5+2k_6)}-\frac{1}{2k_2+3k_3+3k_4+6k_5+6k_6}\,,\end{aligned}$$

which, using the relations in (5.1.7) gives

$$\begin{aligned}\frac{1}{\mu^2}=&-\frac{1}{18p_1}-\frac{1}{2(p_1+2p_2)}+\frac{(2p_1+2p_2+3p_3-p_4)}{(p_1+p_2+p_3)^2}\\&-\frac{1}{2(p_1+p_2+p_3+p_4-p_5)}-\frac{1}{2(p_1+p_2+p_3+p_4+p_5)}\,.\end{aligned}\tag{5.2.3}$$

Similarly, solving the $\widehat{D}_6$ matrix model as described above leads to a total of nine regions and integrating the eigenvalue density gives

$$\begin{aligned}\frac{1}{\mu^2}=&-\frac{1}{48p_1}-\frac{1}{6(p_1+3p_2)}-\frac{1}{2(p_1+p_2+2p_3)}+\frac{2(p_1+p_2+p_3)+3p_4-p_5}{(p_1+p_2+p_3+p_4)^2}\\&-\frac{1}{2(p_1+p_2+p_3+p_4+p_5-p_6)}-\frac{1}{2(p_1+p_2+p_3+p_4+p_5+p_6)}\,,\end{aligned}\tag{5.2.4}$$

for $p_1\geq p_2\geq ...\geq p_6\geq 0$.

5.2.2 General Solution and Polygon Area

By comparing (5.2.2), (5.2.3) and (5.2.4), we propose that the free energy for $\widehat{D}_n$ quivers is determined by:

$$\frac{1}{\mu^2} = \frac{1}{2}\sum_{a=1}^{n-3} \frac{c_a}{\sum_{b=1}^{a-1} p_b + (n-a-1)p_a} + \frac{2\sum_{b=1}^{n-3} p_b + 3p_{n-2} - p_{n-1}}{\left(\sum_{b=1}^{n-2} p_b\right)^2} - \frac{1}{2}\left(\frac{1}{\sum_{b=1}^{n-1} p_b - p_n} + \frac{1}{\sum_{b=1}^{n} p_b}\right), \tag{5.2.5}$$

with $c_a \equiv \frac{-2}{(n-a-1)(n-a-2)}$ and $p_1 \geq p_2 \geq ... \geq p_n > 0$. We have verified that this is correct for the $\widehat{D}_7, ..., \widehat{D}_{10}$ matrix models.

For $\widehat{A}$-quivers, it was shown in [121] that $\mathrm{Vol}(Y)$ can be interpreted as the area of a certain polygon. By rewriting (5.2.5) in a more suggestive form, we will show that there is a certain polygon (or rather a cone) whose area is related to $\mathrm{Vol}(Y)$ for $\widehat{D}$-quivers as well. This construction will be particularly useful in Sections 5.4 and 5.5. We start by observing that the denominators appearing in (5.2.5) can be written as

$$\bar{\sigma}_a = \sum_{b=1}^{n} \left(|p_a - p_b| + |p_a + p_b|\right) - 4\,|p_a|\,; \quad a = 1, ..., n\,,$$
$$\bar{\sigma}_0 = 2(n-2)\,, \qquad \bar{\sigma}_{n+1} = 2\sum_{b=1}^{n} |p_b|\,. \tag{5.2.6}$$

The first step in rewriting (5.2.5) is to combine consecutive terms to get

$$\frac{\mathrm{Vol}(Y)}{\mathrm{Vol}(S^7)} = \frac{1}{2}\left(\frac{1}{\bar{\sigma}_0\,\bar{\sigma}_1} + \sum_{a=1}^{n-1} \frac{p_a - p_{a+1}}{\bar{\sigma}_a\,\bar{\sigma}_{a+1}} + \frac{p_n}{\bar{\sigma}_n\,\bar{\sigma}_{n+1}}\right), \tag{5.2.7}$$

where we have used the relation (5.1.6). The next step is to introduce the vectors $\beta_a = (1, p_a)$ together with $\beta_0 = (0, 1)$ and $\beta_{n+1} = (1, 0)$. Defining the wedge product $(a, b) \wedge (c, d) = (ad - bc)$, we can write all the $\bar{\sigma}_a$'s in (5.2.6) in terms of $\gamma_{a,b} \equiv |\beta_a \wedge \beta_b|$ as follows

$$\bar{\sigma}_a = \sum_{b=1}^{n} \left(\gamma_{a,b} + \gamma_{a,-b}\right) - 4\gamma_{a,n+1}\,; \quad a = 0, ..., n+1\,, \tag{5.2.8}$$

where we have also defined $\beta_{-a} \equiv (1, -p_a)$. This finally leads to

$$\frac{\text{Vol}(Y)}{\text{Vol}(S^7)} = \frac{1}{2}\sum_{a=0}^{n} \frac{\gamma_{a,a+1}}{\bar{\sigma}_a\, \bar{\sigma}_{a+1}}\,. \tag{5.2.9}$$

Now, let us consider the vectors β_a, $a = 0, ..., n+1$ as defining a set of vertices v_a given by

$$v_a = v_0 + \textstyle\sum_{b=0}^{a-1} \beta_b\,,$$

where v_0 is a base point (undetermined for the moment). This set of vertices v_a in turn defines a new set of edges by the equations $v_a \wedge x = 1/2$. Then, the set of intersection points of consecutive edges, given by $w_a = \beta_a/(2\, v_a \wedge v_{a+1})$, together with the origin defines a cone $\mathcal{C}$ whose area is given by

$$\text{Area}(\mathcal{C}) = \frac{1}{8}\sum_{a=0}^{n} \frac{\beta_{a+1} \wedge \beta_a}{(v_a \wedge v_{a+1})(v_{a+1} \wedge v_{a+2})}\,. \tag{5.2.10}$$

The denominators $v_a \wedge v_{a+1} = v_a \wedge (v_a + \beta_a) = v_a \wedge \beta_a = \big(v_0 + \sum_{b=0}^{a-1} \beta_b\big) \wedge \beta_a$ depend on the choice of base point v_0. Choosing $v_0 = (-n+2, -1)$, we can set $(v_a \wedge v_{a+1}) = -1/2\, \bar{\sigma}_a$ leading to

$$\frac{\text{Vol}(Y)}{\text{Vol}(S^7)} = \text{Area}(\mathcal{C})\,. \tag{5.2.11}$$

We also note that by rescaling the cone $\mathcal{C}$ by a factor 2μ, we can actually interpret $\rho(x)$ as the height of the cone. In Figure 5.3 we show the rescaled cone corresponding to the $\widehat{D}_5$ quiver. The x coordinates of the vertices of this cone correspond to the location of the kinks in $\rho(x)$ in Figure 5.2. Thus, $1/2 = \int dx\, \rho(x) = 4\mu^2\, \text{Area}(\mathcal{C})$, from where (5.2.11) follows immediately.

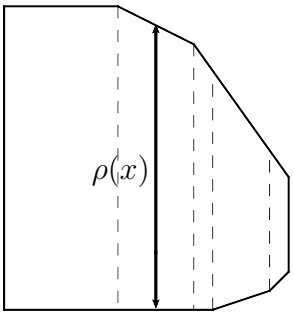

Figure 5.3: Schematic cone for the $\widehat{D}_5$ quiver. The height of the cone gives the density $\rho(x)$ in the regions defined by the x coordinates of the vertices w_a.

This construction is analogous to the polygon for the $\widehat{A}$-quiver [121]. The vectors β_a in that case correspond to the $(1, q_a)$ charges of five-branes involved in the brane description of the theory. The addition of the two extra vectors β_0 and β_{n+1} in the present case seems to suggest that one should also include $(0, 1)$ and $(1, 0)$ branes in the description of these theories.

We would like to comment that solving the matrix model under a different ordering of the p's amounts to permuting them correspondingly in the expression (5.2.9). Moreover, regardless of the sign and ordering of p's, the denominators appearing in the expression for $\mathrm{Vol}(Y)$ are always given by the $\bar{\sigma}$'s in (5.2.8). In the next section we will propose a general expression, which is valid for any value of the CS levels and is explicitly invariant under Seiberg duality.

5.3 General Formula for $\widehat{D}_n$ Quivers

It was shown in [125, 126] that the free energy is invariant under a generalized Seiberg duality [127, 128]. For ADE quivers, Seiberg duality can be reinterpreted as the action of the Weyl group, which acts by permuting and changing the sign of an even number of p's in the case of $\widehat{D}$-quivers. Thus, we would like to have an expression for $\mathrm{Vol}(Y)$ that does not assume any particular relation among CS levels and is explicitly invariant under Seiberg duality. It was proposed in [124] that this can be written as a rational function whose numerator is given by $\sum_{\mathcal{R}_+} \det(\alpha_1 ... \alpha_n)^2 \prod_{a=1}^{n} |\alpha_a \cdot p|$, where $\mathcal{R}_+$ denotes all n-subsets of positive roots. Note that under Weyl transformations the $\bar{\sigma}_a$'s defined in (5.2.8) are simply shuffled among each other. Based on this, we propose that the general expression for the volume corresponding to $\widehat{D}_n$ quivers is given by

$$\frac{\mathrm{Vol}(Y)}{\mathrm{Vol}(S^7)} = \frac{\sum_{\mathcal{R}_+} \det(\alpha_1 ... \alpha_n)^2 \prod_{a=1}^{n} |\alpha_a \cdot p|}{2 \prod_{a=0}^{n+1} \bar{\sigma}_a} \,. \tag{5.3.1}$$

As we will prove below, (5.3.1) reduces to (5.2.9) when the CS levels are ordered.

We recall that in the corresponding formula for $\widehat{A}$-quivers, the numerator could be interpreted as a sum over tree graphs [117]. In a similar way, we will show now that the numerator of (5.3.1) can be interpreted as a sum over certain graphs known as 'signed graphs' [129] (see also [130–132] and references therein). A graph $\Gamma = (V, E)$ consists of a set of vertices V and a set E of unordered pairs from V (the edges). A signed graph (Γ, σ) is a graph Γ with a signing $\sigma : E \to \{+1, -1\}$ associated to each edge. With these definitions, we can associate a signed graph to each term in the numerator of (5.3.1). Recall

that the roots α_a for D_n are of the form $(e_i \pm e_j)$, where e_i are the canonical unit vectors of dimension n and $i \neq j$. To a root of the type $(e_i - e_j)$ we associate a positive edge ($\sigma = 1$) connecting the nodes i and j in the graph, and to a root of the type $(e_i + e_j)$ we associate a negative edge ($\sigma = -1$). Then, we think of the matrix $I = (\alpha_1 ... \alpha_n)$ as an incidence matrix for a diagram with n vertices and n edges[3]. Due to Euler's theorem, such graphs must contain loops. If the graph contains more than one loop then it must be disconnected. Loops are naturally associated a sign as well, given by the product of the signs of all the edges forming the loop. As we shall explain below, the determinant in (5.3.1) selects diagrams containing only negative loops. Some examples of diagrams contributing to the numerator for $\widehat{D}_4$ are shown in Figure 5.4, where dashed lines represent negative edges and solid lines positive ones.

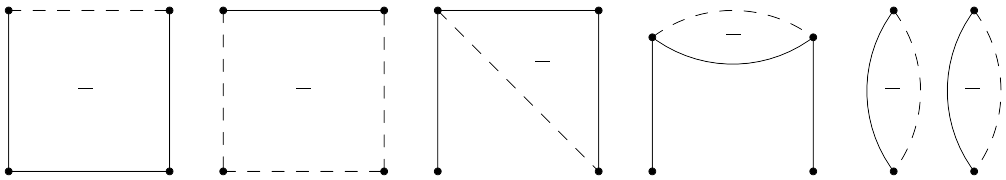

Figure 5.4: Some signed graphs contributing to the numerator for $\widehat{D}_4$. The first diagram, for example, contributes a term $4|(p_1+p_2)(p_2-p_3)(p_3-p_4)(p_4-p_1)|$.

To understand why the determinant vanishes for diagrams with positive loops, it is useful to introduce the operation acting on graphs called 'switching'. Switching is defined with respect to a vertex $v \in V$, and it acts by reversing the signs of all the edges connected to that vertex. This operation preserves the value of $(\det I)^2$ since it corresponds to multiplying some rows and columns of the incidence matrix I by -1. It is easy to see that by various switching operations one can turn any loop with an even number of negative edges into a loop made entirely of positive edges. Then, $\det I$ will vanish simply because the columns in I associated to these edges add up to zero. On the other hand, if there are an odd number of negative edges in the loop, the above argument does not apply. In fact, one can easily check that $(\det I)^2 = 4$ for each negative loop. Thus, we can also write (5.3.1) as

$$\frac{\mathrm{Vol}(Y)}{\mathrm{Vol}(S^7)} = \frac{\sum_{(V,E,\sigma)\in\mathcal{T}^-} 4^{L^-} \prod_{(a,b)\in E} |p_a - \sigma p_b|}{2\prod_{a=0}^{n+1} \bar{\sigma}_a}\,, \tag{5.3.2}$$

where $\mathcal{T}^-$ denotes the set of signed diagrams with n vertices and n edges (con-

[3]Note that due to the absence of roots of the form $2e_i$, one should not consider edges starting and ending on the same node.

nected or disconnected) and no positive loops, L_- is the number of negative loops in the diagram, and σ the sign of the corresponding edge. Using a generalized matrix-tree formula, we now show that (5.3.2) in fact reduces to (5.2.9) for $p_a > p_{a+1}$.

5.3.1 Generalized Matrix-tree Formula

We define the $n \times n$ adjacency matrix A for a signed graph by:

$$A_{aa} = \sum_{b=1}^{n-1} (\gamma_{a,b} + \gamma_{a,-b}) \,, \qquad A_{ab} = -\gamma_{a,b} + \gamma_{a,-b} \,.$$

The generalized matrix-tree formula [131, 132] states that

$$\det A = \textstyle\sum_{(V,E,\sigma)\in\mathcal{T}^-} 4^{L_-} \prod_{(a,b)\in E} |p_a - \sigma p_b| \,. \tag{5.3.3}$$

By row and column operations we can bring A into the tri-diagonal form:

$$\begin{pmatrix}
\bar\sigma_1+\bar\sigma_2+2\gamma_{12} & -\bar\sigma_2 & 0 & \cdots & \cdots & 0 \\
-\bar\sigma_2 & \bar\sigma_2+\bar\sigma_3+2\gamma_{23} & -\bar\sigma_3 & \cdots & \cdots & \vdots \\
0 & -\bar\sigma_3 & \ddots & \ddots & \vdots & \vdots \\
\vdots & \vdots & \ddots & \ddots & -\bar\sigma_{n-1} & 0 \\
\vdots & \cdots & \cdots & -\bar\sigma_{n-1} & \bar\sigma_{n-1}+\bar\sigma_n+2\gamma_{n-1,n} & -\bar\sigma_n \\
0 & \cdots & \cdots & 0 & -\bar\sigma_n & \frac{1}{2}(\bar\sigma_n+\bar\sigma_{n+1})
\end{pmatrix}$$

Using the fact that the determinant of tri-diagonal matrices satisfies a recursion relation, we have

$$\det A = \tfrac{1}{2}\,(\bar\sigma_n + \bar\sigma_{n+1}) \det A_{n-1} - \bar\sigma_n^2 \det A_{n-2} \,, \tag{5.3.4}$$

$$\det A_a = (\bar\sigma_a + \bar\sigma_{a+1} + 2\gamma_{a,a+1}) \det A_{a-1} - \bar\sigma_a^2 \det A_{a-2} \,, \tag{5.3.5}$$

where A_a denotes the $a \times a$ sub-matrix of A for $a = 1, ..., n-1$. Then, using the identities: $\bar\sigma_{a+1} - \bar\sigma_a = -2(n-2-a)\gamma_{a,a+1}$ and

$$\sum_{d=0}^{a-1} \frac{(n-2-d)\gamma_{d,d+1}}{\bar\sigma_d\,\bar\sigma_{d+1}} = \frac{1}{2\,\bar\sigma_a} \,,$$

we can show that the recursion relation (5.3.5) is solved by

$$\det A_{a-1} = \prod_{b=0}^{a} \bar{\sigma}_b \sum_{d=0}^{a-1} \frac{(a-d)\gamma_{d,d+1}}{\bar{\sigma}_d\, \bar{\sigma}_{d+1}} \,. \tag{5.3.6}$$

Using (5.3.6) in (5.3.4), we have

$$\begin{aligned}
\det A &= \frac{1}{2} \prod_{b=0}^{n+1} \bar{\sigma}_b \left[\left(1 + \frac{\bar{\sigma}_n}{\sigma_{n+1}} \right) \sum_{d=0}^{n-1} \frac{(n-d)\gamma_{d,d+1}}{\bar{\sigma}_d\, \bar{\sigma}_{d+1}} - \frac{2\bar{\sigma}_n}{\bar{\sigma}_{n+1}} \sum_{d=0}^{n-2} \frac{(n-1-d)\gamma_{d,d+1}}{\bar{\sigma}_d\, \bar{\sigma}_{d+1}} \right] \\
&= \frac{1}{2} \prod_{b=0}^{n+1} \bar{\sigma}_b \sum_{d=0}^{n-1} \left[2\frac{\gamma_{d,d+1}}{\bar{\sigma}_d\, \bar{\sigma}_{d+1}} + \left(\frac{\bar{\sigma}_{n+1} - \bar{\sigma}_n}{\bar{\sigma}_{n+1}} \right) \frac{(n-2-d)\gamma_{d,d+1}}{\bar{\sigma}_d\, \bar{\sigma}_{d+1}} \right] \\
&= \prod_{b=0}^{n+1} \bar{\sigma}_b \left[\sum_{d=0}^{n-1} \frac{\gamma_{d,d+1}}{\bar{\sigma}_d\, \bar{\sigma}_{d+1}} + \frac{1}{2} \frac{4\gamma_{n,n+1}}{\bar{\sigma}_{n+1}} \frac{1}{2\bar{\sigma}_n} \right] \\
&= \prod_{b=0}^{n+1} \bar{\sigma}_b \sum_{d=0}^{n} \frac{\gamma_{d,d+1}}{\bar{\sigma}_d\, \bar{\sigma}_{d+1}} \,.
\end{aligned}$$

Finally, substituting (5.3.3) in (5.3.2) leads to

$$\frac{\mathrm{Vol}(Y)}{\mathrm{Vol}(S^7)} = \frac{\det A}{2\prod_{b=0}^{n+1} \bar{\sigma}_b} = \frac{1}{2} \sum_{d=0}^{n} \frac{\gamma_{d,d+1}}{\bar{\sigma}_d\, \bar{\sigma}_{d+1}} \,,$$

recovering the expression (5.2.9).

5.4 Flavored $\widehat{D}_n$ Quivers and the F-theorem

The F-Theorem [110] states that the free energy F decreases along RG flows and is stationary at the RG fixed points of any three-dimensional field theory (supersymmetric or not). Thus, F gives a good measure of the number of degrees of freedom, in analogy with the c-function in two dimensions and the anomaly coefficient, a in four dimensions. This theorem was first tested in a variety of field theories [133–135] and recently it has been proven in [136, 137] for any three-dimensional field theory by relating F to the entanglement entropy of a disk-like region. Here we check that it holds for the the class of theories we have discussed. We trigger the RG flow by adding massive non-chiral fundamental flavors in the UV. By integrating out non-chiral flavor fields, there is no effective shift in the CS levels. Thus, we are interested in comparing $F(k_i; n_F)$ to $F(k_i; 0)$. The addition of $n_F \neq 0$ in (5.1.4) introduces

no additional complications and the matrix model is solved as explained in section 5.2. We solved the flavored $\widehat{D}_n$ matrix model for $n = 4, ..., 9$ leading us to

$$\frac{\text{Vol}(Y)}{\text{Vol}(S^7)} = \frac{1}{2}\left(\frac{\gamma_{01}}{\bar{\sigma}_0(\bar{\sigma}_1 + n_F)} + \sum_{a=1}^{n} \frac{\gamma_{a,a+1}}{(\bar{\sigma}_a + n_F)(\bar{\sigma}_{a+1} + n_F)}\right). \tag{5.4.1}$$

By comparing (5.4.1) with (5.2.9), it is clear that $F(k_i; n_F) \geq F(k_i; 0)$ verifying that

$$F_{UV} \geq F_{IR}\,,$$

in accordance with the F-theorem.

In terms of the polygon construction discussed in Section 5.2.2, adding flavor corresponds to adding the vector $\beta_F = (0, n_F/2)$ between β_0 and β_1. Then, (5.4.1) has the same form as (5.2.9) with $b = F, 1, ..., n$ in the definition (5.2.8).

5.5 Unfolding $\widehat{D}_n$ to $\widehat{A}_{2n-5}$

Here we provide a check of the formula (5.2.9), based on the folding/unfolding trick discussed in [138], which relates the free energy of various quiver gauge theories when some CS levels are identified. It can be used to change the gauge groups from unitary to orthosymplectic without changing the quiver or it can be used to change the quiver without changing the type of gauge group. Here we will deal with the latter use, as it relates the free energy of $\widehat{D}$-quivers to that of $\widehat{A}$-quivers.

When the external CS levels of a $\widehat{D}_n$ quiver are identified, it can be unfolded to an $\widehat{A}_{2n-5}$ quiver, as shown in Figure 5.5. Each internal node in the $\widehat{D}$-quiver is duplicated to give two nodes with the same CS level, while the four external nodes combine to give two nodes with doubled CS levels. Each node in the $\widehat{A}$-quiver corresponds to a $U(2N)$ gauge group and the condition $\sum_a n_a k_a = 0$ is automatically satisfied in the unfolded quiver. Using this, it can be shown that in the large N limit, $Z_D = \sqrt{Z_A}$ and therefore the free energies are related by $F_D = \frac{1}{2}F_A$. Here we verify explicitly this proportionality by comparing the formula (5.2.9) to the corresponding formula for $\widehat{A}_{2n-5}$.

Let us first look at the formula for the $\widehat{D}_n$ quiver when external CS levels are identified, *i.e.*, $k_1 = k_2 = k$ and $k_3 = k_4 = k'$. Due to the relations in (5.1.7), this is ensured by setting $p_1 = p_n = 0$. Thus, we need the solution to the matrix model with the ordering $p_2 \geq ... \geq p_{n-1} \geq p_n \geq p_1 \geq 0$. As mentioned at the end of Section 5.2, this is given by permuting the p's in

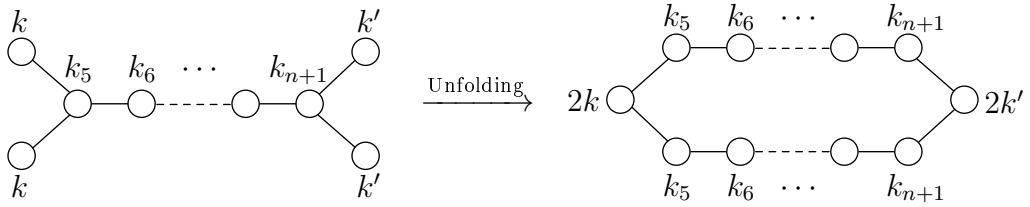

Figure 5.5: Unfolding $\widehat{D}_n$ to $\widehat{A}_{2n-5}$. Each node in the $\widehat{A}$-quiver corresponds to a $U(2N)$ gauge group.

(5.2.9) accordingly. Then, setting $p_1 = p_n = 0$ gives

$$\frac{\mathrm{Vol}(Y_D)}{\mathrm{Vol}(S^7)} = \frac{1}{2}\left(\frac{p_2}{\bar{\sigma}_2^2} + \sum_{a=2}^{n-2}\frac{\gamma_{a,a+1}}{\bar{\sigma}_a\,\bar{\sigma}_{a+1}} + \frac{p_{n-1}}{(\bar{\sigma}_{n-1})^2}\right). \tag{5.5.1}$$

Now we wish to compare this expression with the corresponding one for $\widehat{A}_{2n-5}$ [121], namely

$$\frac{\mathrm{Vol}(Y_A)}{\mathrm{Vol}(S^7)} = \frac{1}{2}\sum_{a=1}^{2n-4}\frac{\gamma_{a,a+1}}{\sigma_a\,\sigma_{a+1}}\,, \tag{5.5.2}$$

where $\sigma_a = \sum_{a=1}^{2n-4}|q_a - q_b|$, $\gamma_{a,b} = |q_a - q_b|$ and $\sum_{a=1}^{2n-4} q_a = 0$. The identification of opposite CS levels in the $\widehat{A}_{2n-4}$ quiver leads to $q_a = -q_{2n-3-a}$ (see Appendix C.1 for details). Then, we assume that $q_1 \geq ... \geq q_{n-2} \geq 0 \geq q_{n-1} \geq ... \geq q_{2n-4}$ and

$$\sigma_a = \sum_{b=1}^{n-2}|q_a - q_b| + \sum_{b=n-1}^{2n-4}|q_a - q_b| = \sum_{b=1}^{n-2}(|q_a - q_b| + |q_a + q_b|)\,; \quad a = 1, ..., n-2\,.$$

Noting that $\sigma_a = \bar{\sigma}_a$ and $q_a = p_{a+1}$ for $a = 1, ..., n-2$, we have

$$\begin{aligned}\frac{\mathrm{Vol}(Y_A)}{\mathrm{Vol}(S^7)} &= \frac{1}{2}\left(\sum_{a=1}^{n-3}\frac{\gamma_{a,a+1}}{\sigma_a\,\sigma_{a+1}} + \frac{\gamma_{n-2,n-1}}{\sigma_{n-2}\,\sigma_{n-1}} + \sum_{a=n-1}^{2n-5}\frac{\gamma_{a,a+1}}{\sigma_a\,\sigma_{a+1}} + \frac{\gamma_{2n-4,2n-3}}{\sigma_{2n-4}\,\sigma_{2n-3}}\right)\\ &= \sum_{a=1}^{n-3}\frac{\gamma_{a,a+1}}{\bar{\sigma}_a\,\bar{\sigma}_{a+1}} + \frac{q_{n-2}}{(\bar{\sigma}_{n-2})^2} + \frac{q_1}{\bar{\sigma}_1^2}\\ &= \frac{p_2}{\bar{\sigma}_2^2} + \sum_{a=2}^{n-2}\frac{\gamma_{a,a+1}}{\bar{\sigma}_a\,\bar{\sigma}_{a+1}} + \frac{p_{n-1}}{(\bar{\sigma}_{n-1})^2}\,.\end{aligned} \tag{5.5.3}$$

Thus, comparing (5.5.3) to (5.5.1) we have

$$\mathrm{Vol}(Y_D) = \tfrac{1}{2}\,\mathrm{Vol}(Y_A)\,. \tag{5.5.4}$$

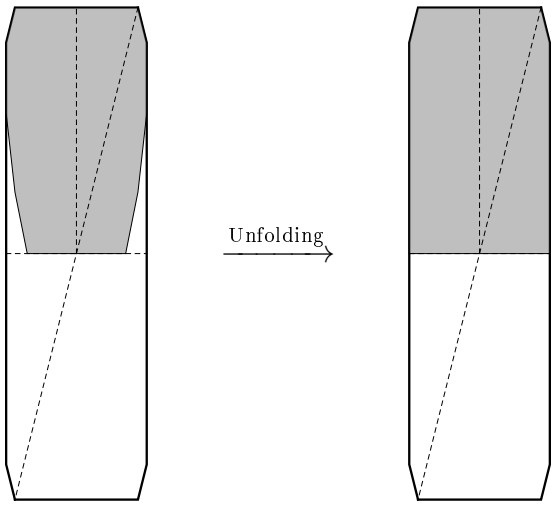

Figure 5.6: Polygons associated to the $\widehat{D}_4$ quiver (shaded region) and $\widehat{A}_3$ quiver (outer polygon). Upon unfolding, $\mathrm{Area}(\mathcal{P}_D) = 1/2\,\mathrm{Area}(\mathcal{P}_A)$.

This relation can also be seen clearly in terms of the areas of the corresponding polygons, as shown in Figure 5.6 (the cone as defined in Section 5.2.2 has been doubled along the dotted line for visual clarity). The outer polygon corresponds to the $\widehat{A}$-quiver with opposite CS levels identified and the shaded region on the left represents the polygon corresponding to a general $\widehat{D}$-quiver; when $p_1 = p_n = 0$, this shaded region expands to fill half of the outer polygon on the right.

Recalling that the nodes of the unfolded $\widehat{A}$-quiver correspond to $U(2N)$ gauge groups, we verify that

$$\frac{F_D}{F_A} = \frac{N^{3/2}}{(2N)^{3/2}}\sqrt{\frac{\mathrm{Vol}(Y_A)}{\mathrm{Vol}(Y_D)}} = \frac{1}{2}\,.$$

5.6 Discussion

In this last chapter we have studied three-dimensional $\widehat{D}_n$ quiver Chern-Simons matter theories by using the localization method of Kapustin, Willet and Yaakov in the large N limit. These field theories are believed to be dual to M-theory on $AdS_4 \times Y$, where Y is a tri-Sasaki Einstein manifold. We

have explicitly solved the corresponding matrix models for various values of n, leading us to conjecture a general expression for the free energy and therefore for the volume of the corresponding space Y given in (5.3.1). We have shown that the numerator of this expression can be interpreted as a sum over a class of graphs with edges that carry a sign, known as signed graphs. Using a generalized matrix-tree formula, we prove that for a particular ordering of CS levels, it can also be interpreted as the area of a certain polygon, given by (5.2.9). When external CS levels in the $\widehat{D}_n$ quiver are identified, the area of this polygon becomes half the area of the polygon corresponding to the $\widehat{A}_{2n-5}$ quiver, in accordance with the unfolding procedure. We have also studied the addition of massive flavor fields, showing that when they are integrated out, the area of the corresponding polygon always increases (thereby decreasing F), in accordance with the F-theorem.

The relevant tri-Sasaki Einstein space for a $\widehat{D}_n$ quiver is the base of the hyperkähler cone defined by the quotient $\mathbb{H}^{4n-8}///U(1)^{n-1}\times SU(2)^{n-3}$. To the best of our knowledge, the volumes of these spaces have not been computed. Thus, (5.3.1) can be considered as an AdS/CFT prediction for these volumes. A possible approach to proving the conjectured expression for the free energy would be to find the general solution to the matrix model, perhaps in terms of the polygon construction presented above, as it has been done for the $\widehat{A}$-quiver in [121]. Some questions which have not been addressed here are whether there is a group theory interpretation of the volume formula and whether its denominator can be written in a form that is universal for any ADE quiver.

References

[1] P. Fayet, "Fermi-Bose Hypersymmetry", *Nucl. Phys.* **B 113** (1976) 135.

[2] M. Sohnius, "Supersymmetry and Central Charges", *Nucl. Phys.* **B 138** (1978) 109.

[3] P. Howe, K. Stelle and P. Townsend, "The Relaxed Hypermultiplet: the Unconstrained $\mathcal{N} = 2$ Superfield Theory", *Nucl. Phys.* **B 214** (1983) 519.

[4] J. Yamron and W. Siegel, "Unified Description of the $\mathcal{N} = 2$ Scalar Multiplet", *Nucl. Phys.* **B 263** (1986) 70.

[5] W. Siegel and M. Roček, "On Off-shell Supermultiplets", *Phys. Lett.* **B 105** (1981) 275.

[6] V. Rivelles and J. Taylor, "Off-shell No-go Theorems for Higher Dimensional Supersymmetries and Supergravities", *Phys. Lett.* **B 121** (1983) 37.

[7] D. Jain and W. Siegel, "Deriving Projective Hyperspace from Harmonic", *Phys. Rev.* **D 80** (2009) 045024 [arXiv:0903.3588 [hep-th]].

[8] D. Jain and W. Siegel, "N=2 Super Yang-Mills Theory from a Chern-Simons Action", *Phys. Rev.* **D 86** (2012) 125017 [arXiv:1203.2929 [hep-th]].

[9] D. Jain and W. Siegel, "On Projective Hoops: Loops in Hyperspace", *Phys. Rev.* **D 83** (2011) 105024 [arXiv:1012.3758 [hep-th]].

[10] D. Jain and W. Siegel, "A Note on Massive Scalar Hypermultiplet in Projective Hyperspace", *Phys. Rev.* **D 86** (2012) 065036 [arXiv:1106.4601 [hep-th]].

[11] D. Jain, Warren Siegel, "Improved Methods for Hypergraphs", *Phys. Rev.* **D 88** (2013) 025018 [arXiv:1302.3277 [hep-th]].

[12] P. M. Crichigno, D. Jain, "Darboux Coordinates and Instanton Corrections in Projective Superspace", *JHEP* **1210** (2012) 027 [arXiv:1204.3899 [hep-th]].

[13] P. M. Crichigno, C. P. Herzog, D. Jain, "Free Energy of $\widehat{D}_n$ Quiver Chern-Simons Theories", *JHEP* **1303** (2013) 039 [arXiv:1211.1388 [hep-th]].

[14] A. Karlhede, U. Lindström and M. Roček, "Selfinteracting Tensor Multiplets in N=2 Superspace", *Phys. Lett.* **B 147** (1984) 297.

[15] U. Lindström and M. Roček, "New Hyperkähler Metrics and New Supermultiplets", *Commun. Math. Phys.* **115** (1988) 21.

[16] U. Lindström and M. Roček, "N=2 Superyang-Mills Theory in Projective Superspace", *Commun. Math. Phys.* **128** (1990) 191.

[17] A. Galperin, E. Ivanov, S. Kalitsyn, V. Ogievetsky and E. Sokatchev, "Unconstrained N=2 Matter, Yang-Mills and Supergravity Theories in Harmonic Superspace", *Class. Quant. Grav.* **1** (1984) 469.

[18] A. Galperin, E. Ivanov, V. Ogievetsky and E. Sokatchev, "Harmonic Superspace: Key to N = 2 Supersymmetry Theories", *JETP Lett.* **40** (1984) 912 [*Pisma Zh. Eksp. Teor. Fiz.* **40** (1984) 155]

[19] B. Zupnik, "Solution of Constraints of Supergauge Theory in the Harmonic SU(2)/U(1) Superspace", *Theor. Math. Phys.* **69** (1986) 1101 [*Teor. Mat. Fiz.* **69** (1986) 207].

[20] A. Galperin, E. Ivanov, V. Ogievetsky and E. Sokatchev, *Harmonic Superspace*, Cambridge Univ. Press, 2001.

[21] W. Siegel, "Supermulti - instantons in Conformal Chiral Superspace", *Phys. Rev.* **D 52** (1995) 1042 [arXiv:hep-th/9412011].

[22] G. Hartwell and P. Howe, "(N, P, Q) Harmonic Superspace", *Int. J. Mod. Phys. A* **10** (1995) 3901 [arXiv:hep-th/9412147].

[23] P. Howe and G. Hartwell, "A Superspace Survey", *Class. Quant. Grav.* **12** (1995) 1823.

[24] P. Heslop and P. Howe, "On Harmonic Superspaces and Superconformal Fields in Four Dimensions", *Class. Quant. Grav.* **17** (2000) 3743 [arXiv:hep-th/0005135].

[25] P. Heslop, "Superfield Representations of Superconformal Groups", *Class. Quant. Grav.* **19** (2002) 303 [arXiv:hep-th/0108235].

[26] M. Hatsuda and W. Siegel, "Superconformal Spaces and Implications for Superstrings", *Phys. Rev.* **D 77** (2008) 065017 [arXiv:0709.4605 [hep-th]].

[27] S. Kuzenko, "Projective Superspace as a Double-punctured Harmonic Superspace", *Int. J. Mod. Phys. A* **14** (1999) 1737 [arXiv:hep-th/9806147].

[28] D. Butter, "Relating Harmonic and Projective Description of $\mathcal{N} = 2$ Nonlinear Sigma Models", *JHEP* **1211** (2012) 120 [arXiv:1206.3939 [hep-th]].

[29] A. Galperin, E. Ivanov, V. Ogievetsky and E. Sokatchev, "Harmonic Supergraphs: Green Functions", *Class. Quant. Grav.* **2** (1985) 601.

[30] A. Galperin, E. Ivanov, V. Ogievetsky and E. Sokatchev, "Harmonic Supergraphs: Feynman Rules and Examples", *Class. Quant. Grav.* **2** (1985) 617.

[31] F. Gonzalez-Rey, M. Roček, S. Wiles, U. Lindström and R. von Unge, "Feynman Rules in N = 2 Projective Superspace I: Massless Hypermultiplets", *Nucl. Phys.* **B 516** (1998) 426 [arXiv:hep-th/9710250].

[32] F. Gonzalez-Rey and R. von Unge, "Feynman Rules in N = 2 Projective Superspace II: Massive Hypermultiplets", *Nucl. Phys.* **B 516** (1998) 449 [arXiv:hep-th/9711135].

[33] F. Gonzalez-Rey, "Feynman Rules in N = 2 Projective Superspace III: Yang-Mills Multiplet", 1997, arXiv:hep-th/9712128.

[34] F. Gonzalez-Rey and M. Roček, "Nonholomorphic N = 2 Terms in N = 4 SYM: 1-loop Calculation in N = 2 Superspace", *Phys. Lett.* **B 434** (1998) 303 [arXiv:hep-th/9804010].

[35] A. Galperin, E. Ivanov, S. Kalitsyn, V. Ogievetsky and E. Sokatchev, "Unconstrained Off-Shell N=3 Supersymmetric Yang-Mills Theory", *Class. Quant. Grav.* **2** (1985) 155.

[36] E. Witten, "Quantum Field Theory and the Jones Polynomial", *Commun. Math. Phys.* **121** (1989) 351.

[37] S. Elitzur, G. Moore, A. Schwimmer and N. Seiberg, "Remarks on the Canonical Quantization of the Chern-Simons-Witten Theory", *Nucl. Phys.* **B 326** (1989) 108.

[38] C-S. Chu and D. Smith, "Multiple Self-Dual Strings on M5-Branes", *JHEP* **1001** (2010) 001 [arXiv:0909.2333 [hep-th]].

[39] I. Buchbinder, E. Buchbinder, E. Ivanov, S. Kuzenko and B. Ovrut, "Effective Action of the N = 2 Maxwell Multiplet in Harmonic Superspace", *Phys. Lett.* **B 412** (1997) 309 [arXiv:hep-th/9703147].

[40] I. Buchbinder, E. Buchbinder, S. Kuzenko and B. Ovrut, "The Background Field Method for N = 2 Super Yang-Mills Theories in Harmonic Superspace", *Phys. Lett.* **B 417** (1998) 61 arXiv:hep-th/9704214].

[41] I. Buchbinder, S. Kuzenko and B. Ovrut, "On the D = 4, N = 2 Non-renormalization Theorem", *Phys. Lett.* **B 433** (1998) 335 [arXiv:hep-th/9710142].

[42] I. Buchbinder, E. Ivanov and A. Petrov, "Complete Low-energy Effective Action in N = 4 SYM: A direct N = 2 Supergraph Calculation", *Nucl. Phys.* **B 653** (2003) 64 [arXiv:hep-th/0210241].

[43] O. Piguet and K. Sibold, "Renormalization Of N=1 Supersymmetrical Yang-Mills Theories: (I). The Classical Theory", *Nucl. Phys.* **B 197** (1982) 257.

[44] O. Piguet and K. Sibold, "Renormalization Of N=1 Supersymmetrical Yang-Mills Theories: (II). The Radiative Corrections", *Nucl. Phys.* **B 197** (1982) 272.

[45] J. Juer and D. Storey, "Nonlinear Renormalization in Superfield Gauge Theories", *Phys. Lett.* **B 119** (1982) 125.

[46] J. Juer and D. Storey, "One Loop Renormalization of Superfield Yang-Mills Theories", *Nucl. Phys.* **B 216** (1983) 185.

[47] M. Grisaru, M. Roček and W. Siegel, "Zero Three Loop beta Function in N=4 Super Yang-Mills Theory", *Phys. Rev. Lett.* **45** (1980) 1063.

[48] M. Grisaru, M. Roček and W. Siegel, "Superloops 3, β 0: A Calculation In N=4 Yang-mills Theory", *Nucl. Phys.* **B 183** (1981) 141.

[49] W. Caswell and D. Zanon, "Vanishing Three Loop Beta Function in N=4 Supersymmetric Yang-Mills Theory", *Phys. Lett.* **B 100** (1981) 152.

[50] W. Caswell and D. Zanon, "Zero Three Loop Beta Function in the N=4 Supersymmetric Yang-mills Theory", *Nucl. Phys.* **B 182** (1981) 125.

[51] M. Grisaru and W. Siegel, "Supergraphity: (II). Manifestly Covariant Rules and Higher Loop Finiteness", *Nucl. Phys.* **B 201** (1982) 292.

[52] P. Howe, K. Stelle and P. Townsend, "Miraculous Ultraviolet Cancellations in Supersymmetry Made Manifest", *Nucl. Phys.* **B 236** (1984) 125.

[53] W. Siegel, "AdS/CFT in Superspace", 2010, arXiv:1005.2317 [hep-th].

[54] I. Buchbinder and S. Kuzenko, "On the Off-Shell Massive Hypermultiplets", *Class. Quant. Grav.* **14** (1997) L157.

[55] S. Gates Jr., S. Penati and G. Tartaglino-Mazzucchelli, "6D Supersymmetry, Projective Superspace and 4D, N=1 Superfields", *JHEP* **0605** (2006) 051 [arXiv:hep-th/0508187].

[56] I. Buchbinder and S. Kuzenko, "Comments on the Background Field Method in Harmonic Superspace: Non-holomorphic Corrections in N=4 SYM", *Mod. Phys. Lett.* **A13** (1998) 1623 [arXiv:hep-th/9804168].

[57] E. Buchbinder, I. Buchbinder and S. Kuzenko, "Non-holomorphic Effective Potential in N = 4 SU(n) SYM", *Phys. Lett.* **B 446** (1999) 216 [arXiv:hep-th/9810239].

[58] S. Kuzenko and I. McArthur, "Effective Action of N = 4 Super Yang-Mills: N = 2 Superspace Approach", *Phys. Lett.* **B 506** (2001) 140 [arXiv:hep-th/0101127].

[59] S. Kuzenko and I. McArthur, "Hypermultiplet Effective Action: N = 2 Superspace Approach", *Phys. Lett.* **B 513** (2001) 213 [arXiv:hep-th/0105121].

[60] I. Buchbinder and A. Petrov, "N=4 Super Yang-Mills Low-Energy Effective Action at Three and Four Loops", *Phys. Lett.* **B 482** (2000) 429 [arXiv:hep-th/0003265].

[61] M. Grisaru, W. Siegel and M. Roček, "Improved Methods for Supergraphs", *Nucl. Phys.* **B 159** (1979) 429.

[62] P. Howe, K. Stelle, P. West, "A Class of Finite Four-Dimensional Supersymmetric Field Theories", *Phys. Lett.* **B 124** (1983) 55.

[63] M. Grisaru and D. Zanon, "New, Improved Supergraphs", *Phys. Lett.* **B 142** (1984) 359.

[64] M. Grisaru and D. Zanon, "Covariant Supergraphs: (I). Yang-Mills Theory", *Nucl. Phys.* **B 252** (1985) 578.

[65] T. Morris, "One Loop Invariant Supergraphs", *Phys. Lett.* **B 164** (1985) 315.

[66] R. Kallosh, "The Effective Action of N=8 Supergravity", 2007, arXiv:0711.2108 [hep-th].

[67] M. Hatsuda, Y-t. Huang and W. Siegel, "First-quantized N=4 Yang-Mills", 2008, arXiv:0812.4569 [hep-th].

[68] A. Galperin, E. Ivanov, S. Kalitsyn, V. Ogievetsky and E. Sokatchev, "N = 3 Supersymmetric Gauge Theory", *Phys. Lett.* **B 151** (1985) 215.

[69] F. Delduc and J. McCabe, "The Quantization of N=3 Super Yang-Mills Off-shell in Harmonic Superspace", *Class. Quant. Grav.* **6** (1989) 233.

[70] N. Seiberg and E. Witten, "Electric-Magnetic Duality, Monopole Condensation, and Confinement in N=2 Supersymmetric Yang-Mills Theory", *Nucl. Phys.* **B 426** (1994) 19; Erratum, *Nucl. Phys.* **B 430** (1994) 485 [arXiv:hep-th/9407087].

[71] N. Seiberg and E. Witten, "Monopoles, Duality and Chiral Symmetry Breaking in N=2 Supersymmetric QCD", *Nucl. Phys.* **B 431** (1994) 84 [arXiv:hep-th/9408099].

[72] N. Seiberg and E. Witten, "Gauge Dynamics and Compactification to Three-dimensions", In *Saclay 1996, The mathematical beauty of physics*, (1996) 333 [arXiv:hep-th/9607163].

[73] M. Kontsevich and Y. Soibelman, "Stability Structures, Motivic Donaldson-Thomas Invariants and Cluster Transformations", 2008, arXiv:0811.2435 [math.AG].

[74] D. Gaiotto, G. Moore and A. Neitzke, "Four-dimensional Wall-crossing via Three-dimensional Field Theory", *Commun. Math. Phys.* **299** (2010) 163 [arXiv:0807.4723 [hep-th]].

[75] S. Alexandrov, B. Pioline, F. Saueressig and S. Vandoren, "Linear Perturbations of Hyperkähler Metrics", *Lett. Math. Phys.* **87** (2009) 225 [arXiv:0806.4620 [hep-th]].

[76] S. Alexandrov, B. Pioline, F. Saueressig and S. Vandoren, "Linear Perturbations of Quaternionic Metrics", *Commun. Math. Phys.* **296** (2010) 353 [arXiv:0810.1675 [hep-th]].

[77] S. Alexandrov, B. Pioline, F. Saueressig and S. Vandoren, "D-Instantons and Twistors", *JHEP* **0903** (2009) 044 [arXiv:0812.4219 [hep-th]].

[78] S. Alexandrov, "D-Instantons and Twistors: Some Exact Results", *J. Phys.* **A 42** (2009) 335402 [arXiv:0902.2761 [hep-th]].

[79] S. Alexandrov, "Twistor Approach to String Compactifications: A Review", 2011, arXiv:1111.2892 [hep-th].

[80] B. Haghighat and S. Vandoren, "Five-dimensional Gauge Theory and Compactification on a Torus", *JHEP* **1109** (2011) 060 [arXiv:1107.2847 [hep-th]].

[81] N. Hitchin, A. Karlhede, U. Lindström and M. Roček, "Hyperkähler Metrics and Supersymmetry", *Commun. Math. Phys.* **108** (1987) 535.

[82] U. Lindström and M. Roček, "Properties of Hyperkähler Manifolds and their Twistor Spaces", *Commun. Math. Phys.* **293** (2010) 257 [arXiv:0807.1366 [hep-th]].

[83] I. Ivanov and M. Roček, "Supersymmetric Sigma Models, Twistors, and the Atiyah-Hitchin Metric", *Commun. Math. Phys.* **182** (1996) 291 [arXiv:hep-th/9512075].

[84] H. Ooguri and C. Vafa, "Summing up D-Instantons", *Phys. Rev. Lett.* **77** (1996) 3296 [arXiv:hep-th/9608079].

[85] N. Seiberg and S. Shenker, "Hypermultiplet Moduli Space and String Compactification to Three-dimensions", *Phys. Lett.* **B 388** (1996) 521 [arXiv:hep-th/9608086].

[86] D. Gaiotto, G. Moore and A. Neitzke, "Wall-Crossing in Coupled 2d-4d Systems", 2011, arXiv:1103.2598 [hep-th].

[87] S. Kuzenko, "N = 2 Supersymmetric Sigma-models and Duality", *JHEP* **1001** (2010) 115 [arXiv:0910.5771 [hep-th]].

[88] S. Kuzenko, "Comments on N = 2 Supersymmetric Sigma-models in Projective Superspace", *J. Phys.* **A 45** (2012) 095401 [arXiv:1110.4298 [hep-th]].

[89] Martin Roček, Unpublished Notes.

[90] S. Cecotti, S. Ferrara and L. Girardello, "Geometry of Type II Superstrings and the Moduli of Superconformal Field Theories", *Int. J. Mod. Phys.* **A4** (1989) 2475.

[91] S. Ferrara and S. Sabharwal, "Quaternionic Manifolds for Type II Superstring Vacua of Calabi-Yau Spaces", *Nucl. Phys.* **B 332** (1990) 317.

[92] S. Gates Jr., T. Hübsch and S. Kuzenko, "CNM Models, Holomorphic Functions and Projective Superspace C-Maps", *Nucl. Phys.* **B 557** (1999) 443 [arXiv:hep-th/9902211].

[93] M. Roček, C. Vafa and S. Vandoren, "Hypermultiplets and Topological Strings", *JHEP* **0602** (2006) 062 [arXiv:hep-th/0512206].

[94] I. Bakas, "Remarks on the Atiyah-Hitchin Metric", *Fortsch. Phys.* **48** (2000) 9 [arXiv:hep-th/9903256].

[95] R. Ionaş, "Elliptic Constructions of Hyperkähler Metrics I: The Atiyah-Hitchin Manifold", 2007, arXiv:0712.3598 [math.DG].

[96] N. Lambert and D. Tong, "Dyonic Instantons in Five-dimensional Gauge Theories", *Phys. Lett.* **B 462** (1999) 89 [arXiv:hep-th/9907014].

[97] N. Seiberg, "Five-dimensional SUSY Field Theories, Nontrivial Fixed Points and String Dynamics", *Phys. Lett.* **B 388** (1996) 753 [arXiv:hep-th/9608111].

[98] A. Lawrence and N. Nekrasov, "Instanton Sums and Five-dimensional Gauge Theories", *Nucl. Phys.* **B 513** (1998) 239 [arXiv:hep-th/9706025].

[99] D. Robles-Llana, F. Saueressig, U. Theis and S. Vandoren, "Membrane Instantons from Mirror Symmetry", *Commun. Num. Theor. Phys.* **1** (2007) 681 [arXiv:0707.0838 [hep-th]].

[100] H-Y. Chen, N. Dorey and K. Petunin, "Wall Crossing and Instantons in Compactified Gauge Theory", *JHEP* **1006** (2010) 024 [arXiv:1004.0703 [hep-th]].

[101] A. Neitzke, "On a Hyperholomorphic Line Bundle over the Coulomb Branch", 2011, [arXiv:1110.1619[hep-th]].

[102] S. Alexandrov, D. Persson and B. Pioline, "Wall-crossing, Rogers Dilogarithm, and the QK/HK Correspondence", *JHEP* **1112** (2011) 027 [arXiv:1110.0466 [hep-th]].

[103] E. Witten, "Topological Quantum Field Theory", *Commun. Math. Phys.* **117** (1988) 353.

[104] V. Pestun, "Localization of Gauge Theory on a Four-sphere and Supersymmetric Wilson Loops", *Commun. Math. Phys.* **313** (2012) 71 [arXiv:0712.2824 [hep-th]].

[105] A. Kapustin, B. Willett and I. Yaakov, "Exact Results for Wilson Loops in Superconformal Chern-Simons Theories with Matter", *JHEP* **1003** (2010) 089 [arXiv:0909.4559 [hep-th]].

[106] D. L. Jafferis, "The Exact Superconformal R-Symmetry Extremizes Z", *JHEP* **1205** (2012) 159 [arXiv:1012.3210 [hep-th]].

[107] N. Hama, K. Hosomichi and S. Lee, "Notes on SUSY Gauge Theories on Three-Sphere", *JHEP* **1103** (2011) 127 [arXiv:1012.3512 [hep-th]].

[108] J. Kallen and M. Zabzine, "Twisted Supersymmetric 5D Yang-Mills Theory and Contact Geometry", *JHEP* **1205** (2012) 125 [arXiv:1202.1956 [hep-th]].

[109] D. L. Jafferis and S. S. Pufu, "Exact Results for Five-dimensional Superconformal Field Theories with Gravity Duals", 2012, arXiv:1207.4359 [hep-th].

[110] D. L. Jafferis, I. R. Klebanov, S. S. Pufu and B. R. Safdi, "Towards the F-Theorem: N=2 Field Theories on the Three-Sphere", *JHEP* **1106** (2011) 102 [arXiv:1103.1181 [hep-th]].

[111] J. M. Maldacena, "The Large N Limit of Superconformal Field Theories and Supergravity", *Adv. Theor. Math. Phys.* **2** (1998) 231 [arXiv:hep-th/9711200].

[112] S. S. Gubser, I. R. Klebanov and A. M. Polyakov, "Gauge Theory Correlators from Noncritical String Theory", *Phys. Lett.* **B 428** (1998) 105 [arXiv:hep-th/9802109].

[113] E. Witten, "Anti-de Sitter Space and Holography", *Adv. Theor. Math. Phys.* **2** (1998) 253 [arXiv:hep-th/9802150].

[114] N. Drukker, M. Marino and P. Putrov, "From Weak to Strong Coupling in ABJM Theory", *Commun. Math. Phys.* **306** (2011) 511 [arXiv:1007.3837 [hep-th]].

[115] O. Aharony, O. Bergman, D. L. Jafferis and J. Maldacena, "N=6 Superconformal Chern-Simons-matter Theories, M2-branes and their Gravity Duals", *JHEP* **0810** (2008) 091 [arXiv:0806.1218 [hep-th]].

[116] I. R. Klebanov and A. A. Tseytlin, "Entropy of Near Extremal Black p-branes", *Nucl. Phys.* **B 475** (1996) 164 [arXiv:hep-th/9604089].

[117] C. P. Herzog, I. R. Klebanov, S. S. Pufu and T. Tesileanu, "Multi-Matrix Models and Tri-Sasaki Einstein Spaces", *Phys. Rev.* **D 83** (2011) 046001 [arXiv:1011.5487 [hep-th]].

[118] D. Martelli and J. Sparks, "The Large N Limit of Quiver Matrix Models and Sasaki-Einstein Manifolds", *Phys. Rev.* **D 84** (2011) 046008 [arXiv:1102.5289 [hep-th]].

[119] S. Cheon, H. Kim and N. Kim, "Calculating the Partition Function of N=2 Gauge Theories on S^3 and AdS/CFT Correspondence", *JHEP* **1105** (2011) 134 [arXiv:1102.5565 [hep-th]].

[120] D. L. Jafferis and A. Tomasiello, "A Simple Class of N=3 Gauge/Gravity Duals", *JHEP* **0810** (2008) 101 [arXiv:0808.0864 [hep-th]].

[121] D. R. Gulotta, C. P. Herzog and S. S. Pufu, "From Necklace Quivers to the F-theorem, Operator Counting, and T(U(N))", *JHEP* **1112** (2011) 077 [arXiv:1105.2817 [hep-th]].

[122] H.-U. Yee, "AdS/CFT with Tri-Sasakian Manifolds", *Nucl. Phys.* **B 774** (2007) 232 [arXiv:hep-th/0612002].

[123] B. Assel, C. Bachas, J. Estes and J. Gomis, "IIB Duals of D=3 N=4 Circular Quivers", 2012, arXiv:1210.2590 [hep-th].

[124] D. R. Gulotta, J. P. Ang and C. P. Herzog, "Matrix Models for Supersymmetric Chern-Simons Theories with an ADE Classification", *JHEP* **1201** (2012) 132 [arXiv:1111.1744 [hep-th]].

[125] B. Willett and I. Yaakov, "N=2 Dualities and Z Extremization in Three Dimensions", 2011, arXiv:1104.0487 [hep-th].

[126] F. Benini, C. Closset and S. Cremonesi, "Comments on 3d Seiberg-like Dualities", *JHEP* **1110** (2011) 075 [arXiv:1108.5373 [hep-th]].

[127] O. Aharony, "IR Duality in d=3 N=2 Supersymmetric USp(2N(c)) and U(N(c)) Gauge Theories", *Phys. Lett.* **B 404** (1972) 71 [arXiv:hep-th/9703215].

[128] A. Giveon and D. Kutasov, "Seiberg Duality in Chern-Simons Theory", *Nucl. Phys.* **B 812** (2009) 1 [arXiv:0808.0360 [hep-th]].

[129] F. Harary, "On the Notion of Balance of a Signed Graph", *Michigan Math. J.* **2** (1953-54) 143.

[130] Thomas Zaslavsky, "The Geometry of Root Systems and Signed Graphs", *The American Math. Monthly* **88** (1981) 88.

[131] Thomas Zaslavsky, "Signed Graphs", *Discrete Applied Math.* **4** (1982) 47.

[132] Seth Chaiken, "A Combinatorial Proof of the All Minors Matrix Tree Theorem", *SIAM. J. on Algebraic and Discrete Methods*, **3** (1982) 319.

[133] I. R. Klebanov, S. S. Pufu and B. R. Safdi, "F-Theorem Without Supersymmetry", *JHEP* **1110** (2011) 038 [arXiv:1105.4598 [hep-th]].

[134] A. Amariti and M. Siani, "Z-extremization and F-theorem in Chern-Simons Matter Theories", *JHEP* **1110** (2011) 016 [arXiv:1105.0933 [hep-th]].

[135] I. R. Klebanov, S. S. Pufu, S. Sachdev and B. R. Safdi, "Entanglement Entropy of 3-d Conformal Gauge Theories with Many Flavors", *JHEP* **1205** (2012) 036 [arXiv:1112.5342 [hep-th]].

[136] H. Casini, M. Huerta and R. C. Myers, "Towards a Derivation of Holographic Entanglement Entropy", *JHEP* **1105** (2011) 036 [arXiv:1102.0440 [hep-th]].

[137] H. Casini and M. Huerta, "On the RG Running of the Entanglement Entropy of a Circle", *Phys. Rev.* **D 85** (2012) 125016 [arXiv:1202.5650 [hep-th]].

[138] D. R. Gulotta, C. P. Herzog and T. Nishioka, "The ABCDEF's of Matrix Models for Supersymmetric Chern-Simons Theories", *JHEP* **1204** (2012) 138 [arXiv:1201.6360 [hep-th]].

Appendix A

y-Calculus

We present here some sample hoop calculations in projective hyperspace using the diagrammatic rules outlined in Section 3.2.4.

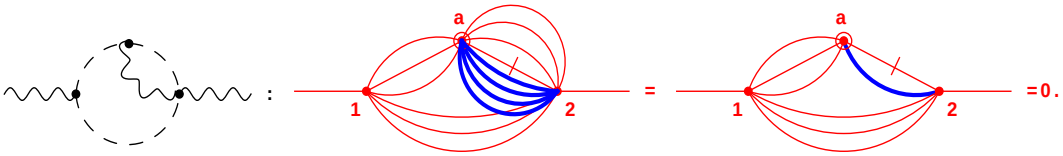

Figure A.1: Vanishing of a 2-hoops diagram with ghost propagators.

In Figure A.1, the emergence of $y\delta(y)$ factor is shown when only three y_{2a}'s in the y_{2a}^4 factor (produced via d-algebra) are cancelled by y_{2a}^3 factor present in the ghost propagator.

Actual evaluation of 'q' y-integrals (for the divergent pieces) is possible in '$\leq q$' steps as shown in the following calculations involving vector propagators. First, we look at one 1-hoop 3-point diagram:

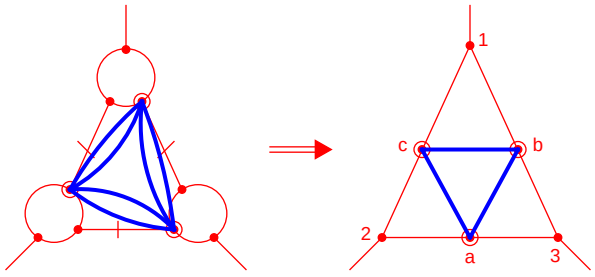

Figure A.2: Setting up y-integrals for diagram 1.(a) in Figure 3.6.

$$
\begin{aligned}
\text{F.A.2} \equiv & \int \frac{dy_{1,2,3,a,b,c}}{y_a\, y_b\, y_c} \frac{V_1 V_2 V_3\, y_{ba}\, y_{ac}\, y_{cb}}{y_{1c}\, y_{c2}\, y_{2a}\, y_{a3}\, y_{3b}\, y_{b1}} \\
= & \int dy_{1,2,3} \frac{V_1 V_2 V_3}{y_{12}\, y_{23}\, y_{31}} \oint dy_{a,b,c} \left(\frac{1}{y_{2a}} + \frac{1}{y_{a3}}\right)\left(\frac{1}{y_{3b}} + \frac{1}{y_{b1}}\right)\left(\frac{1}{y_{1c}} + \frac{1}{y_{c2}}\right) \times \\
& \qquad \times \left(1 - \frac{y_a}{y_b}\right)\left(1 - \frac{y_c}{y_a}\right)\left(1 - \frac{y_b}{y_c}\right) \\
= & \int dy_{1,2,3} \frac{V_1 V_2 V_3}{y_{12}\, y_{23}\, y_{31}} \oint dy_{a,b} \left(\frac{1}{y_{2a}} + \frac{1}{y_{a3}}\right)\left(\frac{1}{y_{3b}} + \frac{1}{y_{b1}}\right)\left(1 - \frac{y_a}{y_b}\right) \times \\
& \qquad \times \left(1 - \frac{y_2}{y_a} - \frac{y_b}{y_1} + \frac{y_b}{y_a}\right) \\
= & \int dy_{1,2,3} \frac{V_1 V_2 V_3}{y_{12}\, y_{23}\, y_{31}} \oint dy_a \left(\frac{1}{y_{2a}} + \frac{1}{y_{a3}}\right) \times \\
& \qquad \times \left(-\frac{y_a}{y_3} - \frac{y_2}{y_a} + \frac{y_2}{y_3} + \frac{y_a}{y_1} + \frac{y_1}{y_a} - 1\right) \\
= & \int dy_{1,2,3} \frac{V_1 V_2 V_3}{y_{12} y_{23} y_{31}} \left(-3 + \left\updownarrow \frac{y_1}{y_2} \right\updownarrow\right).
\end{aligned}
$$

This is the result we used in (3.3.7). Next we look at two 2-hoop 2-point diagrams:

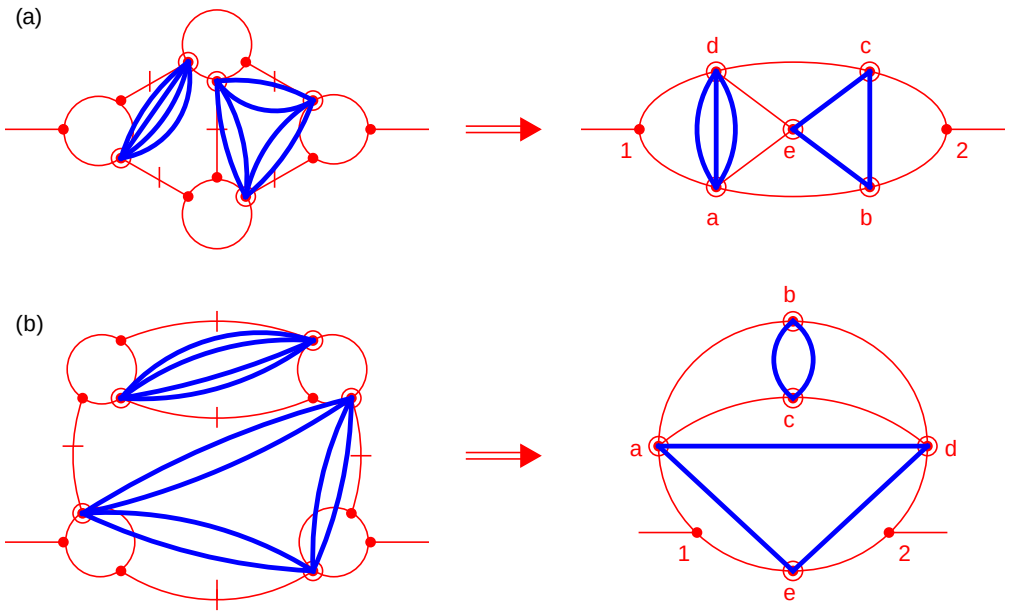

Figure A.3: Setting up y-integrals for the last two diagrams in Figure 3.8.

$$
\begin{aligned}
\text{F.A.3.(a)} \equiv & \int \frac{dy_{1,2,a,b,c,d,e}}{y_a\, y_b\, y_c\, y_d\, y_e} \frac{V_1 V_2\, y_{ad}^3\, y_{bc}\, y_{ce}\, y_{eb}}{y_{1a}\, y_{ab}\, y_{b2}\, y_{2c}\, y_{cd}\, y_{de}\, y_{ea}\, y_{d1}} \\
= & \int \frac{dy_{1,2,a,b,c,d}}{y_a\, y_b\, y_d} \frac{V_1 V_2\, y_{ad}^2\, y_{bc}}{y_{1a}\, y_{ab}\, y_{b2}\, y_{2c}\, y_{cd}\, y_{d1}} \left(1 - \frac{y_a}{y_c} - \frac{y_b}{y_d} + \frac{y_b}{y_c}\right) \\
= & \int \frac{dy_{1,2,a,b,d}}{y_a\, y_d} \frac{V_1 V_2\, y_{ad}^2}{y_{1a}\, y_{ab}\, y_{b2}\, y_{d1}\, y_{2d}} \left(1 - \frac{y_a}{y_d} - \frac{y_b}{y_d} + \frac{y_b}{y_2} - \frac{y_d}{y_b} + \frac{y_a}{y_b}\right) \\
= & \int \frac{dy_{1,2,a,d}}{y_a\, y_d} \frac{V_1 V_2\, y_{ad}^2}{y_{1a}\, y_{d1}\, y_{2d}\, y_{a2}} \left(3 - \frac{y_a}{y_d} - \frac{y_2}{y_d} - \frac{y_d}{y_a}\right) \\
= & \int dy_{1,2,a} \frac{V_1 V_2}{y_{1a}\, y_{a2}\, y_{21}} \left(-6 + 4\frac{y_a}{y_2} + 5\frac{y_1}{y_a} - \left(\frac{y_a}{y_2}\right)^2 - \frac{y_2}{y_a} - \left(\frac{y_1}{y_a}\right)^2\right) \\
= & -\int dy_{1,2} \frac{V_1 V_2}{y_{12}\, y_{21}} \frac{1}{2} \left(2 - \left\updownarrow \frac{y_1}{y_2} \right\updownarrow\right) \\
\Rightarrow & -\frac{1}{2} \int d^8\theta \int dy_1 dy_2 \frac{V_1 V_2}{y_1\, y_2} = 0.
\end{aligned}
$$

$$
\begin{aligned}
\text{F.A.3.(b)} \equiv & \int \frac{dy_{1,2,a,b,c,d,e}}{y_a\, y_b\, y_c\, y_d\, y_e} \frac{V_1 V_2\, y_{bc}^2\, y_{ae}\, y_{ed}\, y_{da}}{y_{1a}\, y_{ba}\, y_{ac}\, y_{cd}\, y_{db}\, y_{d2}\, y_{2e}\, y_{e1}} \\
= & \int \frac{dy_{1,2,a,b,d,e}}{y_a\, y_d\, y_e} \frac{V_1 V_2\, y_{ae}\, y_{ed}\, y_{da}}{y_{1a}\, y_{ba}\, y_{ad}\, y_{db}\, y_{d2}\, y_{2e}\, y_{e1}} \left(-2 + \frac{y_b}{y_a} + \frac{y_d}{y_b}\right) \\
= & \int \frac{dy_{1,2,a,d,e}}{y_a\, y_d\, y_e} \frac{V_1 V_2\, y_{ae}\, y_{ed}}{y_{1a}\, y_{ad}\, y_{d2}\, y_{2e}\, y_{e1}} (-2 + 1 + 1) = 0.
\end{aligned}
$$

Thus, the claim made in Section 3.3.3 that these vector self-energy diagrams are not divergent holds.

Appendix B

c-Map

The c-map [90,91] relates classical hypermultiplet moduli spaces in compactifications of type II strings on a Calabi-Yau threefold to vector multiplet moduli spaces via a further compactification on a circle. In [92, 93], it was shown that the c-map has a natural description in projective superspace. It can be regarded as taking a vector multiplet from four to three dimensions and reinterpreting it as a tensor multiplet when returning to four dimensions. This is possible because in three-dimensions, a vector multiplet is equivalent to a tensor multiplet, which can then be dualized into a hypermultiplet in four dimensions.

This means that given an $\mathcal{N}=2$ holomorphic prepotential $\mathcal{F}(W)$ describing a vector multiplet:

$$\mathcal{L}_v = -\mathrm{Im}\left[\int d^2\theta d^2\vartheta \mathcal{F}(W)\right],$$

there is a corresponding dual projective hypermultiplet Lagrangian $\mathcal{G}$ describing a hyperkähler moduli space given by

$$\begin{aligned}\mathcal{L}_s &= \int d^2\theta d^2\bar{\theta} \oint \frac{dy}{y}\mathcal{G}(y;\eta_e) = \int d^2\theta d^2\bar{\theta} \oint \frac{dy}{y}\overline{\mathrm{Im}}\left[\frac{\mathcal{F}(y\eta_e)}{y^2}\right] \\ &= -i\int d^2\theta d^2\bar{\theta} \oint \frac{dy}{y}\left[\frac{\mathcal{F}(y\eta_e)}{y^2} - \overline{\mathcal{F}(y\eta_e)}\,y^2\right].\end{aligned}$$

This expression determines the semiflat projective Lagrangian f^{sf} in (4.2.9).

We now show how this duality works, following [93]. Rewriting $\mathcal{L}_v$ in $\mathcal{N}=1$ superspace, we get

$$\mathcal{L}_v = -\mathrm{Im}\left[\int d^2\theta d^2\bar{\theta}\mathcal{F}'(\Phi)\bar{\Phi} + \int d^2\theta \mathcal{F}''(\Phi)W^\alpha W_\alpha\right],$$

where $\Phi = W_|$ and $W_\alpha = \mathcal{D}_{\vartheta,\alpha} W_|$ are $\mathcal{N} = 1$ chiral superfield and vector multiplet's spinor field strength, respectively. When we reduce from four to three dimensions, the above Lagrangian is still valid but we can write W_α in terms of a (real linear) field strength G as $W_\alpha = \frac{i}{\sqrt{2}} \bar{\mathcal{D}}_\alpha G$ such that $\mathcal{D}^2 G = \bar{\mathcal{D}}^2 G = 0$. This is because in $d = 3$ there is no distinction between the dotted and undotted spinor indices (the conjugate representations of SL(2,C) in $d = 4$ reduce to same representation of SL(2,R) in $d = 3$). Thus the above Lagrangian turns into

$$\mathcal{L}_v = \mathrm{Im} \int d^2\theta d^2\bar{\theta} \left(-\mathcal{F}'(\Phi)\bar{\Phi} + \tfrac{1}{2}\mathcal{F}''(\Phi) G^2 \right).$$

We can now compare this to the hypermultiplet Lagrangian. Using (4.3.2), we first expand $\mathcal{F}(y\eta_e) \equiv \mathcal{F}\left(a + \theta_e y - \bar{a} y^2\right)$ in terms of its $\mathcal{N} = 1$ component fields. Then we do the y-integral which picks out only two terms proportional to y^2, leading us to

$$\mathcal{L}_s = \mathrm{Im} \int d^2\theta d^2\bar{\theta} \left(-\mathcal{F}'(a)\bar{a} + \tfrac{1}{2}\mathcal{F}''(a)\theta_e^2 \right).$$

Thus $\mathcal{L}_s$ and $\mathcal{L}_v$ precisely match if we identify a with Φ and θ_e with G.

Appendix C

Quiver Theories

This appendix covers notation for roots of affine Lie algebras used in Chapter 5, showcases the detailed calculation of free energy for the $\widehat{D}_5$ quiver and provides the expression for free energy of exceptional quiver theories.

C.1 Roots of $\widehat{A}_{m-1}$ and $\widehat{D}_n$

Here we give some useful information about the roots for $\widehat{A}$ and $\widehat{D}$ Lie algebras. For $\widehat{A}_{m-1}$ we choose the following root basis

$$\tilde{\alpha}_a = e_a - e_{a+1}\,, \quad a = 1, ..., m-1\,; \qquad \tilde{\theta} = -e_1 + e_m\,,$$

where e_a are canonical unit vectors of dimension m. For $\widehat{D}_n$ we choose

$$\alpha_i = e_i - e_{i+1}\,, \quad i = 1, ..., n-1\,; \qquad \alpha_n = e_{n-1} + e_n\,, \qquad \theta = -(e_1 + e_2)\,,$$

where e_i are the unit vectors of dimension n.

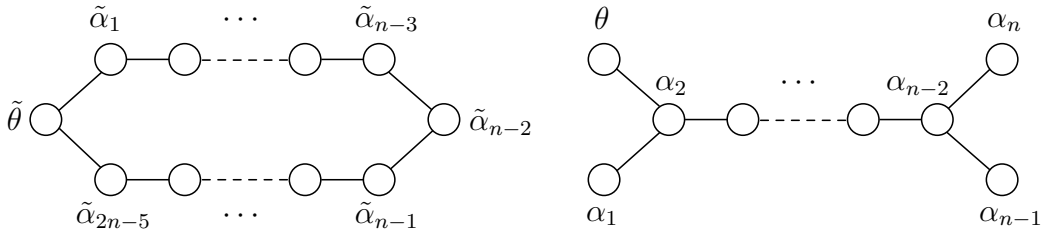

Figure C.1: Dynkin diagrams for $\widehat{A}_{2n-5}$ and $\widehat{D}_n$.

In Figure C.1 we show the affine Dynkin diagrams for the $\widehat{A}$ and $\widehat{D}$ Lie algebras along with the roots associated with every node. At each node, the

CS level is given by $\tilde{\alpha}\cdot q$ and $\alpha\cdot p$ for $\widehat{A}$ and $\widehat{D}$, respectively. The identification of opposite CS levels in the $\widehat{A}_{2n-5}$ quiver imposes $\tilde{\alpha}_a \cdot q = \tilde{\alpha}_{2n-4-a}\cdot q$ and hence $q_a = -q_{2n-3-a}$ for $a = 1, ..., n-2$. With these conventions, unfolding the $\widehat{D}$-quiver to the $\widehat{A}$-quiver relates $q_a = p_{a+1}$.

C.2 $\widehat{D}_5$

Here we give the detailed solution of the matrix model for the $\widehat{D}_5$ quiver gauge theory. As discussed in Section 5.2, there are 7 regions defining a generic solution of this model. To keep the notation simple, the second index for the four y's corresponding to the external nodes is suppressed.

Region 1: $0 \le x \le \frac{\mu}{3(k_2+k_3+k_4+2k_5+2k_6)}$

$$\rho = \frac{\mu}{3}\,;$$
$$y_1 - y_{6,2} = \frac{(2k_1-k_3-k_4-2k_6)\,x}{4\rho}\,,\quad y_2 - y_{6,2} = \frac{(2k_2-k_3-k_4-2k_6)\,x}{4\rho}\,,$$
$$y_3 - y_{6,2} = \frac{k_3 x}{2\rho}\,,\quad y_4 - y_{6,2} = \frac{k_4 x}{2\rho}\,,\quad y_{5,1} - y_{6,2} = y_{5,2} - y_{6,2}\,,$$
$$y_{5,2} - y_{6,2} = -\frac{(k_3+k_4+2k_6)x}{4\rho}\,,\quad y_{6,1} - y_{6,2} = 0\,.$$

Region 2: $\frac{\mu}{3(k_2+k_3+k_4+2k_5+2k_6)} \le x \le \frac{4\mu}{6k_2+9k_3+9k_4+12k_5+18k_6}$

$$\rho = \frac{\mu}{3}\,;$$
$$y_1 - y_{5,2} = -\frac{1}{2}\,,\quad y_2 - y_{6,2} = \frac{(2k_2-k_3-k_4-2k_6)\,x}{4\rho}\,,\quad y_3 - y_{6,2} = \frac{k_3 x}{2\rho}\,,$$
$$y_4 - y_{6,2} = \frac{k_4 x}{2\rho}\,,\quad y_{5,1} - y_{6,2} = -\frac{1}{2} - \frac{(2k_1+k_3+k_4+2k_6)\,x}{4\rho}\,,$$
$$y_{5,2} - y_{6,2} = \frac{1}{2} + \frac{(2k_1-k_3-k_4-2k_6)\,x}{4\rho}\,,\quad y_{6,1} - y_{6,2} = 0\,.$$

Region 3: $\frac{4\mu}{6k_2+9k_3+9k_4+12k_5+18k_6} \leq x \leq \frac{2\mu}{3(2k_2+k_3+k_4+2k_5+2k_6)}$

$$\rho = \frac{\mu}{3}\,;$$
$$y_1 - y_{5,2} = -\frac{1}{2}\,, \quad y_2 - y_{6,2} = -1 - \frac{(k_1-k_2)\,x}{2\rho}\,,$$
$$y_3 - y_{6,2} = -1 - \frac{(2k_1-3k_3-k_4-2k_6)\,x}{4\rho}\,,$$
$$y_4 - y_{6,2} = -1 - \frac{(2k_1-k_3-3k_4-2k_6)\,x}{4\rho}\,, \quad y_{5,1} - y_{6,2} = -\frac{3}{2} - \frac{k_1 x}{\rho}\,,$$
$$y_{5,2} - y_{6,2} = -\frac{1}{2}\,, \quad y_{6,1} - y_{6,2} = -2 - \frac{(2k_1-k_3-k_4-2k_6)\,x}{2\rho}\,.$$

Region 4: $\frac{2\mu}{3(2k_2+k_3+k_4+2k_5+2k_6)} \leq x \leq \frac{2\mu}{2k_2+3(k_3+k_4+2k_5+2k_6)}$

$$\rho = \frac{\mu}{2} + \frac{x}{4}\,(k_1-k_2)\;;$$
$$y_1 - y_{5,2} = -\frac{1}{2}\,, \quad y_2 - y_{6,2} = 0\,, \quad y_3 - y_{6,2} = -\frac{1}{2} + \frac{(2k_3+k_4+k_5+2k_6)\,x}{2\rho}\,,$$
$$y_4 - y_{6,2} = -\frac{1}{2} + \frac{(k_3+2k_4+k_5+2k_6)\,x}{2\rho}\,, \quad y_{5,1} - y_{6,2} = -\frac{1}{2} - \frac{(k_1-k_2)\,x}{2\rho}\,,$$
$$y_{5,2} - y_{6,2} = -\frac{1}{2}\,, \quad y_{6,1} - y_{6,2} = -1 + \frac{(k_3+k_4+k_5+2k_6)\,x}{\rho}\,.$$

Region 5: $\frac{2\mu}{2k_2+3(k_3+k_4+2k_5+2k_6)} \leq x \leq \frac{2\mu}{2k_2+3k_3+5k_4+4k_5+6k_6}$

$$\rho = \mu + x k_1\,;$$
$$y_1 - y_{5,2} = -\frac{1}{2}\,, \quad y_2 - y_{6,2} = 0\,, \quad y_3 - y_{6,2} = \frac{(3k_3+k_4+2k_6)\,x}{4\rho}\,,$$
$$y_4 - y_{6,2} = \frac{(k_3+3k_4+2k_6)\,x}{4\rho}\,, \quad y_{5,1} - y_{6,2} = \frac{1}{2}\,,$$
$$y_{5,2} - y_{6,2} = -\frac{1}{2}\,, \quad y_{6,1} - y_{6,2} = \frac{(k_3+k_4+2k_6)\,x}{2\rho}\,.$$

Region 6: $\frac{2\mu}{2k_2+3k_3+5k_4+4k_5+6k_6} \leq x \leq \frac{2\mu}{2k_2+5k_3+3k_4+4k_5+6k_6}$

$$\rho = \frac{3\mu}{2} + \frac{x}{4}\left(6k_1 - k_3 - 3k_4 - 2k_6\right) ;$$
$$y_1 - y_{5,2} = -\frac{1}{2}\,, \quad y_2 - y_{6,2} = 0\,, \quad y_3 - y_{6,2} = \frac{1}{6} + \frac{(2k_3+k_6)\,x}{3\rho}\,,$$
$$y_4 - y_{6,2} = \frac{1}{2}\,, \quad y_{5,1} - y_{6,2} = \frac{1}{2}\,, \quad y_{5,2} - y_{6,2} = -\frac{1}{2}\,,$$
$$y_{6,1} - y_{6,2} = \frac{1}{3} + \frac{(k_3+2k_6)\,x}{3\rho}\,.$$

Region 7: $\frac{2\mu}{2k_2+5k_3+3k_4+4k_5+6k_6} \leq x \leq \frac{2\mu}{2k_2+3k_3+3k_4+4k_5+6k_6}$

$$\rho = 2\mu + x\left(2k_1 - k_3 - k_4 - k_6\right) ;$$
$$y_1 - y_{5,2} = -\frac{1}{2}\,, \quad y_2 - y_{6,2} = 0\,, \quad y_3 - y_{6,2} = \frac{1}{2}\,, \quad y_4 - y_{6,2} = \frac{1}{2}\,,$$
$$y_{5,1} - y_{6,2} = \frac{1}{2}\,, \quad y_{5,2} - y_{6,2} = -\frac{1}{2}\,, \quad y_{6,1} - y_{6,2} = \frac{1}{2} + \frac{k_6 x}{2\rho}\,.$$

Finally, the last saturation occurs at the end of this region with $y_{6,1} = y_{6,2} + 1$.

C.3 Exceptional Quivers

We have also solved the matrix models for the exceptional quivers $\widehat{E}_6$, $\widehat{E}_7$ and $\widehat{E}_8$. They consist of eleven, seventeen and twenty-nine regions, respectively. Here we give the corresponding free energies for a particular ordering of the CS levels. In Figure C.2, we show our conventions in labelling the nodes.

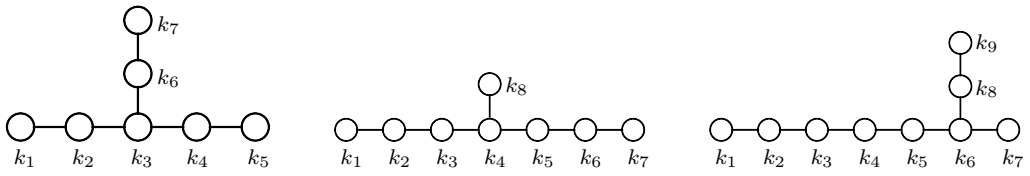

Figure C.2: Labelling of Chern-Simons levels for $\widehat{E}_6$, $\widehat{E}_7$ and $\widehat{E}_8$.

$\widehat{\boldsymbol{E}}_{\boldsymbol{6}}$**.** The matrix model for $\widehat{E}_6$, with the assumptions $k_6 \geq k_5 \geq k_4 \geq k_3 \geq k_2 \geq 0$ and $k_7 > 3k_2 + 6k_3 + 4k_4 + 2k_5 + 4k_6$, gives:

$$\begin{aligned}\frac{2}{\mu^2} = &\frac{2(4k_2 + 11k_3 + 8k_4 + 4k_5 + 6k_6 + 4k_7)}{(2k_2 + 5k_3 + 4k_4 + 2k_5 + 3k_6 + 2k_7)^2} \\ &- \frac{1}{42(3k_2 + 6k_3 + 4k_4 + 2k_5 + 5k_6 + k_7)} \\ &- \frac{1}{77(13k_2 + 12k_3 + 8k_4 + 4k_5 + 3k_6 + 2k_7)} \\ &- \frac{1}{3(3k_2 + 6k_3 + 4k_4 + 2k_5 + 5k_6 + 4k_7)} \\ &- \frac{9}{6k_2 + 14k_3 + 13k_4 + 6k_5 + 9k_6 + 6k_7} \\ &- \frac{9}{11(6k_2 + 14k_3 + 13k_4 + 12k_5 + 9k_6 + 6k_7)}\,.\end{aligned}$$

$\widehat{\boldsymbol{E}}_{\boldsymbol{7}}$**.** The matrix model for $\widehat{E}_7$ gives:

$$\begin{aligned}\frac{2}{\mu^2} = &\frac{8k_2 + 24k_3 + 42k_4 + 4(8k_5 + 6k_6 + 3k_7 + 5k_8)}{(2k_2 + 6k_3 + 10k_4 + 8k_5 + 6k_6 + 3k_7 + 5k_8)^2} \\ &- \frac{1}{2k_2 + 7k_3 + 10k_4 + 8k_5 + 6k_6 + 3k_7 + 5k_8} \\ &- \frac{1}{2k_2 + 6k_3 + 10k_4 + 9k_5 + 6k_6 + 3k_7 + 5k_8} \\ &- \frac{1}{180(2k_2 + 3k_3 + 4k_4 + 3k_5 + 2k_6 + k_7 + 2k_8)} \\ &- \frac{4}{15(4k_2 + 11k_3 + 2(9k_4 + 8k_5 + 7k_6 + 6k_7) + 9k_8)} \\ &- \frac{27}{7(6k_2 + 17k_3 + 28k_4 + 24k_5 + 20k_6 + 9k_7 + 15k_8)} \\ &- \frac{32}{21(8k_2 + 25k_3 + 42k_4 + 32k_5 + 22k_6 + 12k_7 + 27k_8)}\,,\end{aligned}$$

assuming that $k_7 \geq k_6 \geq k_5 \geq k_4 \geq k_3 \geq k_2 \geq 0$ along with

$$\begin{gathered}k_4 + k_5 > k_6, \\ k_3 + 2k_4 + k_5 > k_7, \\ 4k_3 + k_4 > 2k_5 + k_6, \text{ and} \\ 3k_8 > 6k_3 + 12k_4 + 15k_5 + 10k_6 + 5k_7.\end{gathered}$$

$\widehat{\boldsymbol{E}}_{\boldsymbol{8}}$**.** The matrix model for $\widehat{E}_8$ gives:

$$\begin{aligned}\frac{2}{\mu^2} = & \frac{8k_2+24k_3+48k_4+74k_5+92k_6+48k_7+64k_8+32k_9}{(2k_2+6k_3+12k_4+18k_5+23k_6+12k_7+16k_8+8k_9)^2} \\ & - \frac{1}{3150(2k_2+3k_3+4k_4+5k_5+6k_6+3k_7+4k_8+2k_9)} \\ & - \frac{1}{2(k_2+3k_3+6k_4+9k_5+12k_6+6k_7+8k_8+4k_9)} \\ & - \frac{1}{2k_2+6k_3+13k_4+18k_5+23k_6+12k_7+16k_8+8k_9} \\ & - \frac{27}{7(6k_2+18k_3+35k_4+52k_5+69k_6+38k_7+48k_8+24k_9)} \\ & - \frac{108}{35(12k_2+36k_3+70k_4+104k_5+138k_6+69k_7+103k_8+48k_9)} \\ & - \frac{36}{55(12k_2+36k_3+70k_4+104k_5+138k_6+69k_7+103k_8+68k_9)} \\ & - \frac{9}{154(6k_2+17(3k_3+4k_4+5k_5+6k_6+3k_7+4k_8+2k_9))}\,,\end{aligned}$$

with assumptions that

$$\begin{gathered}k_6 \geq k_5 \geq k_4 \geq k_3 \geq k_2 \geq 0, \\ k_7 > 3k_4+6k_5+4k_6, \\ 2k_4+4k_5+6k_6+9k_7 > k_8, \\ 2k_3+4k_4+6k_5+8k_6+4k_7+6k_8 > k_9, \text{ and} \\ 2k_9 > 6k_3+12k_4+18k_5+24k_6+16k_7+11k_8\,.\end{gathered}$$

C.4 Mathematica® Code

Most of the matrix model calculations were preformed using Mathematica®. Here we give the basic code used to generate the volume in terms of k's. Let us take the example of $\widehat{D}_5$ again to do the initial setup. First, we define the nodes and edges of the extended Dynkin diagram.

```
n={1,1,1,1,2,2};
e={{1,5},{2,5},{5,6},{6,3},{6,4}};
```

Then we construct the Lagrangian with 'independent' k's and specify the relations among them.

```
k[1]=-(k[2]+k[3]+k[4]+2k[5]+2k[6]);
```

```
Lm=(f0[x,n]+f1[x,n,e]-2\[Pi]\[Mu]\[Rho][x]+Nf\[Pi]\[Rho][x]x);
assumk={k[6]>=k[5]>=k[4]>=k[3]>=k[2]>=0&&\[Mu]>0&&Nf>=0};
```

The functions depending on the Dynkin diagram data are defined separately.

```
f[x_]:=(2\[Pi]Floor[-x+1/2]+2\[Pi]x)^2
f0[x_,n__]:=2\[Pi]x\[Rho][x]Sum[k[a]y[a,i,x],{a,1,Length[n]},
{i,1,n[[a]]}]
f1[x_,n__,e__]:=\[Rho][x]^2/(4\[Pi])(Sum[f[y[a,i,x]-y[a,j,x]-1/2],
{a,1,Length[n]},{i,1,n[[a]]},{j,1,n[[a]]}]-Sum[f[y[e[[a,1]],i,x]
-y[e[[a,2]],j,x]],{a,1,Length[e]},{i,1,n[[e[[a,1]]]]},
{j,1,n[[e[[a,2]]]]}])
```

A function to generate all the required inequalities (5.2.1) for a given region is crucial and looks as follows:

```
GenReg[RegO__,Rp_:1,satin__:{},ysat__:{}]:=Block[{RegN=RegO,n,e,m,
satinq,satvars,satval,eqTchg,bifvar,slope,inqTchk,inqpos},
If[Rp==1,n=RegN[[1]];e=RegN[[2]];RegN={Table[y[a,i,x]==y[a,j,x],
{a,1,Length[n]},{i,1,n[[a]]-1},{j,i+1,n[[a]]}],
Table[Less[-1/2,y[e[[a,1]],i,x]-y[e[[a,2]],j,x],1/2],
{a,1,Length[e]},{i,1,n[[e[[a,1]]]]},{j,1,n[[e[[a,2]]]]}]}
//Flatten;, If[Head[satin[[1]]]===Inequality,satinq={Less[
satin[[1,1]],satin[[1,3]],satin[[1,5]]]};,satinq=satin;];
satinq=(satinq/.Less[L_,a_+y[x__]-y[z__],U_]:>
Less[L-a,y[x]-y[z],U-a]);
satvars=Cases[satinq,y[x__]:>y[x],\[Infinity]];
eqTchg=Table[Select[Select[RegN,(Head[#]===Equal)&],
MemberQ[#,satvars[[m]], \[Infinity]]&], {m,1,2}]//Flatten;
If[Length[eqTchg]!=0,bifvar=
Intersection[(List@@@eqTchg)//Flatten,satvars];
If[Length[bifvar]>1,PrintTemporary["Region␣"<>ToString[Rp]<>":␣
Colliding␣Degeneracies:␣Choose␣another␣xmin."]; Return["R"],
bifvar=bifvar[[1]];];
satinq=satinq/.Less[L_,y__,U_]/;Coefficient[satinq[[1,2]],
bifvar]==-1:>Less[-U,-y,-L]; satval=satinq[[1,2]]/.ysat;];
For[m=1,m<=Length[eqTchg],m++, If[(satval<0)&&(satinq[[1,-1]]<0),
If[Position[satinq[[1]],satval,1][[1,1]]==1,
RegN=ReplacePart[RegN,Position[RegN,eqTchg[[m]]]->Less[0,bifvar
-DeleteCases[List@@eqTchg[[m]],bifvar][[1]],1]];,
RegN=ReplacePart[RegN,Position[RegN,eqTchg[[m]]]->Less[0,
DeleteCases[List@@eqTchg[[m]],bifvar][[1]]-bifvar,1]];];,
If[(satval>=0)&&(Position[satinq[[1]],satval,1][[1,1]]>1),
RegN=ReplacePart[RegN,Position[RegN,eqTchg[[m]]]->Less[0,
DeleteCases[List@@eqTchg[[m]],bifvar][[1]]-bifvar,1]];,
RegN=ReplacePart[RegN,Position[RegN,eqTchg[[m]]]->Less[0,
```

```
bifvar-DeleteCases[List@@eqTchg[[m]],bifvar][[1]],1]];];];];
RegN=DeleteCases[RegN/.ysat//Simplify,False];
inqTchk=Select[Tally[chkreg[RegN]],#[[2]]>1&];
For[m=1,m<=Length[inqTchk],m++,
inqpos=Position[chkreg[RegN],inqTchk[[m,1]]];
RegN=Delete[RegN,inqpos[[2;;-1]]];];
If[(And@@RegN//FullSimplify)===False, Print["Region␣
"<>ToString[Rp]<>":␣Impossible␣Region:␣Something␣went␣horribly␣
wrong."]; Return["R"]];]; Return[RegN]]
chkreg[reg__]:=(Replace[DeleteCases[List@@@reg,_Symbol,2],
{a_,b_,c_}:>Cases[b,y[x__]:>y[x],
\[Infinity]],2])/.{a_+y[x__]:>y[x],b_-y[x__]:>y[x]}
chgeq[reg__,satval__,eqTchg__,bifvar__]:=If[satval<=0,
ReplacePart[reg,Position[reg,eqTchg]->Less[0,bifvar
-DeleteCases[List@@eqTchg,bifvar][[1]],1]],
ReplacePart[reg,Position[reg,eqTchg]->Less[0,
DeleteCases[List@@eqTchg,bifvar][[1]]-bifvar,1]]]
```

We can use this on its own but its usefulness is manifest only when we want to automatize all the steps outlined in Section 5.2.1 to solve the matrix model. So we hand over our basic setup directly to the following recursive function:

```
SolMatModRec[Regions__,assuk__,L__,satinqP__:{},ysatsP__:{y[0]->0},
solYRsP__:{{}},xminsP__:{0},P_:1]:=Module[{Regs=Regions,
assuK=assuk,p=P,n,e,j,s,nRegs,LR,vars,str,solYR,eqsYR,reginq,xlist,
xpos,xgrt,xmin,reclen,assutp,satinq,satvar,sateq,satval,solYRs,
xmins,\[Rho]s=\[Rho][x]/.solYRsP,ysats={},sol\[Mu],volMM=0},
n=Regs[[1,1]]; e=Regs[[1,2]]; nRegs=Plus@@n-1;
Regs=Append[Regs,GenReg[Regs[[p]],p,satinqP,ysatsP]];
If[Regs[[p+1]]==="R",Return[{assuk,
Regs[[1;;-2]],solYRsP,"x",\[Rho]s,ysatsP,0}]];
Monitor[str={"Evaluating␣Lagrangian..."};
LR=Assuming[{And@@Regs[[p+1]]},FullSimplify[L//.ysatsP]];
vars=Sort[DeleteDuplicates[Cases[LR,y[a__]->y[a],\[Infinity]]]];
str={"Solving␣equations␣of␣motion..."};
eqsYR={Sequence@@(vars/.y[a__]:>D[LR,y[a]]),D[LR,\[Rho][x]]};
solYR=Select[Solve[eqsYR==0,{Sequence@@(vars[[1;;-2]]),\[Rho][x]}],
!MatchQ[\[Rho][x]/.#,0]&]//Flatten; If[Length[solYR]==0,
xmins="x"; str={"No␣Non-trivial␣Solutions␣Found."};
Pause[1];Return[]]; If[Length[solYRsP[[-1]]]!=0,
If[((\[Rho][x]/.solYRsP[[-1]]/.x->xminsP[[-1]])/
(\[Rho][x]/.solYR/.x->xminsP[[-1]])//Simplify)!=1,xmins="x";
str={"Discontinuity␣Encountered␣in␣\[Rho]."};
Pause[1];Return[]];]; str={"Finding␣upper␣x-limit␣(xmin)␣for␣this␣
```

```
region..."};
reginq=DeleteDuplicates[DeleteCases[Assuming[{And@@Regs[[p+1]]},
Simplify[Regs[[p+1]]//.solYR]]//.solYR//Simplify,_Symbol,2]];
xlist=If[Length[reginq]!=1,Replace[DeleteCases[List@@@reginq,
_Symbol,2], {{a_,b_,c_}:>{(x/.Solve[b==a,x]),
(x/.Solve[b==c,x])},{a_,b_}:>(x/.Solve[a==b,x])},2]//Flatten,
DeleteCases[List@@@reginq//Flatten,_Symbol]/.{a_,b_,c_}:>
{(x/.Solve[b==a,x]),(x/.Solve[b==c,x])}//Flatten];
xpos=DeleteCases[Select[xlist,Assuming[assuK,
Simplify[NonNegative[#]]]&],0]; If[Assuming[assuK,
(xminsP[[-1]]!=0)//FullSimplify],xgrt=Extract[xpos,
Position[Table[Assuming[assuK,
Simplify[1/xpos[[j]]<1/xminsP[[-1]]]],{j,1,Length[xpos]}],
Except[False],{1},Heads->False]],xgrt=xpos];
If[Length[xgrt]==0,Print["Region␣May␣Not␣Exist!"];
xgrt={xminsP[[-1]]};]; xmin=Assuming[assuK, Min[xgrt]//Simplify];
If[Head[xmin]===Piecewise,xmin=Min@@({Table[xmin[[1,m,1]],
{m,1,Dimensions[xmin[[1]]][[1]]}],xmin[[2]]}//Flatten)];
If[Head[xmin]===Min,reclen=Length[xmin];,reclen=1;];
Monitor[For[j=1,j<=reclen,j++, Print["Region:",p,"xmin:",j];
If[reclen!=1,assutp={assuK[[1]]&&Assuming[assuK,
And@@Delete[Table[Reduce[xmin[[m]]>xmin[[j]]],{m,1,reclen}],
j]]}//FullSimplify; If[assutp[[1]]===False,xmins="x";
Continue[],xmins=xmin[[j]];],assutp=assuK;xmins=xmin;];
str={"Identifying␣the␣saturated␣inequality..."};
satinq=If[Length[Regs[[p+1]]]!=1,Extract[Regs[[p+1]],
Position[(Simplify[Regs[[p+1]]//.solYR]//Flatten)/.x->xmins
//Simplify,False]],Regs[[p+1]]]; For[s=1, s<=Length[satinq]-1,
s++,satinq[[s]]=satinq[[s]]//.ysats//Simplify;
satvar=Cases[List@@satinq[[s]],y[a__,x]:>y[a,x],\[Infinity]];
sateq=satvar[[1]]-satvar[[2]]; satval=sateq//.solYR/.x->xmins
//Simplify; ysats=Append[ysats,Solve[sateq==satval,
Sort[satvar][[1]]]]//Flatten//Simplify; Regs=Append[Regs,
GenReg[Regs[[-1]],p+s,{satinq[[s]]},{ysatsP,ysats}//Flatten]];
If[Regs[[-1]]==="R",Return[{assuk,Regs[[1;;-2]],solYRsP,"x",
\[Rho]s,ysatsP,0}]];]; satinq={satinq[[s]]}//.ysats//Simplify;
satvar=Cases[List@@satinq,y[a__,x]:>y[a,x],\[Infinity]];
sateq=satvar[[1]]-satvar[[2]];
satval=sateq//.solYR/.x->xmins//Simplify; ysats={ysatsP,ysats,
Solve[sateq==satval,Sort[satvar][[1]]]}//Flatten//Simplify;
solYRs=PadRight[solYRsP,p+s,{solYR}];
xmins=PadRight[xminsP,p+s,xmins]; str={"Done."}; If[p+s<=nRegs,
{assutp,Regs,solYRs,xmins,\[Rho]s,ysats,volMM}=
```

```
SolMatModRec[Regs,assutp,L,satinq,ysats,solYRs,xmins,p+s];
If[volMM===0,Continue[],assuK=assutp;Break[]];];];,
Refresh["xmins:␣"<>ToString[j]<>"/"<>ToString[reclen],
TrackedSymbols->{j}]];, Refresh["Region␣"<>ToString[p]<>":␣
"<>str, TrackedSymbols->{str}]]; If[xmins==="x", Return[{assuk,
Regions,solYRsP,xmins,\[Rho]s,ysatsP,0}]]; If[p==nRegs,
PrintTemporary["Calculating␣Volume..."];
\[Rho]s=\[Rho][x]/.solYRs;
sol\[Mu]=Solve[(Sum[Integrate[\[Rho]s[[m+1]],{x,xmins[[m]],
xmins[[m+1]]}],{m,1,Length[\[Rho]s]-1}])==1/2,\[Mu]];
volMM=1/(8\[Mu]^2)/.sol\[Mu][[2]];]; Return[{assuK,Regs,
solYRs,xmins,\[Rho]s,ysats,volMM}]]
```

This function is called via the command

```
{assumkM,Regions,solYs,Xmins,\[Rho]s,ySats,volD5}=
SolMatModRec[{{n,e}},assumk,Lm];
```

whose output contains

`assumkM` Modified (if at all) assumptions (`assumk`),

`Regions` y-inequalities (5.2.1) defining each region,

`solYs` $y_{a,I}(x)$ in each region,

`Xmins` Boundaries (x_i's in Table 5.1) of each region,

`ρs` $\rho(x)$ in each region,

`ySats` Saturated y-inequality for each region, and (finally)

`volD5` Vol(Y) in terms of k's. We can use `Apart[]` function to achieve partial function decomposition and then convert k's to p's as explained in the beginning of this Appendix.